GGU

Apatite mineralisation in carbonatite and ultramafic intrusions in Greenland

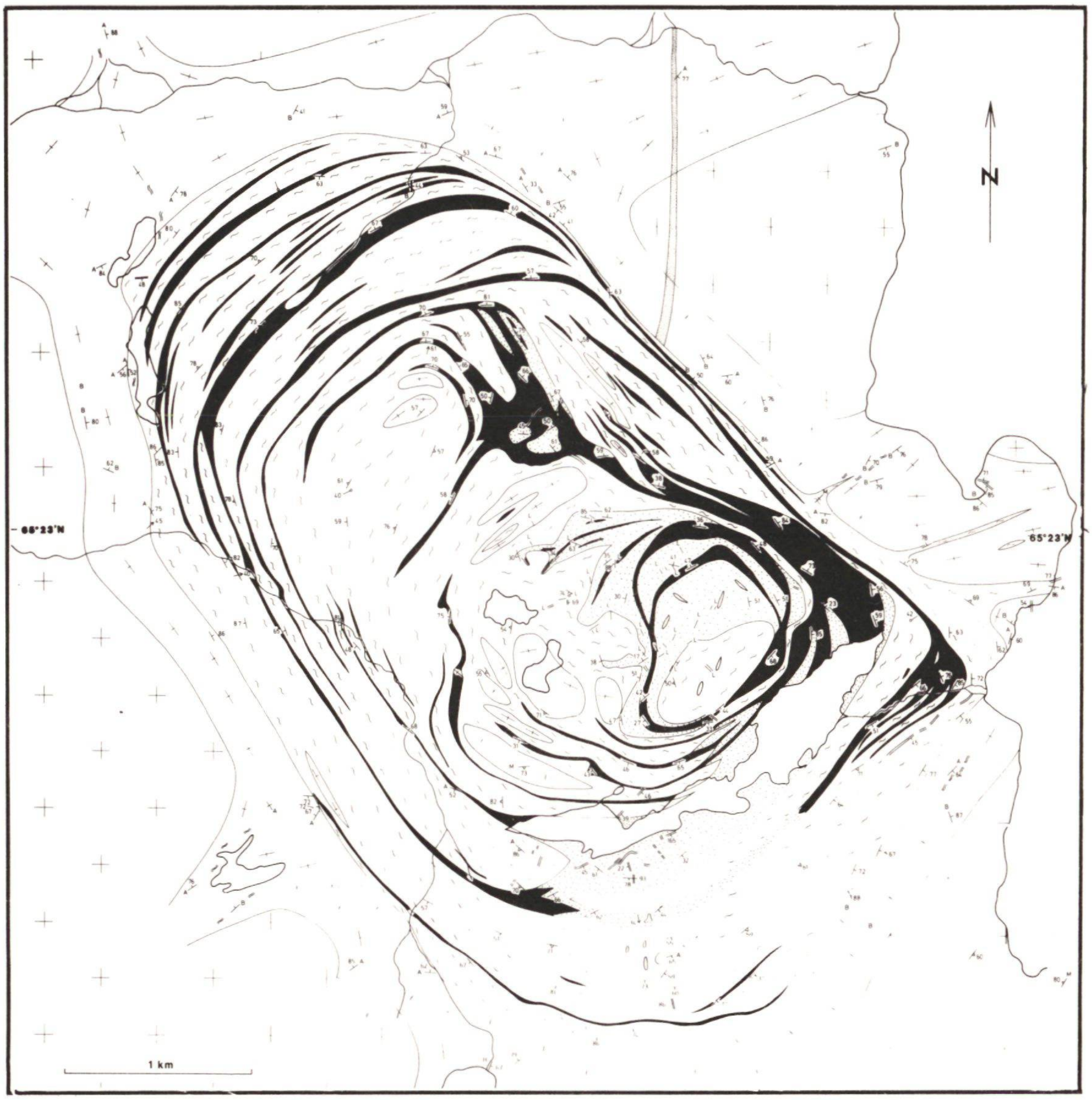

Final Report

2. edition

GRØNLANDS GEOLOGISKE UNDERSØGELSE
The Geological Survey of Greenland
ØSTER VOLDGADE 10, 1350 KØBENHAVN K, DANMARK

"RAW MATERIALS" R & D PROGRAMME

Sub-programme: *Metals and mineral substances*

By *Christian Knudsen*

Final report:	1 Sep. 1983 to 31 Dec. 1985
Contractor:	GEOLOGICAL SURVEY OF GREENLAND
Contract No:	*MSM-119-DK (G)*
Project leader:	KARSTEN SECHER
Project geologist:	CHRISTIAN KNUDSEN
Title of project:	APATITE MINERALISATION IN CARBONATITE AND ULTRAMAFIC INTRUSIONS IN GREENLAND

CONTENTS:

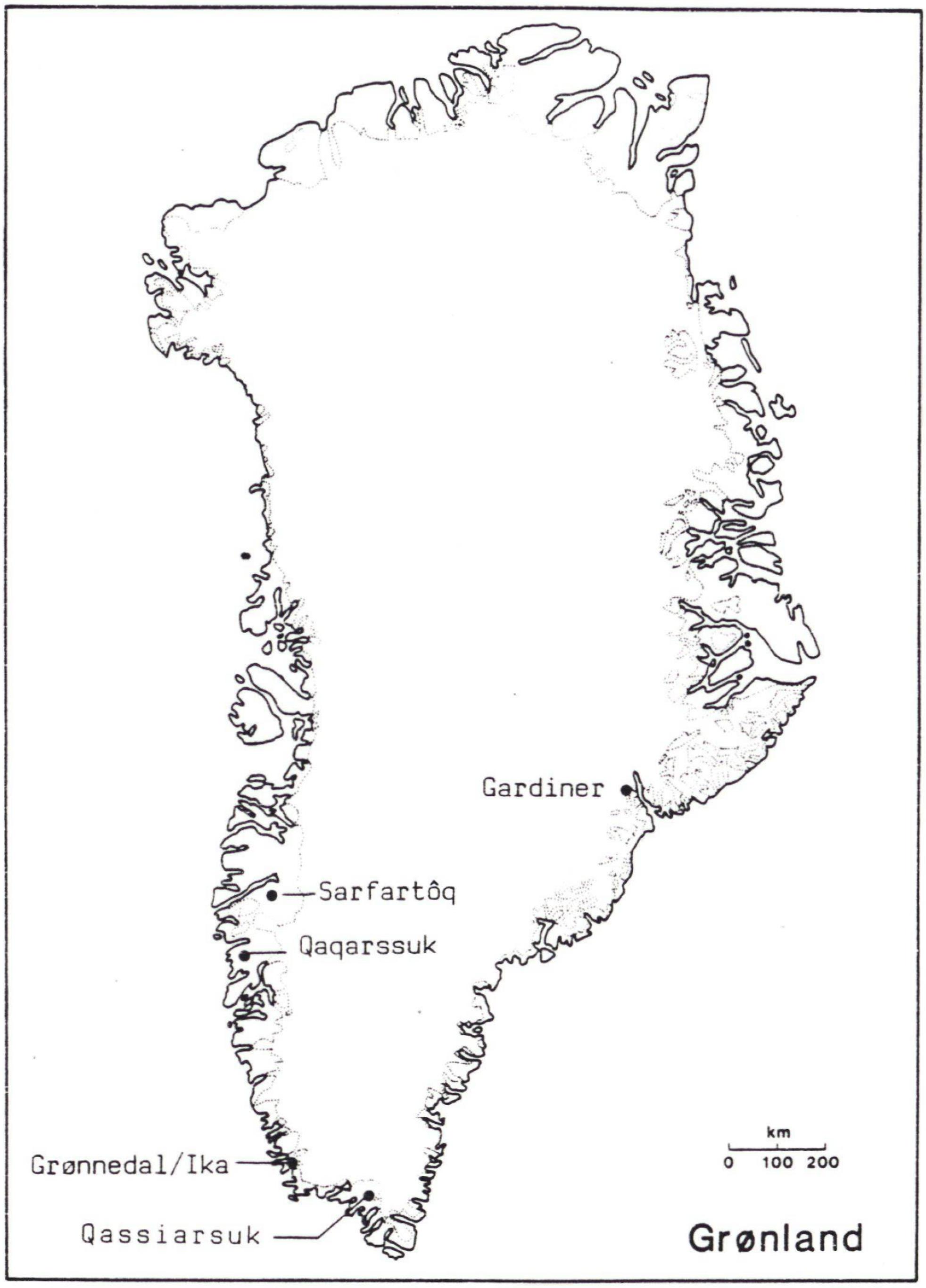

Fig. 1. The apatite-bearing carbobatite and ultramafic intrusions in Greenland.

1. INTRODUCTION

The project has been carried out at The Geological Survey of Greenland (GGU), and the project was partly (5o%) funded by EEC and partly (50%) by GGU. The project period was 1st September 1983 to 31st december 1985.

The project has been carried out in cooperation with British Geological Survey (BGS) and Warren Spring Laboratory (WSL). BGS is writing a review of apatite occurrences in igneous rocks, of the major deposits and economic potential of the different apatite associations. WSL is carrying out beneficiation studies on igneous apatite including apatite from carbonatites in Greenland.

1.1. ORIGINAL OBJECTIVES

The objective of the project is to investigate the phosphate potential of a number of intrusive complexes in Greenland as part of a study of the geology, distribution and mode of occurrence of low-grade igneous apatite deposits in the North Atlantic realm.

1.2. AREAS OF HIGHEST PRIORITY

The main emphasis of the work has been on the Qaqarssuk Carbonatite Complex because there is drill core and geophysical information available for the complex, and because several types of phosphate-rich rocks are present in significant amounts. Further the complex contains pyrochlore, lanthanide-rich carbonatites and vanadium-rich magnetite, which could support a phosphate production. The Qaqarssuk Carbonatite Complex is located 55 km east of the town Sukkertoppen and 20 km from the west coast.

Some work has been done on the effusive carbonatites at Qassiarssuk because relatively high phosphate contents could be expected. This combined with the horizontal orientation and surface near character of the deposit, and the location in an area with existing infrastructure and near the sea and just opposite to the Narsarsuaq airport, South Greenland - makes the area interesting as a potential phosphate source.

Finally, short reviews are given of two well-studied carbonatite occurrences, the Sarfartôq and Gardiner intrusions, which also contain economically interesting phosphate deposits.

1.3. MEMBERS OF THE PROJECT

The following persons have been involved in the project.

Christian Knudsen acted as project geologist, Inge Rytved as lab-technician (mainly working with data processing), Aase Hasselsteen as secretary and Karsten Secher as project leader. Morten Kjærgaard and Kim Olsen carried out geophysical field investigations during the summer 1984. Morten Kjærgaard has processed magnetic date, provided by Kryolitselskabet Øresund A/S. Trine Boiesen carried out radiometric measurements during the summer 1985.

2. PHOSPHATE ROCK

2.1. RESERVES AND MARKET

The following is only a short review, and a more throughout description will be given by BGS.

Commercial grade phosphate "rock" (concentrate) ranges from 60 to 88% BPL (bone phosphate of lime 1% BPL = 0.458% P_2O_5) or 28 to 40 wt% P_2O_5. Sedimentary phosphorites constitute the bulk of the exploited rock and yield phosphate concentrates with average 70% BPL. This is lower than concentrates from igneous sources yielding average 83% BPL. The difference is caused by the substitution of P by C in the apatite (francolite) in the sedimentary phosphates.

Global reserves of recoverable phosphate reserves are estimated to 35,700 mill t phosphate "rock", of which 61% are located in Morocco and western Sahara and 19% in USA. 1600 mill. t are recoverable at costs less than 30 $/t and 10,600 mill t at costs less than 40 $/t. (Anon, 1985). Many older mines mainly in the USA are producing at low cost relative to new mines but these resources are likely to be exhausted by the end of the century.

The *annual production* of phosphate "rock" was 147 mill t (table No 1) in 1984, with a capacity utilisation of 78%. An oversupply has led to a drop in the price after peak prices in 1974-75. However, the latest years have seen an increase in phosphate rock demands (Mew, 1985).

Demand: Almost all phosphate rock is used as raw material in the fertiliser industry, and hence the demand for phosphate rock is

Table I

PHOSPHATE ROCK PRODUCTION

(From Mew, 1985)

(10^3t product)

USA	48.820
USSR	28.890
Marocco	21.133
China	13.200
Tunesia	5.346
Jordan	6.263
Brazil	3.400
Israel	3.312
South Africa	2.593
Togo	2.696
Nauru	1.359
Senegal	1.874
Syria	1.514
Iraq	850
Christmas Island	1.252
Others	4.095
Total	142.997
Capacity	172.390

dependent on the agricultural production in the industrialised countries, and the ability to buy fertilizer in the Third world countries. The economic growth in e.g. the Far East has resulted in growth in demand for phosphate.

The *price* of a given concentrate is further determined by:

- The grade of the concentrate: - (lower grade means higher consumption of acid in the production of phosphoric acid).
- The quality of the concentrate:

1. Certain impurities as Mg, Si, Fe, Al and Na cause increased consumption of sulphuric acid when opening the raw phosphate.
2. Other impurities as Cu and Cd lower the quality of the fertilizer, being poisonous.

Igneous phosphate generally has very low contents of impurities and is regarded as high quality phosphate. The export market for igneous phosphate is very small, though. The former large USSR output of Kola phosphate is decreasing. In the long term the USSR will probably not be able to export phosphate, as domestic consumption is expected to increase beyond the production (Anon, 1983). In the new five year plan, it is decided not to export phosphate to western countries and to cut deliveries to other eastern European countries with 25%.

Igneous phosphate is currently exported from South Africa (Palabora).

Igneous phosphate is further produced in Brazil, Finland, East Africa and Sri Lanka, but this is almost entirely used on the domestic market.

TABLE 2

CADMIUM IN APATITE

Sedimentary deposits:

Morocco 2)	24.6 ppm
Togo 2)	65.6 -
Senegal 2)	92.3 -
Tunesia/Algeria 2)	24.6 -
Israel/Jordan 2)	14.4 -
Western USA 2)	61.5 -
Eastern USA 2)	14.4 -

Igneous deposits:

USSR (Kola) 1)			0.2 -
Kola 4)			0.05 -
South Africa (Palabora) 3)			3.4 -
Sweden 1)	Gränges		1.1 -
	LKAB		0.3 -
Finland	Siilinjärvi 4)		0.07 -
	Sokli 4)		2.8 -
Greenland	Qaqarssuk 4)	Søvite	0.11 -
		Silico-søvite	0.10 -
		Rauhaugite	0.18 -
		Late søvite	0.21 -
	Sarfartôq 4)	Rauhaugite	0.11 -
		-	0.14 -
		Apatite-rich rauhaugite	0.23 -
		Pegmatic carbonatite	0.13 -
	Gardiner 4)		0.02 -

1) From Gunnarsson, 1983
2) Calculated after Hutton, 1981
3) Calculated after Sauerbeck, 1982
4) Analysed by GGU, this work

2.2. THE CADMIUM PROBLEM

Most phosphate rock producers exploit sedimentary phosphate, with relatively high cadmium (Cd) contents (table 1). Cd is toxic, even in small quantities (Gunnarsson, 1983) and outlet of Cd from phosphate fertilizer production and use has attracted attention (e.g. from the EEC-Commission).

The outlet of Cd to the environment happens at two stages:

1. To produce phosphoric acid, for further treatment in the fertilizer industry, the raw phosphate is treated with sulphuric acid $Ca_5(PO_4)_3F + 5\ H_2SO_4 \rightleftharpoons 5\ CaSO_4 + 3\ H_3PO_4 + HF$. In this process gypsum is a by-product. Two thirds of the Cd is distributed into the phosphoric acid and one third into the gypsum (Wakefield, 1980). The gypsum is often dumped in coastal waters, and e.g. in 1978 there was a worldwide discharge of approximately 62 t Cd via the gypsum (Hutton, 1983).

2. The annual contribution of Cd from phosphate fertilizer into agricultural soil is 5 g/ha on average (Hutton, 1983), which is equal to 1% of the average concentration in soil and more than the input from the atmosphere (3 g/ha). This Cd pollution is hence not rapid, but a long term effect, increasing the Cd concentration in the soil with approximately 0.25%/year (Dam and Klausen, 1983), which according to Hutton, (1983) is likely to raise the dietary intake of Cd in e.g. Denmark above the (WHO) tolerable values in 100 years' time.

To circumvent these problems there are two strategies:

1. To use raw-phosphate with low Cd contents, i.e. igneous phosphate.
2. To remove the Cd from the gypsum and the fertilizer.

Regarding the first strategy, there is limited access to igneous phosphate on the export markets because output is limited and most igneous phosphate is produced for domestic market. One of the major exporters of igneous phosphate is South Africa (Palabora), which from a political point of view must be regarded as a problematic trade partner for the time being. Further the Palabora phosphate has a very high content of Cu which causes other environmental problems. The other large producer of igneous phosphate, USSR, is likely to need the phosphate for the domestic market on a long term basis (Anon, 1983).

Regarding the second strategy, the problem with the Cd discharge via gypsum can be solved either by use of the gypsum in the building industry or by removal of the Cd from the gypsum. The Danish company Superfos has solved this (on pilot plant scale) by an ion exchange process $2\ KCl + CaSO_4 \rightleftharpoons K_2SO_4 + CaCl_2$, where the K_2SO_4 is used as fertilizer and the Cd is easily subtracted from the $CaCl_2$).

No process (to the author's knowledge) is in function for removing Cd from phosphoric acid or fertilizer.

Sweden has introduced regulations of the Cd content in phosphate fertilizers, and other countries, e.g. the EEC, may do the same. Because purification processes are rather costly, an ensuing increase in the demand, and hence the price, for igneous phosphate must be expected.

3. PHOSPHORUS IN IGNEOUS PROCESSES

3.1. DISTRIBUTION OF PHOSPHORUS ON THE EARTH

The total amount of phosphorus on the earth - based on cosmochemical arguments (Smith, 1981) is likely to be 11 to 13 x 10^{21} kg, of which approximately 29 x 10^{18} kg is found in the crust.

Fluorapatite is the dominating phosphorous mineral in the crust (Smith, 1981). The positive correlation between P_2O_5 and F in oceanic basalts (Smith, 1981) and the P_2O_5 and lanthanide content in alkali basalts, nephelinites and kimberlites (Bergman, 1979) indicates that apatite is the main phosphorous mineral in the upper mantle and the source for P in igneous rocks. Considerations of the relative abundances of P and F indicate that only 1/20 of the total amount of P on the earth is found as fluorapatite (Smith, 1981), whereas the remaining part, situated in the lower mantle and core, probably is found as phosphides. The concentration of P may reach 0.7 wt% in the core.

Igneous rocks of the crust have a wide range of P_2O_5 contents (in wt%) from ultrabasic rocks (appr. 0.01), ocean ridge tholeiites (0.08), alkali basalts (0.3 to 1.0) and granites (0.02 to 0.15). Some strongly alkaline rocks, e.g. in the Kola and Gardar alkaline igneous provinces, have P_2O_5 over 1 wt%, and carbonatites have in average 2 wt% (Gold, 1966). Chondrite values are appr. 0.2 wt% and lherzolite contains 0.06 wt% (Nash, 1984).

3.2. BEHAVIOUR OF PHOSPHORUS IN IGNEOUS PROCESSES

Atomic number = 15

Atomic weight = 30.97376

Oxidation state = 5^+

Ionic radius = 0.34 Å (tetrahedral coordination)

Due to the high field strength of P^{5+}, phosphorus is found as PO_4^{3-} complexes in melts (Ringwood, 1955).

Phosphorus can substitute for Si^{4+} in silicate minerals, but in general the phosphate distribution into silicate and oxide minerals is very small with distribution coefficients from 0.01 to 0.06 (Andersen and Greenland, 1969). Due to this *incompatible character*, phosphorus is enriched in the melt fraction during early stages of crystallisation. In later stages, when the phosphorus concentration has reached a certain (threshold) level, phosphate minerals - generally apatite - start to crystallise. In carbonatite lavas isokite ($CaMgPO_4F$) may be found as the phosphate species, and in lanthanide-rich magmas monazite ($(Ce,La,Y,Th)PO_4$) or xenotime (YPO_4) may be found.

High concentrations of PO_4^{3-} complexes strongly affect the melt properties, melting points are lowered, and extensive fields of liquid immiscibility may appear (McBirney and Nakamura, 1974). PO_4^{3-} form complexes with some heavy ions in alkaline environment and may serve as transporting agent for such ions (Kosterin, 1959, and Möller & Morteani, 1983).

The solubility of phosphate in silicate melts decreases with increasing silica content of the melt (Watson, 1979).

Phosphorus is a volatile element (Wyllie and Tuttle, 1964), and high phosphorus concentrations have been measured in the air over fumaroles.

The lower content of phosphorus in extrusive rocks compared to intrusive rocks is interpreted as due to loss of phosphorus during degassing of the lava (Liebau and Koritnig, 1978). As could be expected from the volatile character of phosphorus, the element is enriched in pegmatites, where a wide range of phosphate minerals is found - often associated with Mn, Fe, Li, Be, lanthanides and Nb (Moore, 1973). Apatite is also found in vesicles in olivine leucitite crystallised from the vapour phase (Birch, 1980)*.

3.3. APATITE

3.3.1. *The properties of apatite*

In igneous rocks, the - by far - most abundant phosphate mineral is fluorapatite ($Ca_{10}(PO_4)_6F_2$). There is, however, a large number of substitutions for the various components, and the formula can be expressed: $A_{10}(ZO_4)_6X_2$ (Cockbain, 1968). The most important elements are respectively: (Mc Connell, 1973):

A: Ca^{2+}, Sr^{2+}, Ba^{2+}, Na^{+} and lanthanides^{3+}.

Z: P^{5+}, Si^{4+}, C^{3+} and Mn^{6+}.

X: F^{-}, Cl^{-} and OH^{-}.

The A position in fluorapatite can accept ionic radii from 0.95 to 1.35 Å and valences of 1 to 3.

The Z position can accept radii of 0.29 to 0.6 Å and valences of 3 to 6 (Kreidler and Hummel, 1970).

The substitutions are often coupled, with end-members, e.g. vitusite $Na_3(La,Ce)(PO_4)_2$ or britholite $Ce_3Ca_2(SiO_4)_3OH$.

Apatite is *hexagonal,* and optically negative with refractive index omega from 1.6356 to 1.6497 and epsilon from 1.6326 to 1.6462 depending on the composition (Mc Connell, 1973).

The *colour* is generally greenish-yellow, but high contents of Mn^{5+} can give a blue colour (Mc Connell, 1973).

The *density* of apatite (theoretical fluorapatite) is 3,199 g/cm^3, but varies with composition and content of fluid and solid inclusions.

Apatite crystallised in equilibrium with liquid and vapour form equidimensional crystals, whereas apatite crystallised from cooling liquids forms acicular prisms, locally with cavities (Wyilie et al., 1962).

3.3.2. *Factors controlling the apatite composition*

The apatite composition depends on a number of different factors, as melt composition and temperature.

- The *temperature* affects the entry of both F and lanthanides into the apatite. There is a negative correlation between K_{Ap}^{F} and temperature, and the distribution of OH and F between biotite and apatite has been proposed as a geothermometer by Stormer and Charmichel (1971).

There is a negative correlation between temperature and K_{Ap}^{REE}, and Watson and Green (1981) found a factor 2 increase in lanthanide concentration in apatite with a temperature decrease of 130° C.

The apatite composition is affected by the *melt composition*. There is a negative correlation between Si in apatite and in melt in silicic melts (Taborsky, 1962). This is because the entry of Si^{+4} into apatite in silicate melts is negatively correlated to the degree of polymerisation of $(Si, Al)O_4$ tetrahedrons in the melt, increasing with the silica concentration. Nash (1972) found a positive, linear correlation between silica in melt and apatite in alkaline silicic rocks and carbonatites at Iron Hill. Lanthanide partitioning into apatite (K_{Ap}^{REE}) is higher in silicate-rich rocks than in basic rocks (an increase from 50 to 68 wt% SiO2 gives an increase in partition coefficient from 7 to 30 (Watson and Green, 1981)).

The *alkalinity* of the melt/environment affects the lanthanide entry into apatite, - increasing with increasing alkalinity (Landa et al., 1983). In contrast, the lanthanides are kept in solution where they form complexes with chlorine (Flynn & Burnham, 1978), fluorine or carbonate (Landa et al, 1983, Möller and Morteani, 1983).

The lanthanide partition coefficient is not the same for all lanthanides, but a function of the difference between the lanthanide ionic radius from the optimum radius of the available site in the apatite (Ca) (Eby, 1975). Samarium (Sm) has the most ideal size (Key et al., 1964), and the chondrite normalised lanthanide patterns are downwards concave as a result of this. The partition coefficients for Nd, Sm and Dy lie in the range of 28 to 40 (Nash 1984), 15 to 24 for La and 19 to 27 for Ce (Larsen, 1979) in peralkaline rocks.

F/Cl in apatite has a systematic variation during fractionation with up to 30 fold increase (Nash, 1984).

The apatite rarely has any Eu anomaly relative to the coexisting melt. Where a negative Ce anomaly is present, this indicates that the melt had high pO_2 before apatite crystallised.

Fig. 2 and 3. Seismic field work at Qaqarssuk 1984.

4. METHODS

4.1. FIELD WORK

4.1.1.

The geological field work was carried out on the basis of 1:10,000 and 1:2,000 orthophoto maps and 1:40,000 aerial photographs in stereo pairs. Strike and dip were measured with magnetic compass where possible - care had to be taken due to the strongly anomalous magnetic field adjacent to magnetite-rich rocks. Saphymo SPP-2 scintillometer was used as a mapping tool.

Soil samples were taken in profiles dug with hand spade down to 80 cm where possible, and approximately 500 g soil samples from the B horizon (where present) were collected in paper bags.

The seismic investigations were done with a 12 channel OYO McSeis 1500 enhance and display unit and 12 single geophones. Both hammer and explosives (Dynamex B) were used as energy sources (fig. 2 and 3). Power supply was delivered from a 12 V accumulator (Kjaergaard and Olsen, 1985).

The geoelectrical investigations were carried out with an ABEM SAS 300 terrameter, a SAS 200 booster, two 400 m sounding cables and two Wenner-cables for fixed spread measurements (electrode spacings 20 m and 10 m).

Magnetic investigations have been carried out in different periods. In 1970 and 1971, Kryolitselskabet Øresund A/S (KØ) made a survey of the vertical field (50 m x 50 m grid) in a 35 km^2 large area, with an Askania 56 magnetometer. In 1975 KØ made a survey of the total magnetic field in the core (25 m x 10 m grid) covering 2.5 km^2. Mesurements were carried out with a proton precision magnetometer - Scintrex MP-2.

Investigations of susceptibility were made by Kjærgaard and Olsen (1985) with hand-held kappameter - Geofyzika Bruo kT-5.

Radiometric investigations were first carried out by KØ in 1970. The whole complex was covered by a (one channel > 1.6 MeV) PRI scintillometer survey (50 m x 50 m grid).

In 1985 *radiometric investigations* were made in selected areas, with a Geometrics Gr 410 four channel gamma-ray spectrometer (total, K, U and Th). The instrument was carried on the back (1 m above ground). Counting time was 2 minutes. Background radiation was measured twice a day over 2 m water. The instrument was calibrated on concrete pads at RISØ. Equilibrium U and Th concentrations were calculated using: U sensitivity = 10.23 counts/sec per ppm eU, Th sensitivity = 0.1174 counts/sec per ppm eTh and stripping ratio: Th into U = 0.5236. The calculated values were corrected for reduced signal because of the distance to the ground of 1 m. The factors of 1.2 (Th) and 1.38 (U) were determined in the field.

4.1.2.

The geological field work was carried out by Christian Knudsen in the periods 25. June to 3. July 1984 in Qassiarssuk; 5. to 7. July 1984 in Grønnedal/Ika (together with I. Morteani, B. Kronimus and P. Möller); and 10. July to 31. August 1984 and 9. July to 15. August 1985 in Qaqarssuk.

The geoelectric and seismic field work was carried out by Morten Kjærgaard and Kim Bak Olsen in the period 10. July to 31. August 1984.

The gamma spectrometric measurements were carried out by Trine Boiesen in the period 9. July to 18. August 1985.

4.2. LABORATORY WORK

4.2.1.

Major elements were analysed at the Geological Survey of Greenland (Ib Sørensen) by X-ray fluorescence analysis of glass discs prepared with a sodium tetraborate flux (sample:flux = 1:7 in rock samples and 1:23 in soil samples) using a 28 channel Phillips PW 1606 X-ray spectrometer (Rh tube, 50 kV, 50 mA). Na was analysed by atomic absorption spectrometry, FeO by titration and volatiles by loss on ignition.

4.2.2.

Trace elements in rocks were measured by X ray fluorescence analyses on pressed powder pellets at the Institute of Petrology, University of Copenhagen (John Bailey), using a Philips PW 1400 spectrometer and the techniques of Norrish and Chappel (1977). The analysed elements are: Rb, Sr, Y, Zr, Nb, Th, Pb, Ga, Ta and Zn (Mo tube, 80 kV, 30 mA), Cu and Ni, (Mo tube, 70 kV, 35 mA), La, Ce and Nd (W tube, 60 kV, 40 mA), Co, V and Cr (W tube,70 kV, 35 mA), Ba, Ti and Sc (Cr tube, 60 kV, 40 mA).

Results were corrected for background and interference from tube and sample spectral lines, and for matrix variation, using both major and trace element composition (trace element composition was hence determined by 2 iterations). USGS standards (G-2, GSP-1, AGV-1, W-1, BCR-1 and PCC-1) were used for calibration.

4.2.3.

Trace elements in soil (Nb, La, Y and Zr). After crushing of the soil it was analysed by Haldis Bollingberg at the Institute of Petrology using optical emission spectrography (Hilger Large Quartz Glass spectrograph), and synthetic standards calibrated against G-1, W-1 and NBS minerals.

4.2.4.

Microprobe analyses of minerals were carried out on the JEOL 733 superprobe at the Institute of Mineralogy, University of Copenhagen under the supervision of Jørn Rønsbo.

A reconnaissance study of the mineral parageneses of all rock types was carried out with the energy dispersive equipment (15 kV, 1 nA, 100 sec live time, focussed beam). Elements determined were Na, Mg, Al, Si, P, K, Ca, Ti, Fe, Mn, Zr, Nb and Ce, and in some cases also for S, Sr, Ba and Nd. Raw data were (ZAF) corrected on line. Simple natural and syntethic standards were used.

Pyrochlore was analysed using 4 wavelength dispersive X-ray spectrometers (15 kV, 30 nA, focussed beam). Raw data were ZAF corrected on line. The analysed elements are Nb, Ta, Ti, Fe, La, Ce, Pr, Nd, Sm, Y, Na, Ca, U, Th, Zr and Si.

Apatite compositions were analysed in two runs. The *trace elements* were analysed with the 4 channel wavelength dispersive equipment operated at 20 kV, 200 nA with 10 sec livetime, with the beam defocussed to a diameter of 20 μ using a stepping procedure, so that each analysis is an average of 4 points in a square (20μ x 20μ). The following elements were analysed: La, Ce, Pr, Nd, Sm, Dy, Y, Yb, Mn, Sr and Ba. Raw data were ZAF corrected off line, using standard apatite composition. The results were corrected for background interference from sample spectral lines (Mn -> Dy, Ba -> Ce, Ba -> Nd, Sr -> Y). The results were calibrated relative to synthetic standards (Drake and Weill, 1972), also used as drift control.

Apatite major element composition was determined with the 4 channel wavelength dispersive equipment (15 kV, 20 nA, 10 sec, beam defocussed to a diameter of 20μ). The following elements were analysed: F, Na, Si, P, Cl, Ca, Sr, Y, La, Ce and Nd. Raw data were ZAF corrected on line, and results calibrated relative to the Wilberforce apatite.

Instrumental neutron activation analyses (INAA)

3o whole-rock analyses were carried out by L. H. Christensen, Isotope Division, Risø National Laboratory. The analytical procedure is described in Christensen and Damsgaard (1985).

Cathodoluminescence

The cathodoluminescence studies were carried out with Lumenoscope equipment, supervised by P. Frykman, Institute for Historical Geology and Paleontology, University of Copenhagen.

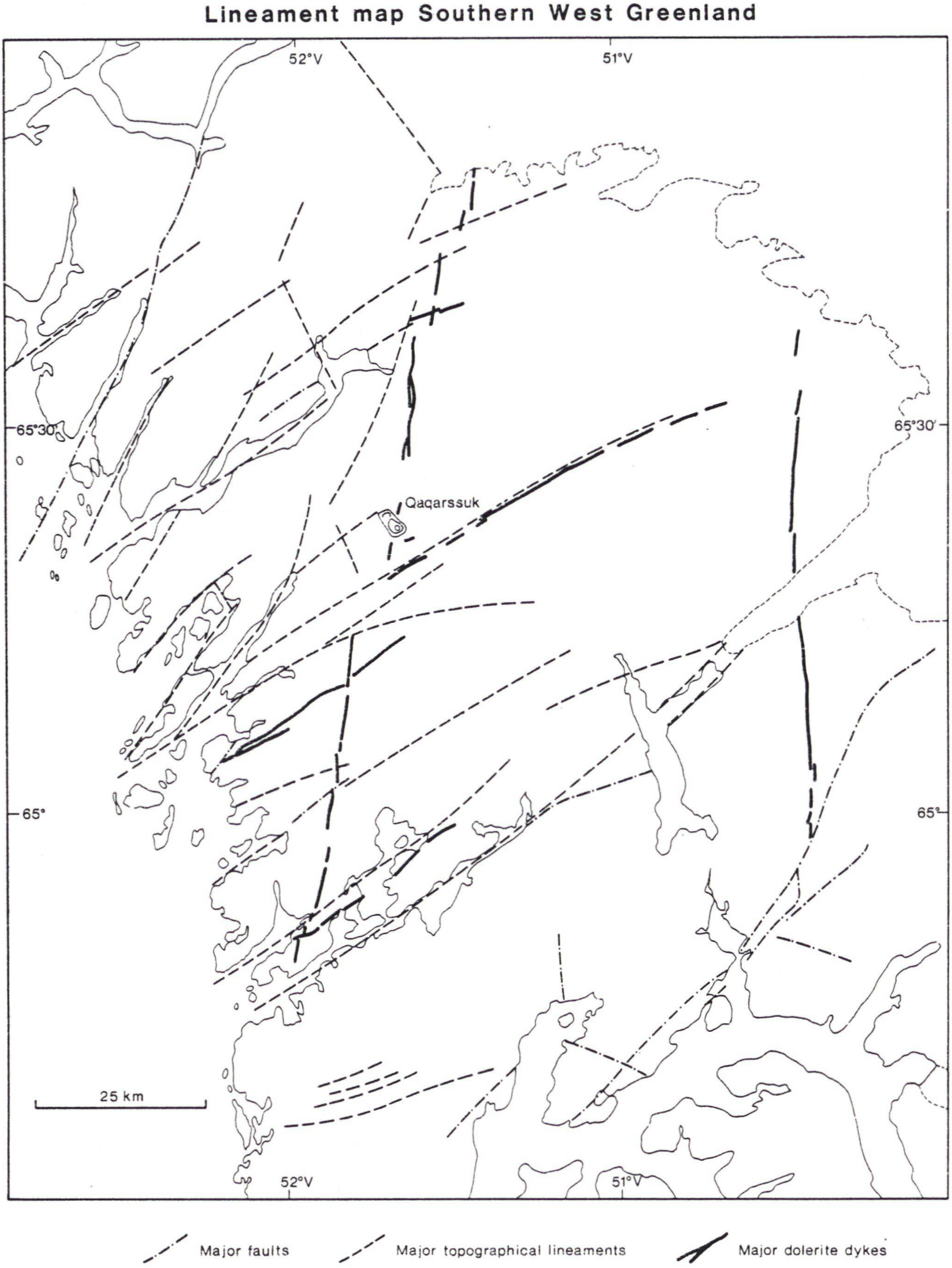
Lineament map Southern West Greenland

Fig. 4.

5. THE QAQARSSUK CARBONATITE COMPLEX

5.1. PREVIOUS INVESTIGATIONS

The Qaqarssuk Carbonatite Complex, situated 60 km east of the town Sukkertoppen, was found by Kryolitselskabet Øresund A/S in 1962 because of the rust staining, and was later verified during a regional airborne aeromagnetic survey in 1965. The complex was considered as a metamorphic limestone until chemical analyses showed high content of Nb, Sr, Ba and lanthanides. The complex was revisited in 1969, and was mapped at a scale of 1.10,000 in 1970 (Vuotovesi, 1974) and radiometric (scintillometry) and magnetic surveys (vertical field measurements) were carried out in a 50 m x 50 m point grid, covering the whole complex (Kurki et al. 1973). The radiometric survey showed that the radioactive elements - mainly Th - were concentrated in the rim of the complex. Because a correlation between Th and lanthanides was observed, the radiometric anomaly pattern was used as a guide in a drilling programme in 1970 (Kurki and Juhava, 1971) where 10 shallow drill holes were made in the rim of the complex. No substantial lanthanide mineralisations were found.

In 1975 the complex was revisited, and the strongly magnetic core was subjected to a total magnetic field survey in a 10 m x 25 m grid. Because a correlation between pyrochlore and magnetite was observed, the magnetic anomalies were used as a guide for a drilling programme (Gothenborg and Pedersen, 1976). In 1975 222 shallow drill holes (average 8 m) were made and in 1976 16 deep drill holes (average 150 m). This work delineated two

Qaqarssuk Carbonatite Complex

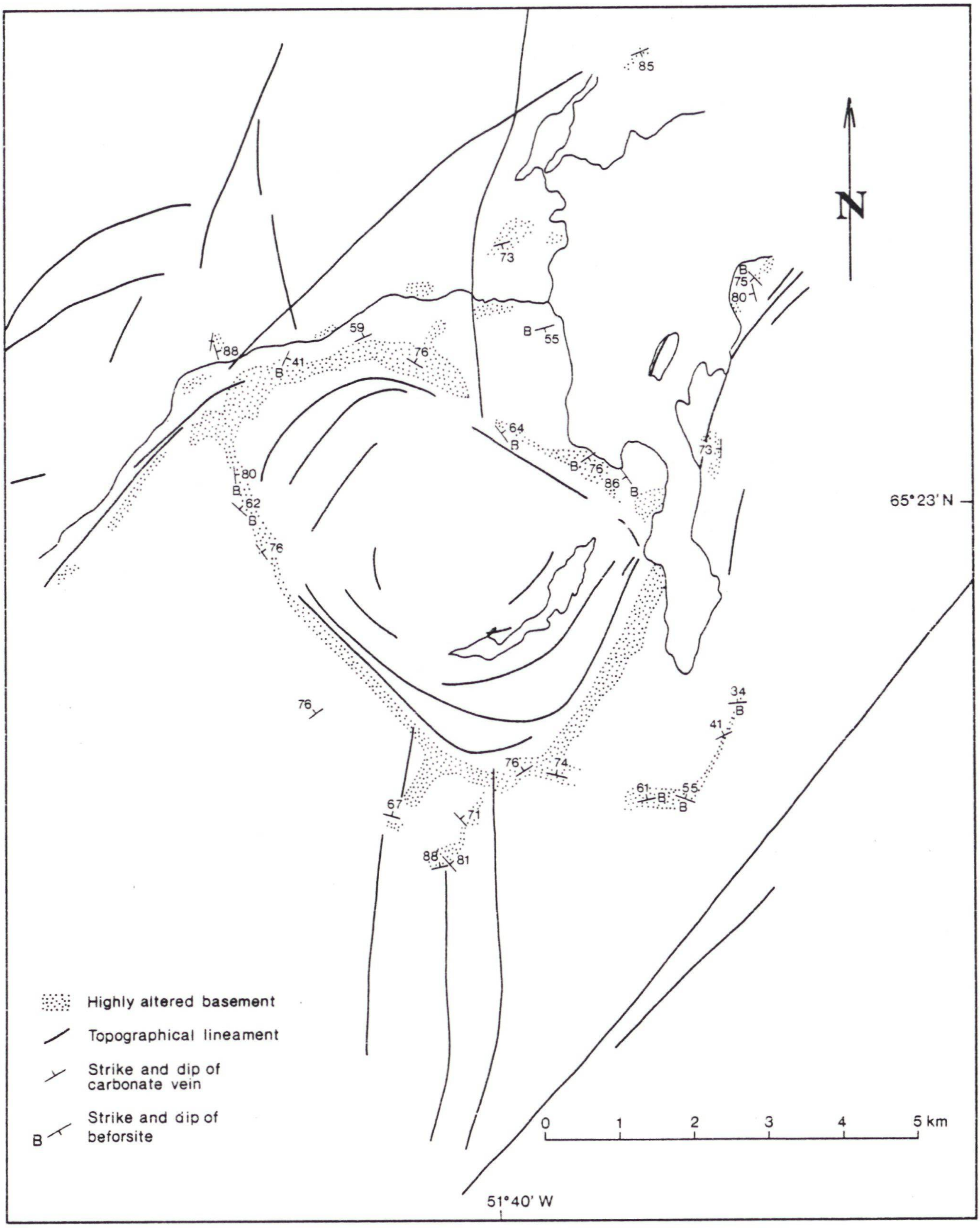

Fig. 5.

pyrochlore mineralised zones with a total of 3.5 mill tons of rock with 0.5 % Nb_2O_5 or 1.2 mill t of rock with 0.8 % Nb_2O_5 (Gothenborg et al., 1977). Apart from this the drilling programme indicated substantial amounts of lanthanide-rich carbonatite and apatite-rich carbonatite and glimmerite. However, the carbonatite was considered uneconomic by Kryolitselskabet Øresund A/S, and the concession was given up in 1983.

The Qaqarssuk Carbonatite Complex has since 1976 been investigated by the Geological Survey of Greenland (Secher 1977, Kunzendorf and Sørensen, 1982, Larsen et al, 1983 and Kunzendorf and Secher, in press, a). Kunzendorf and Sørensen concluded that stream sediment sampling is of minor use in the area, whereas (radioactive) Nb mineralisations can be outlined by systematic soil sampling. Kunzendorf and Secher found enrichment of Si, Ti, Al, Fe and P in the soil (A horizon). This is interpreted as due to leaching of carbonate and preservation of resistant minerals such as apatite. Nb and U enrichment in certain soils is interpreted as upwards migration of these elements after chemical alteration of pyrochlore. Kunzendorf and Secher further report gradually increasing Ca, Mg and P and decreasing Si and Al from the country-rock to carbonatite.

Larsen et al (1983) found ages around 173 my by K/Ar dating of phlogopite from carbonatites as well as from a discordant lamprophyre dyke.

5.2. GEOLOGICAL SETTING

The carbonatite was intruded into the Archaean basement 173 my ago (Larsen et al. 1983). The Archaean basement consists of granitic to

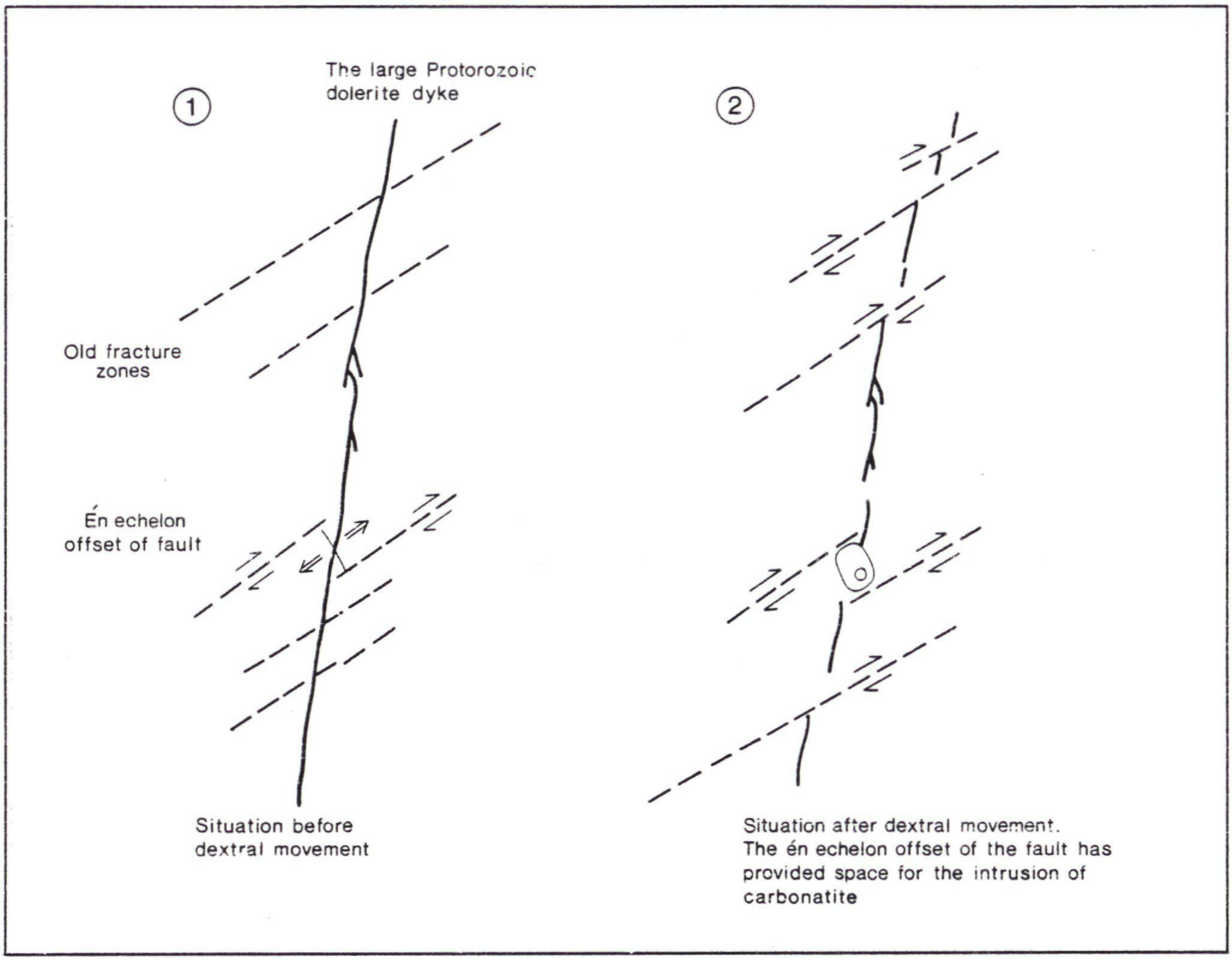
①
The large Protorozoic dolerite dyke
Old fracture zones
Én echelon offset of fault
Situation before dextral movement
②
Situation after dextral movement. The én echelon offset of the fault has provided space for the intrusion of carbonatite

Fig. 6.

tonalitic rocks, and of mafic to ultramafic layers and lenses, probably of supracrustal origin. The metamorphic grade ranges from amphibolite to granulite facies. The basement contains a large (20 to 200 m wide) dolorite dyke, rich in clinopyroxene and orthopyroxene (of early Protorozoic age) trending N - S, and several less mafic dolerite dykes generally trending NE - SW (fig. 4). These dykes are cut by the carbonatite. By the intrusion of the carbonatite, the basement was fenitised both within and around the complex.

5.3. STRUCTURE AND TECTONIC CONSIDERATION

5.3.1. *Structure*

The structure of the carbonatite appears from the map (plate 1 in the appendix).

The carbonatite complex has a rounded rectangular outline with the long side trending approximately 140° and the short side trending 50°. The complex consists of an outer suite of steeply outwards dipping concentric carbonatite sheets which follow and define the rounded, rectangular shape, and an inner suite of less steeply dipping circular sheets. There seems to be two centres of these inner, circular sheets, of which the southern centre is by far the most dominating. The noncircular appearance on the map of this centre is a topographic effect, resulting from the western part being capped by fenite on a hill. The carbonatite sheets vary widely in thickness, from several tens of metres to a few centimetres, and the composition varies from søvitic to rauhaugitic. The thick sheets are generally of søvitic composition, and the thickness of the carbonatite sheets is generally highest near the "corners" of the complex.

The carbonatite as well as the fenite generally contain a well developed foliation and often mineral lineation and layering. The dip of the foliation and layering in the complex increases outwards, and in the NW corner of the complex (at low altitude) the layering locally dips towards the core. The abundant folds generally plunge outwards perpendicularly to the strike of the layering. This indicates that the carbonatite sheets are curved giving the complex a diapir (or onion-)like shape).

The frequency of carbonatite sheets in the fenite is by far highest in the eastern part of the complex, and correspondingly the deformation of the fenite and carbonatite is more intense here.

The carbonatite contains varying amounts of fenite inclusions and ultramafic inclusions or layers, and the described carbonatitic rocks range from pure carbonatite (fig. 23) to carbonatite seen as a braided pattern between fenite lenses (fig. 17). Hence it has been necessary to use arbitrary boundaries (at 50% carbonatite) in the mapping of the complex (plate 1 in the appendix).

There is a general decrease in grain size from the core of the complex (the large carbonatite sheets) and outwards. This holds both for the carbonatite and the associated fenites. In the core, the deformation of the feldspar-rich country rocks has led to a granoblastic texture with complete recrystallisation of the feldspar, whereas the albite lamellae in the plagioclase found in the marginal shear zones often are bended. Shear zones with very fine-grained quartz-rich mylonites are found as well, with beautiful flattened high-angle boundary subgrains (fig. 11). Most of these shear zones have a concentric orientation relative to the complex, but some radiate out from the complex with a general trend of 50^o to 80^o.

The carbonatite and the fenite aureole are surrounded by a rim of highly altered quartz-bearing basement rocks (fig. 5), cut by radioactive ankerite veins or calcite veins and shear zones. Radioactive, narrow beforsite dykes and vents (with subcircular outline), rich in altered basement fragments are also found in the highly altered basement, often located in radioactive shear zones.

5.3.2. *Tectonic considerations*

The direction of the dominating lineament direction in the region is 50^o-60^o (fig. 4). Recurrent shear, faulting and fracturing have taken place along this direction, which is very important in the post Archaean evolution in central West Greenland. The movement in these fault zones has mainly been dextral, as can be seen from the offset of the N - S trending early Proterozoic dolerite dyke. Fault movements in the Fossilik area, a few km east of Qaqarssuk, of post Ordovician age are reported (Secher, 1983 a).

The actual timing of the dextral faulting is not known, but some movement may be related to large dextral movements associated to the opening of the North Atlantic and the Polar Basin. Jones (1983) suggests that large dextral movements in the de Geers transform fault zone, along the margin of the Polar Basin and in Northern Canada, is related to a large transform fault zone, caused by the offset between the spreading

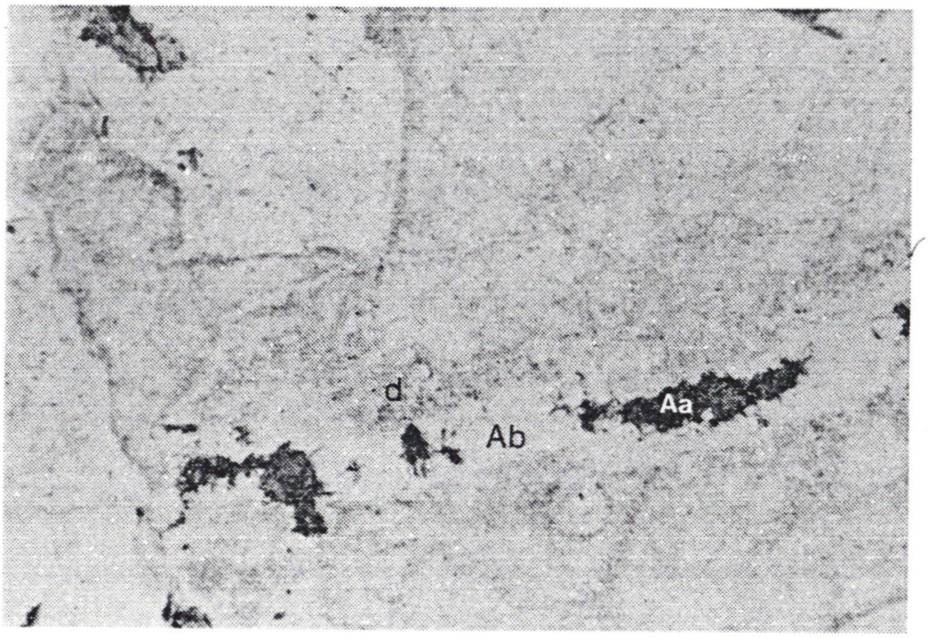

Fig. 7. Aegerine-augite (Aa) in recrystallised albite (Ab). The albite is dusty up to the vein (d). Quartzbearing altered basement, GGU 320431. The microphotograph is 1 mm vertically.

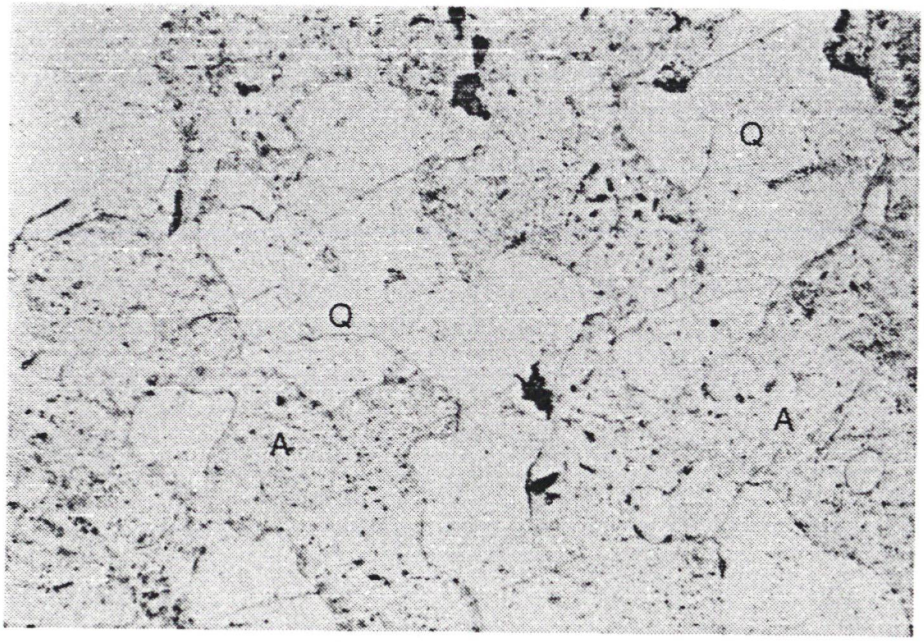

Fig. 8. Rounded quartz grains (Q) in dusty albite (A). Quartzbearing altered basement, in which the texture is completely changed, GGU 320442. The microphotograph is 2 mm vertically.

ridges in the Polar Basin and in the North Atlantic. These movements are active from early Mesozoic time, and may have caused reactivation of the West Greenland fracture zones.

If dextral movement is assumed, a small en échelon offset, possibly caused by the large dolerite dyke, would cause tension parallel to the faults and perpendicular to the long side of the carbonatite thus giving space for the intrusion (fig. 6). A very large proportion of the carbonatite sheets in the Qaqarssuk Carbonatite Complex is parallel to this 140° direction, and also to the 50°- 60° trending fractures which probably are determinating the direction of the short "side" of the complex.

5.4. ROCK DESCRIPTIONS

The nomenclature in the following is as follows (based on Currie, 1976):

Beforsite:	Fine-grained dolomite-dominated dyke.
Carbonatite:	Igneous rock with more than 50% carbonate.
Fenite:	Metasomatically altered basement rock, in which no quartz has survived.
Glimmerite:	Rock composed essentially of mica.
Rauhaugite:	Medium- to coarse-grained dolomite-dominated carbonatite.
Silico-søvite:	Søvite with 25-50% silicate minerals.
Søvite:	Medium- to coarse-grained calcite dominated carbonatite.

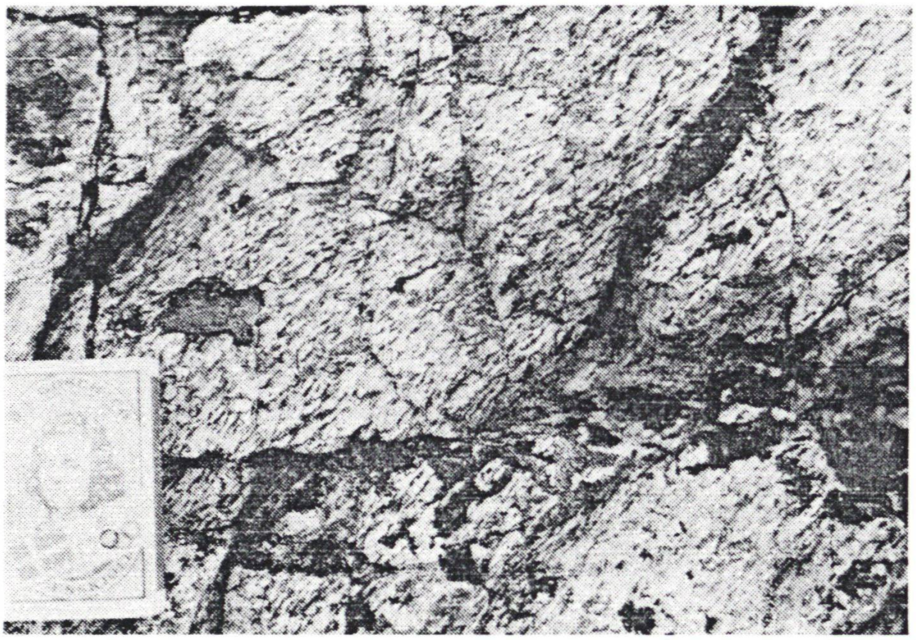

Fig. 9. Quartzbearing altered basement, in which the texture is completely altered.

Fig. 10. Mylonite with alternating quartz and amphibole rich layers.

5.4.1. *Altered basement rocks*

The basement is progressively altered approaching the carbonatite complex, and apart from this altered zones are found in the basement, mainly along the dominating lineaments in the area parallel to the 60° NE - SW striking lineaments, e.g. in the Kangia Valley (fig. 5).

5.4.1.1. *Altered basement with preserved quartz*

Different types of quartz-bearing altered basement can be recognised in the field. They occur as an outer aureole to the complex, as the least altered rocks inside the complex, and in shear-zones further off - mainly in the NE - SW trending fault or fracture zones in the area.

5.4.1.1.1. Distal altered basement rocks

The altered basement along the above-mentioned fault or fracture zones appears as gossans and is easily recognised from the air. The rock is intensely carbonated and often sheared. The iron content in the carbonate increases with increasing distance from the complex, and siderite is found 10 km from the core of the complex. These gossans are often slightly radioactive. They form magnetic lows because the magnetite is altered. Beforsite dykes or vents are localised in these areas.

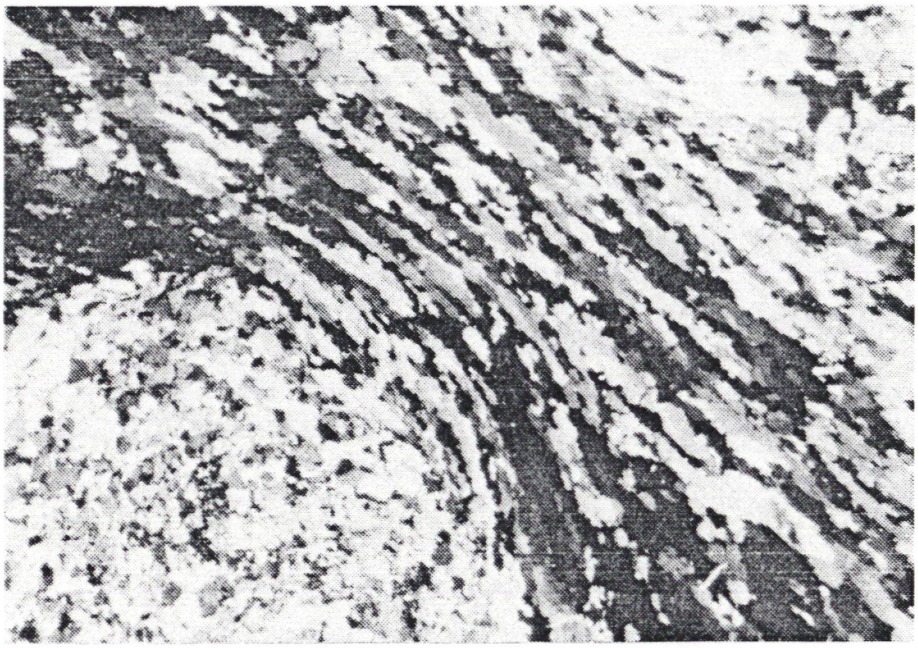

Fig. 11. Highly strained quartz grains wrapped around a rounded fenite fragment. Mylonite. The microphotograph is 2 mm vertically, crossed Nicols. GGU 320406.

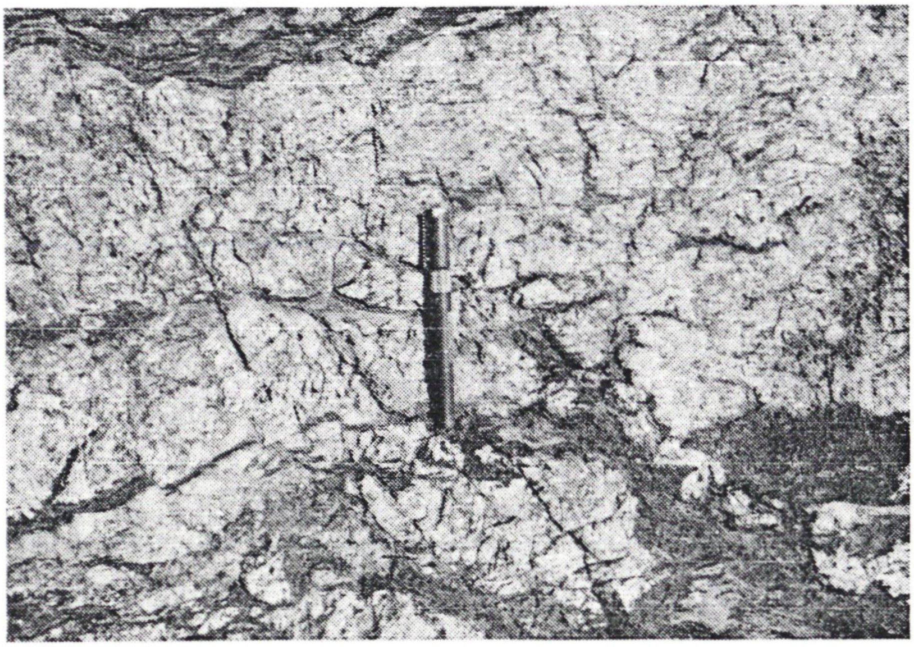

Fig. 12. Felsic fenite with carbonatite veins rimmed by ultramafite. The black veins are hornblende dominated, the grey are pyroxene dominated.

5.4.1.1.2. Proximal altered basement rocks

A coarse-grained, foliated, red rock (fig. 9) is typical for the parts of the altered basement within 500 m from the fenite margin - and internally in the complex. The texture of the basement is totally reworked, and the rock consists of *quartz-schlieren* composed of unstrained, rounded quartz grains (1 - 3 mm) (fig. 8) often enclosing radiating clusters of fibrous aegirine augite. The *plagioclase* - (antiperthite) is coarse and zoned, composed of a dusty oligoclase to albite core with sericite and carbonate inclusions (1 - 5 μ). This is overgrown by clean albite.

Aegirine-augite is abundant along cracks and joints in the rock (fig. 7), locally overgrown by *alkali amphibole*. Magnetite is overgrown by sphene. Where pyroxene and amphibole in cracks are abundant, the rock gets a green appearance. *Carbonate* occurs as veins as well as inclusions in the feldspar. In the innermost part of this zone, a *very fine-grained* strongly sericitised/chloritised rock is found. Calcite and ankerite veins are frequent, and pyrite is a common accessory mineral.

5.4.1.1.3. Mylonite

The altered basement is cut by mylonites, either developed as a nicely layered and folded rock (fig 10) with a compositional layering of alternating quartz and amphibole-albite layers with rounded fenite inclusions (fig.11) or as an aphanitic almost pseudo-tachylytic rock with feldspar augens.

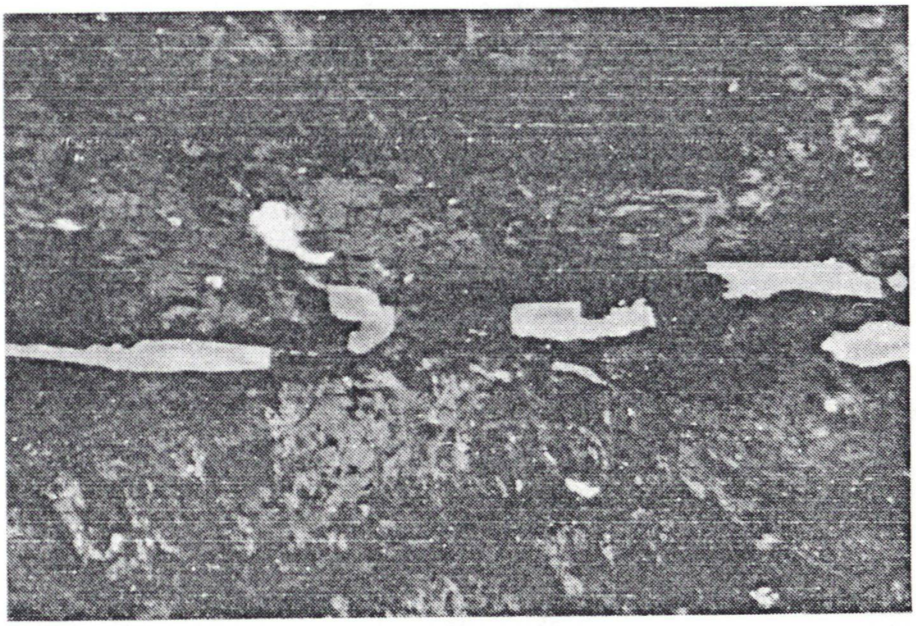

Fig. 13. Zoned apatite along vein in fenite. The microphotograph is 0.5 mm vertically, cathodoluminescence. GGU 320121.

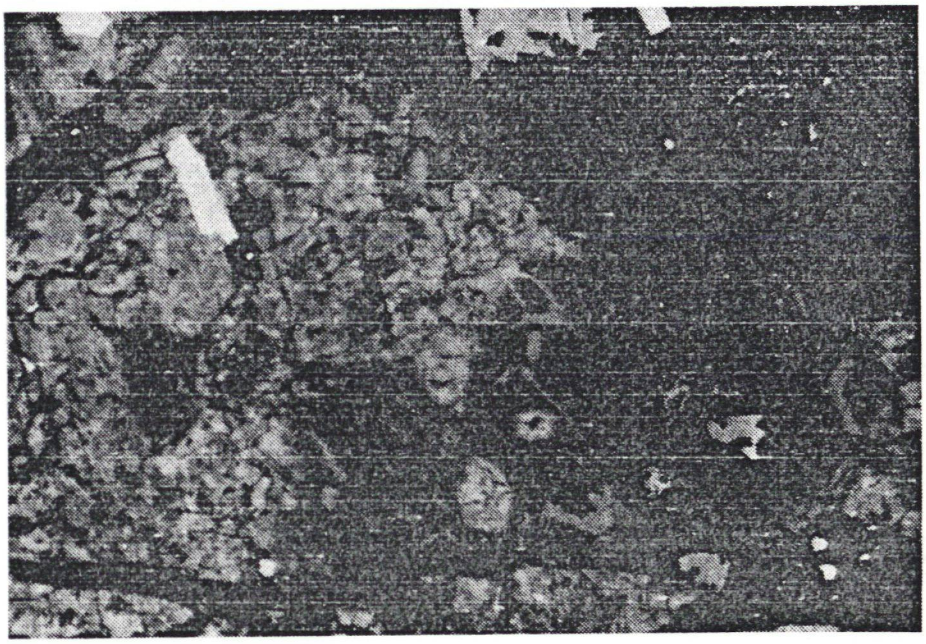

Fig. 14. Apatite enclosed in albite. Both the apatite and the albite are compositionally zoned. The microphotograph is 1 mm vertically, cathodoluminescence. GGU 320424.

5.4.1.2. *Felsic fenite*

The felsic fenite occurs as an inhomogeneous rock with layering and veining of mafic material in a felsic rock (fig. 12). The felsic part consists of *albite* with subordinate *biotite, alkali amphibole* and *aegirine-augite*. The texture is medium-grained granoblastic, but with a foliation defined by parallel orientation of mafic minerals or aggregates of mafic minerals. The mafic minerals are often is concentrated along joints or carbonate veins. The thickness of these mafic "veins" varies from 1 to 20 mm and apart from carbonate they consist of aegirine-augite often overgrown by alkali amphibole. Layered fenites are found where this veined pattern has been transposed into parallelism by deformation.

Apatite is found both as elongated medium-grained crystals in veins (fig. 13), and disseminated as euhedral fine-grained crystals enclosed in the albite (fig. 14) and in the albite rock.

Accessory *zircon* and metamict *pyrochlore* are locally found.

Occasionally very coarse albitite rock with up to 3 cm large albite crystals is seen as small veins in the glimmerite.

5.4.1.3. *Shear zones in the fenite*

The layering in the fenite is locally cut by shear zones. The rock in these zones consists of a very fine-grained albite and biotite matrix together with rounded apatite. In this groundmass large plagioclase and phlogopite crystals are found.

Fig. 15. Diopside rimmed by hornblende and nucleation of alkaliamphibole in the albite. Mafic fenite. The microphotograph is 0.2 mm vertically. GGU 320429.

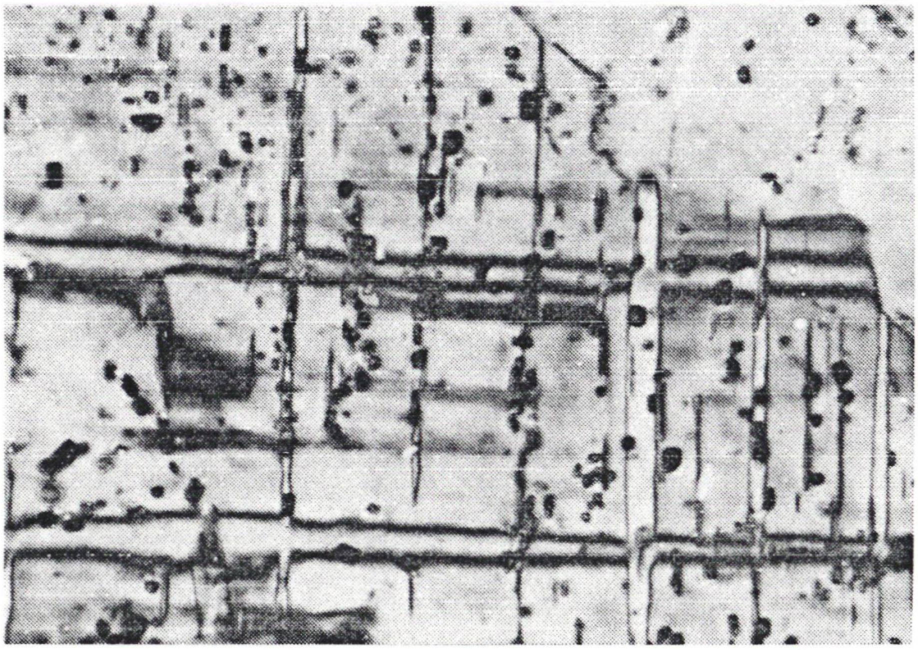

Fig. 16. Nucleation of alkaliamphibole parallel to twin lamellae in albite. Mafic fenite. The microphotograph is 100 μ vertically, crossed Nicols. GGU 320429.

5.4.1.4. *Mafic fenite*

The mafic fenites occur as dark green to black medium-grained rocks. They can be traced back to little altered mafic basement rocks where they occur e.g. as garnet pyribolites. The mafic fenites are characterised by *diposide* or *augite* rimmed by *hornblende* (fig. 15). The *hornblende* rim may continue into a colourless *richterite* and bluish *arfvedsonite* outer rim, and may be altered to *arfvedsonite* along cracks. The interstitial *plagioclase* is medium to fine-grained and granoblastic. The plagioclase may be zoned with an anorthite-rich core and albite rim. The albite contains inclusions of very fine-grained amphibole often oriented relative to the albite structure (fig. 16). *Carbonate* is present as veins, as inclusions in or corrosive to albite or interstitial to the silicate minerals. The rock is often foliated due to parallel orientation of pyroxene and varying proportions of mafic minerals.

There is a gradual transition from the mafic fenite to the pyroxenite and hornblendite, as the albite content decreases.

5.4.1.5. *Pyroxenite*

The pyroxenite consists of medium- to coarse-grained (0.2 to 5 mm), subhedral *diopside* or *augite* crystals often with alkali pyroxene or hornblende rim in interstitial carbonate (calcite) (0.05 to 0.1 mm). The pyroxenite is transitional into both the hornblendite and black glimmerite by alteration of the pyroxene to hornblende or phlogopite,

Fig. 17.
Søvite with a vertical foliation defined by parallel arrangement of phlogopite.

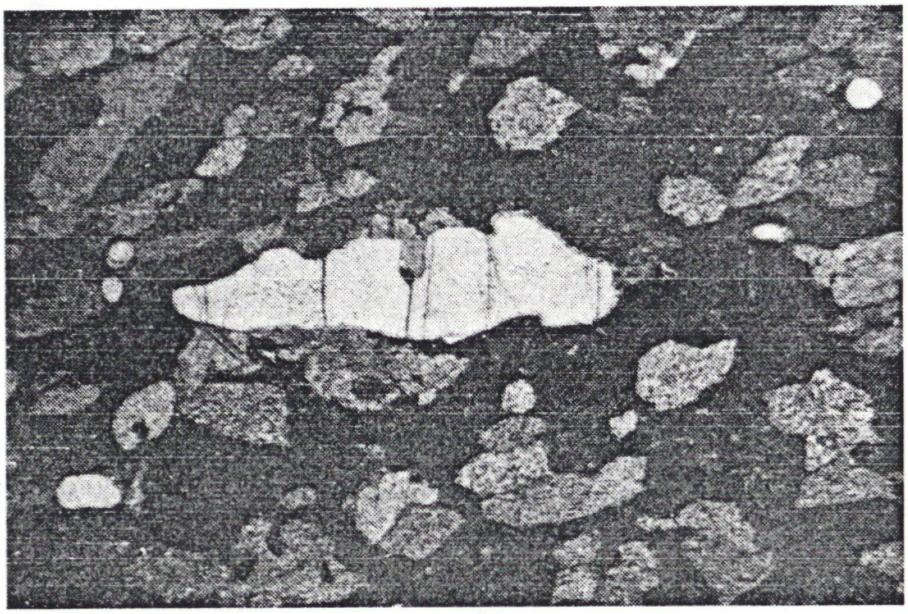

Fig. 18. Embayments in apatite. Søvite. The thinsection is stained with alizarine red, and calcite is dark, dolomite is grey and apatite is white. The microphotograph is 1 mm vertically. GGU 249806.

respectively. The pyroxenite often contains small amounts of granoblastic albite. The pyroxenite may contain up to 10% *apatite* mainly localised in the interstitial carbonate, but apatite enclosed in pyroxene and albite is frequently found. *Pyrrhotite* or *magnetite* are common accessories together with *zircon*.

5.4.1.6. *Hornblendite*

The hornblendite is a medium- to coarse-grained (0.5 to 10 mm) rock consisting of zoned euhedral *hornblende* crystals often with *pyroxene* core in a *calcite* matrix with 5 to 20% modal apatite. *Albite* with *apatite* and carbonate inclusions may be present. The *hornblende* is replaced by *phlogopite* along the rims, mimicking the hornblende structure and phlogopite is common as subhedral zoned crystals with normal pleochroitic scheme.

The hornblendite is foliated with parallel arrangement of phlogopite and hornblende.

5.4.1.7. *Glimmerite*

The glimmerite is transitional into the hornblendite and pyroxenite, and is the most proximal rock relative to major carbonatite sheets. The glimmerite is a coarse-grained rock consisting of *phlogopite*, *hornblende*, *alkali amphibole*, *pyroxene*, *carbonate*, *apatite* and *magnetite* with accessory *zircon* and *pyrochlore*. The colour of the glimmerite varies from brown to black depending on whether the

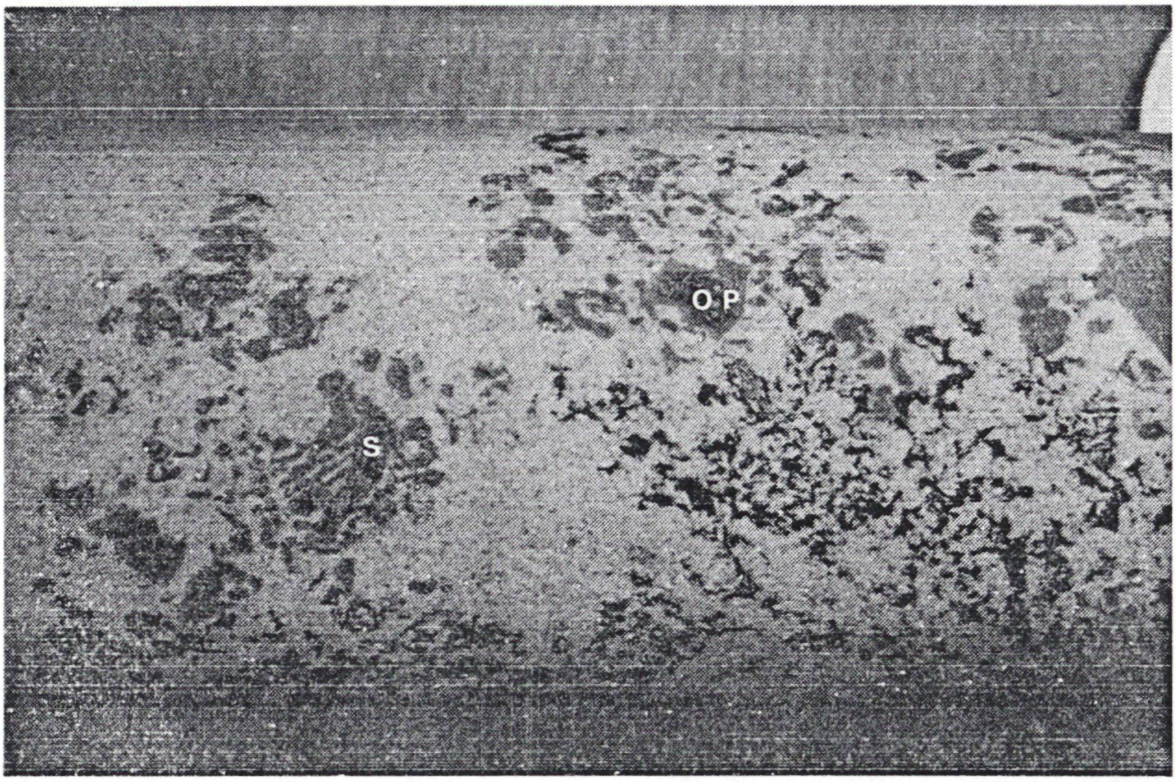

Fig. 19. Skeletal olivine (S), olivine partly replaced by phlogopite (OP) and dendritic magnetite. Søvite. Drill core

Fig. 20. Relict olivine. The primary crystal shape is outlined by a magnetite rim. Dendritic magnetite is also seen. Søvite. Drill core.

phlogopite is reversely pleochroitic (tetraferri phlogopite) or not.

Hornblende and pyroxene occur as partly digested cores in some phlogopite grains. *Calcite and apatite* occur interstitially in the glimmerite. The *apatite* is coarse-grained, rounded, and may locally constitute up to 50% of the rock.

The glimmerite may contain considerable amounts of very coarse poikiloblastic *magnetite* grains with ilmenite exsolution lamellae. This magnetite is locally corroded by calcite leaving the ilmenite lamellae in a conspicuous pattern.

5.4.2. *Carbonatites*

In the field the carbonatites can be roughly divided into seven groups, based on modal composition and texture, described in the following.

Due to the concentric development of the complex it is difficult to make a relative chronology of these rock types. The only rock types with discordant relations are 1. the late søvite which cuts søvite, siliocosøvite, ultramafic rocks, fenites and beforsite; and 2. the lanthanide-rich carbonatite veins which cut søvite, silico-søvite, ultramafites and fenite.

5.4.2.1. *Søvite*

The søvite has a widely varying mineralogical composition, with varying contents of calcite, dolomite, apatite, phlogopite, alkali

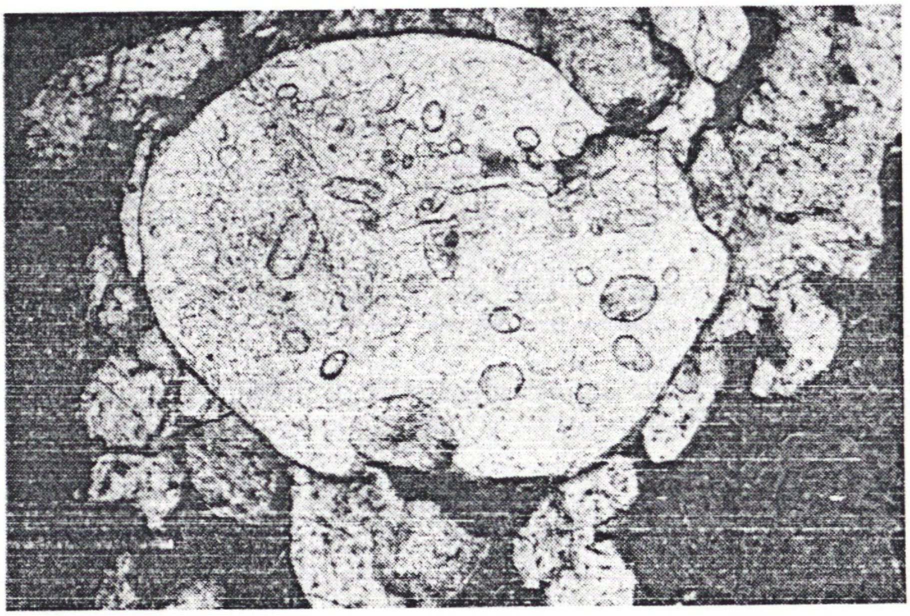

Fig. 21. Rounded apatite with dolomite inclusions. The thin-section is stained and calcite is dark, dolomite grey and apatite white. Søvite. The microphotograph is 0.5 mm vertically. GGU 253662.

amphibole, magnetite and olivine. Accessory strontianite, ancylite, zircon and pyrochlore are found locally.

Calcite, which is the dominating mineral, is found as medium-grained interlobate crystals enclosing the slightly coarser subhedral *dolomite* crystals. Inclusions of fine-grained calcite in the dolomite - and of dolomite in calcite are abundant in little deformed carbonatites, and locally the two carbonates are intimately intergrown. In shaded areas (e.g. in hollow olivine crystals) calcite is very rich in rounded dolomite blebs (fig. 38). The small blebs of one carbonate in another are interpreted as an exsolution texture.

The *apatite* is found as rounded, slightly elongated, coarse-grained crystals with carbonate inclusions - mainly of dolomite (fig. 21). The apatite is compositionally zoned. Carbonate is corrosive in the apatite and embayments (fig. 18) often cut the compositional zoning of the apatite. Apatite enclosed by olivine occurs as slender euhedral needles with a length/width ratio on up to 20/1 (fig. 46). This is in contrast to the little elongated apatite crystals usually found in the carbonate.

The *magnetite* is found both disseminated and as almost massive layers in the søvite. The magnetite in these layers consists of coarse, euhedral crystals of titano magnetite with ilmenite exsolution lamellae (fig. 26). The magnetite disseminated in the carbonatite is found both as coarse euhedral magnetite crystals and in a conspicuous dendritic or skeletal texture (fig. 19), where the magnetite is intimately intergrown with calcite (with dolomite exsolution blebs). This magnetite also contains exsolved ilmenite, both as irregular ilmenite patches in the magnetite and as lamellae in the magnetite. The skeletal magnetite is often associated with olivine.

Fig. 22. Silico søvite. The rock is highly strained and homogenised in both sides of the photo. In the centre fenite inclusions rimmed by ultramafite is seen in an isoclinally folded structure.

The *olivine* is found as coarse euhedral to resorbed or totally replaced crystals. The olivine is often skeletal (fig. 19 and fig. 38). The olivine is often altered in a zoned pattern (fig. 20 and 39). The innermost zone is serpentine, which also is found along cracks in the olivine. Then follows a zone of very fine-grained tetraferri phlogopite, which in turn is followed by fibrous orthoamphibole in apparent optical continuity with the olivine. Finally there is a rim of fine-grained anhedral magnetite generally outlining the original shape of the olivine crystal. The carbonate adjacent to such altered olivine is dolomite within a distance of 0.2 to 0.5 mm from the relict olivine surface. This sequence of minerals is not always complete. The olivine may be completely altered to some of the above-mentioned minerals and only recognisable by the shape of the magnetite rim, within which lies a core of tetraferri phlogopite or fibrous amphibole.

Locally, bands of olivine, magnetite and apatite-rich carbonatite are found, not exceeding 15 cm in thickness.

The *phlogopite* is, apart from the above-described, found as coarse-grained, zoned, brown, reversely pleochroic, subhedral crystals which are often slightly deformed. The *alkali amphibole* occurs as fine-grained, zoned euhedral crystals with a colourless core and a bluish-green, pleochroic rim.

The søvite is often *foliated*, with a foliation defined by parallel arrangement of dolomite, amphibole, phlogopite and apatite crystals, and the texture resembles the texture in gneiss (fig. 17 and 22).

The søvite contains rounded inclusions of fenite with ultramafic rim. There is a gradual transition from the søvite to the below described silico søvite.

Fig. 23. Rauhaugite as thin veins in a braided pattern between fenite inclusions. Notice the thin ultramafic alteration rim on the fenite inclusion.

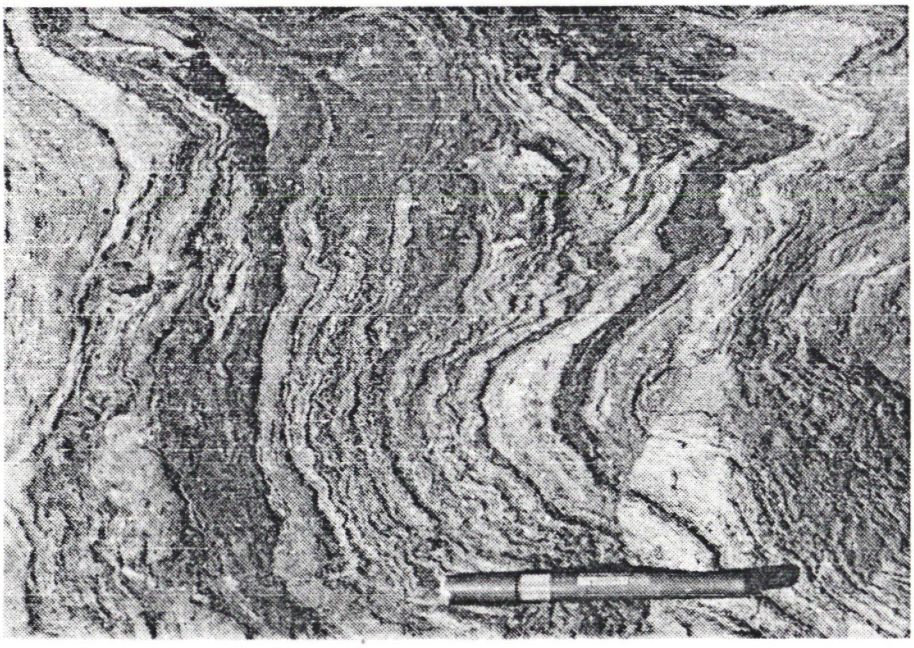

Fig. 24. Highly deformed rauhaugite where the altered fenite inclusions have been transformed into concordant ultramafic layers.

Olivine-bearing søvite is found as relatively narrow (< 0.2m) conformable layers in thick søvite sheets, and is often associated with skeletal magnetite.

5.4.2.2. *Silico-søvite*

The silico søvite is in this work defined as a rock with 25 to 50% silicate minerals in carbonate (calcite dominated) matrix. The silico-søvite appears as a strongly foliated, inhomogeneous rock, often with fenite and ultramafic inclusions varying from 10 to 100 cm in diameter (fig. 22). The silicates are mainly phlogopite and alkali amphibole. Both amphibole and phlogopite are zoned: the phlogopite in places has a green, normally pleochroic core overgrown with a reddish brown, reversely pleochroic rim, while the amphibole may have a colourless core (richterite) and a bluish-green rim (magnesio-arfvedsonite). Adjacent to large ultramafic bodies, the silico søvite may consist of coarse-grained diopside rimmed by hornblende or of coarse-grained hornblende in a søvitic matrix.

The silico-søvite has an elevated apatite content relative to the søvite (average) and the apatite appears as medium- to coarse-grained resorbed crystals. Large apatite crystals may have a prismatic shape. On a large scale the silico søvite forms a transitional contact from the søvite into the fenite and the ultramafic rocks with increasing contents of fenite inclusions or ultramafic inclusions and layers, repectively.

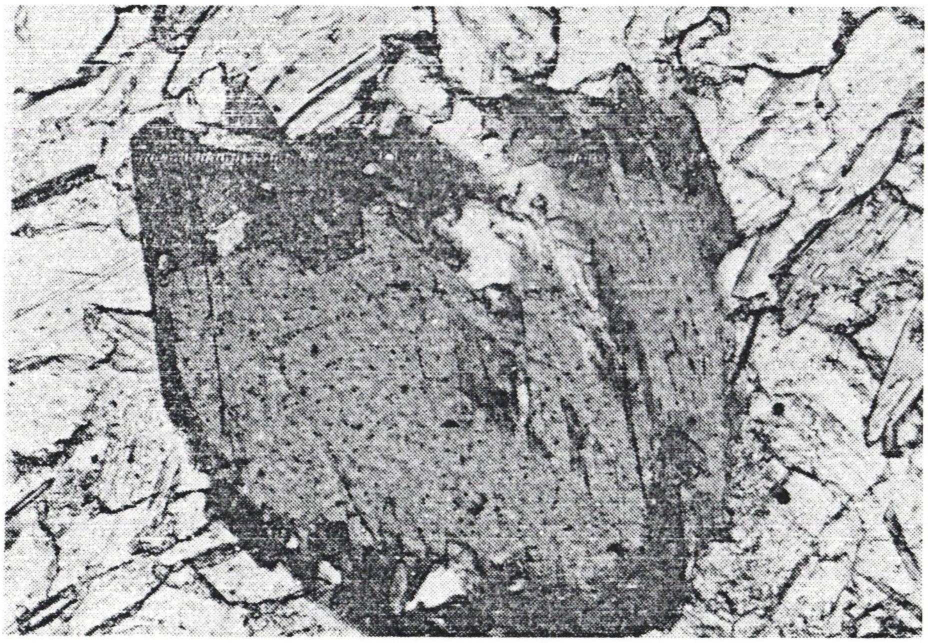

Fig. 25. Zoned amphibole with a light richterite core and dark arfvedsonite rim. Silico søvite. The microphotograph is 0.2 mm. GGU 224853.

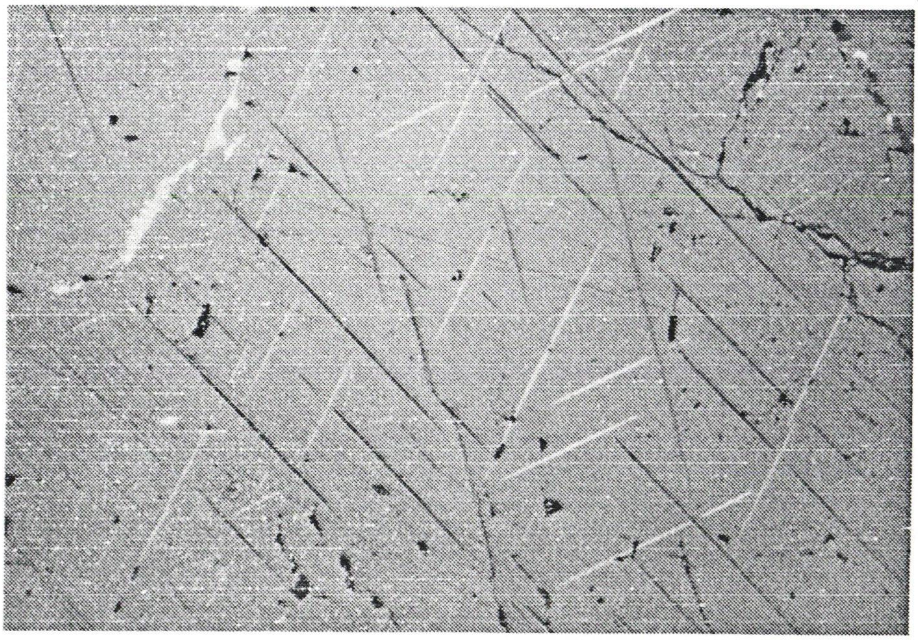

Fig. 26. Magnetite with ilmenite exsolution lamellae Glimmerite. The microphotograph is 0.5 mm vertically, polished section, reflected light, crossed Nicols (80°). GGU 223817.

5.4.2.3. *Rauhaugite*

The rauhaugite appears typically as a brownish weathering fine- to medium-grained rock consisting of dolomite, alkali amphibole and phlogopite with coarse apatite crystals and magnetite grains. The rauhaugite forms sheets that are generally thinner than the søvite, and contain a higher portion of fenite inclusions. The rauhaugite forms a braided pattern between the fenite inclusions (fig. 23) or forms 5 to 50 cm thick veins within the fenite. Locally the rauhaugite is highly deformed and appears as a highly deformed heterogeneous rock with silicic layers (deformed fenite inclusions and their ultramafic rims), minor søvite layers and rauhaugite layers (fig. 24). The rauhaugite is often found along strike of major søvite sheets.

The *dolomite* is fine- to medium-grained (0.02 - 0.05 mm), subhedral and may contain calcite inclusions.

The *apatite* is very similar to the apatite in the søvite and silico-søvite. Locally a zoning of alternating clear and light brown zones (probably due to submicroscopic fluid inclusions) is seen, and fluid inclusions parallel to the C-axis are abundant. The apatite often forms a mineral lineation parallel to fold axes in the rauhaugite.

The *amphibole* forms fine- to medium-grained, euhedral, zoned crystals with light green to light olive (pleochroic) richterite core and bluish to brown (pleochroic) arfvedsonite rim (fig. 25). Twinning parallel to the long diagonal is abundant.

The *phlogopite* forms coarse, sub- to euhedral, reversely pleochroitic, redbrown, zoned tetraferriphlogopite crystals.

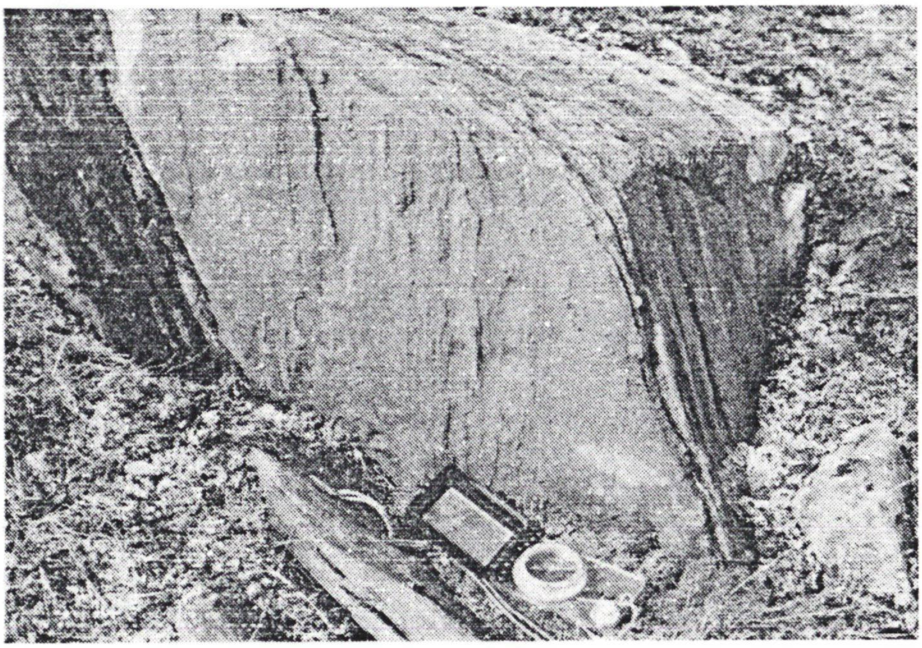

Fig. 27. Highly strained, fine-grained rauhaugite with steeply dipping lineation.

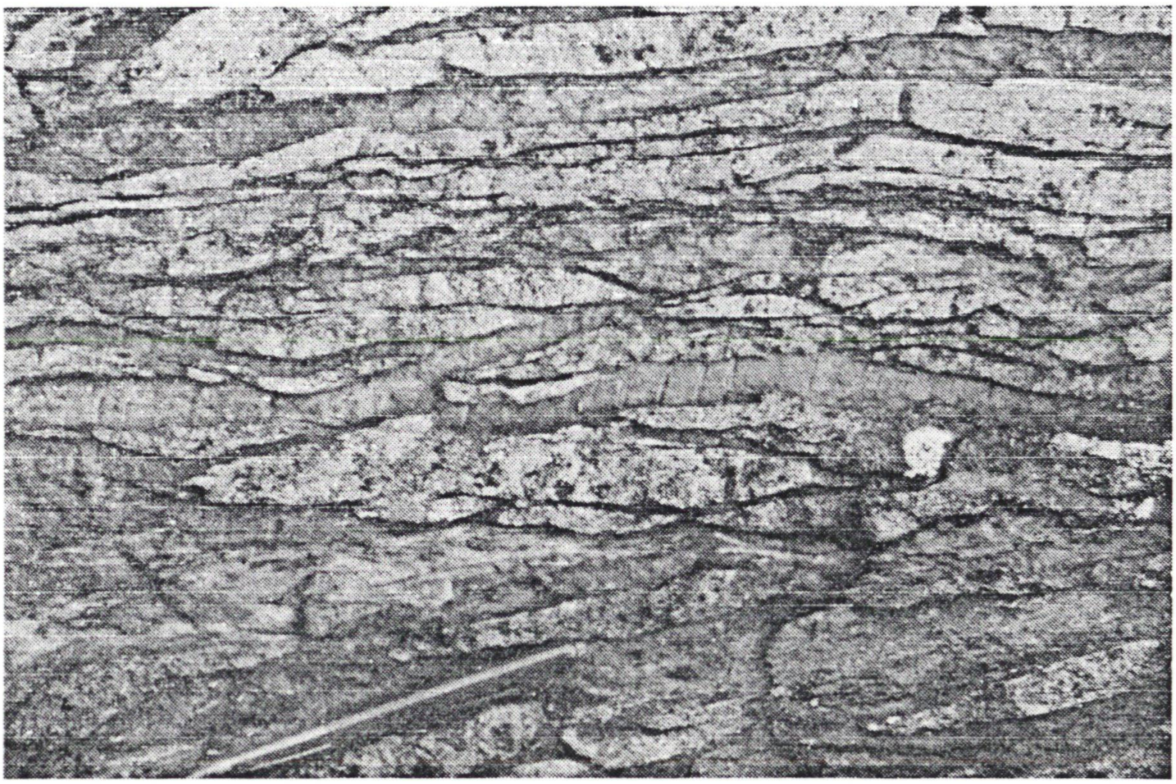

Fig. 28. Fine-grained rauhaugite in a braided pattern between fenite "inclusions". The carbonatite contains isoclinal folds (above the pencil).

The *magnetite* forms large poikilitic grains with ilmenite exsolution lamellae and inclusions of all the other minerals (fig. 26).

The rauhaugite is foliated with parallel arrangement of dolomite, amphibole, apatite and phlogopite. The rauhaugite contains clusters of fibrous amphibole together with redbrown very fine-grained mica and magnetite, often in silicate-rich layers in the rauhaugite. These clusters resemble the altered olivine in the søvite and may indicated that olivine was a primary mineral in the rauhaugite.

5.4.2.4. *Highly deformed rauhaugite*

The rocks located near the outer margin of the fenite-carbonatite are generally highly strained (fig. 27) with steeply outwards dipping foliation and crenulation lineation. The fenites are strongly deformed, but the carbonatites are even more deformed and very fine-grained (1 - 100μ). The dominating carbonate is iron-rich dolomite, which together with very fine-grained silicate (mica?) constitute the matrix of the rock.

The foliated and lineated appearance (fig. 27) is caused by highly strained and corroded fenite inclusions. Where quartz is present this is preferentially corroded by dolomite, and where K-feldspar is present, e.g. in antiperthite, the K-feldspar is preferentially corroded by dolomite relative to the plagioclase. The plagioclase is heavily sericitised and rich in carbonate inclusions, except in the rim, where a fresh albite is found. Plagioclase is often found as rounded xenocrysts with slightly bended albite lamellae. The carbonate is directly corrosive in the fenite inclusions, whereas the contact between carbonatite and

Fig. 29. Beforsite rich in angular basement and fenite fragments.

fenite is transitional via an ultramafic rim in the søvite and in the coarser rauhaugites.

The shape of the deformed fenite inclusions indicates that the deformation has been plastic.

Apatite is found as tiny needles in the groundmass, and in the few slightly coarser crystals a rounded core overgrown with an euhedral rim may be seen. Rounded medium-grained apatite is found, too.

In small cavities dolomite has crystalled with successively more iron-rich composition, indicating iron enrichment in the late fluids. Finally an unidentified zeolite mineral is seen in cavities.

5.4.2.5. *Beforsite*

Beforsite occurs both as subcircular intrusions (vents) associated with the radiating radioactive shear zones, and as narrow (5 to 30 cm thick) dykes, generally striking parallel to the outline of the complex and steeply dipping (often towards the core)(fig. 5).

The beforsite is easily recognisable on its orange-brown appr. 1 cm thick weathering crust and high (Th) radioactivity (Secher, 1980). The beforsite is always located outside the fenite/carbonatite part of the complex, in the altered basement. The beforsite is associated with a high frequency of ankerite veins, ankerite-calcite veins and an increase of alteration of the basement.

The beforsite consists of a very fine-grained groundmass of carbonate (ankerite to dolomite) and mica(?), with 10 to 50% subangular to rounded fenite and basement inclusions (fig.- 29). The inclusions are slightly corroded along the margin, but differ from the inclusions in the mylonite

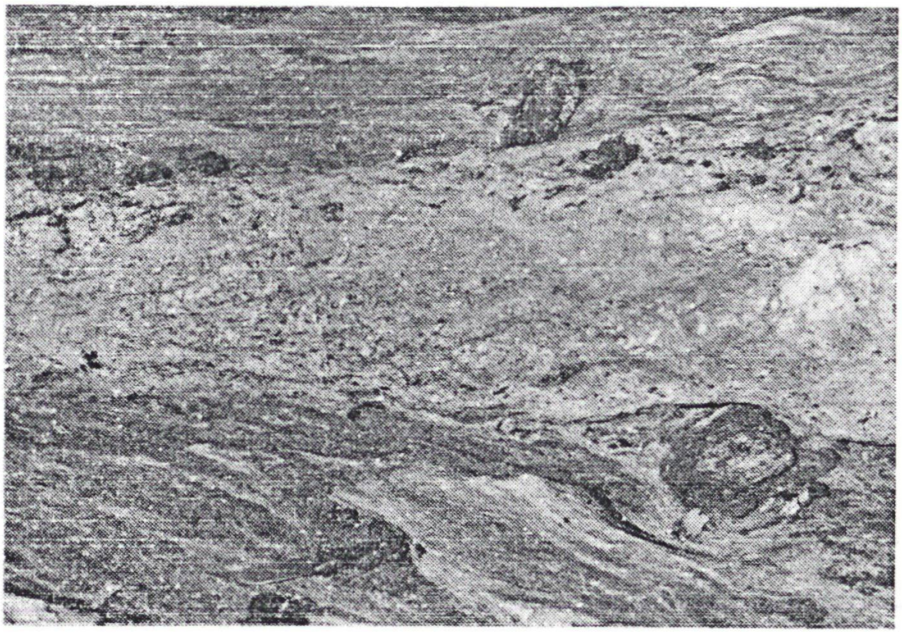

Fig. 30. Late søvite with coarse calcite, cutting silico carbonatite. Notice the fenite inclusion with thick ultramafic alteration rim.

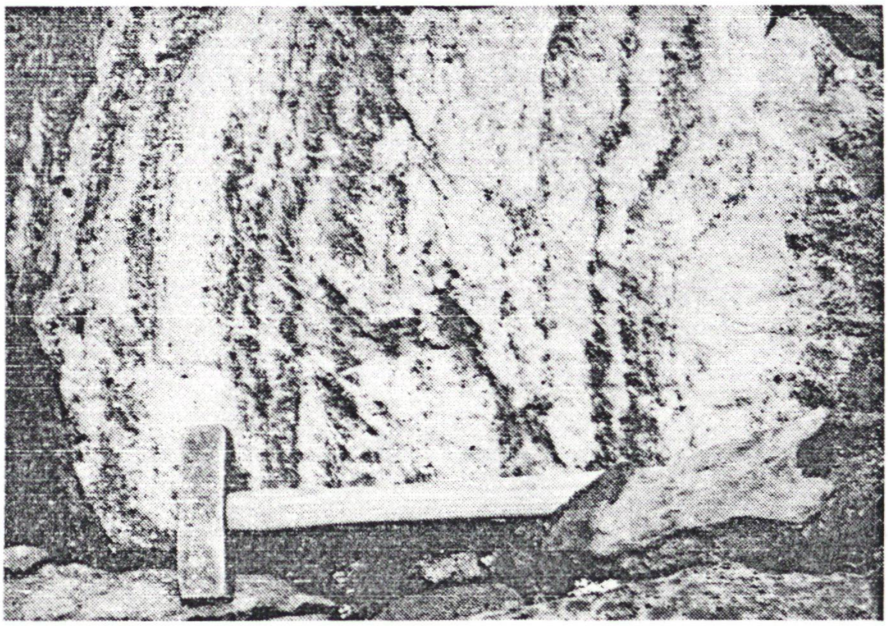

Fig. 31. Late søvite with alternating calcite and phlogopite-rich layers and coarse platy calcite. Slightly deformed.

in that they has not been plastically deformed.

Several generations of beforsite can locally be observed.

5.4.2.6. *Ankerite veins*

The ankerite veins differ from the beforsites in their lack of basement inclusions, their slightly coarser nature and frequent content of calcite which locally forms a rhytmical interlamination with the ankerite. In these layered veins carbonate crystals are oriented perpendicular to the vein. The ankerite veins are Th radioactive and have high contents of lanthanides. Ancylite may be seen as light specks in this brown rock. Further pyrrhotite and pyrite are found.

5.4.2.7. *Late søvite*

The late søvite occurs as 0.1 to 10 m thick sheets which are characterised by large platy calcite crystals. The late søvite consists of calcite, phlogopite, alkali amphibole, apatite and magnetite. Pyrochlore, zircon and pyrrhotite locally occur in large quantities. Dolomite and ancylite are found as inclusions in calcite. The late søvite often shows a repeated layering parallel to the sheet, with varying proportions of minerals (fig. 31). Locally the magnetite and apatite is dominating the rock and up to 10 m thick sheets of magnetite-apatite-pyrochlore-rich rock is found.

The *phlogopite* is coarse-grained, zoned tetraferri phlogopite.

The *amphibole* is colourless richterite, generally fine-grained to fibrous.

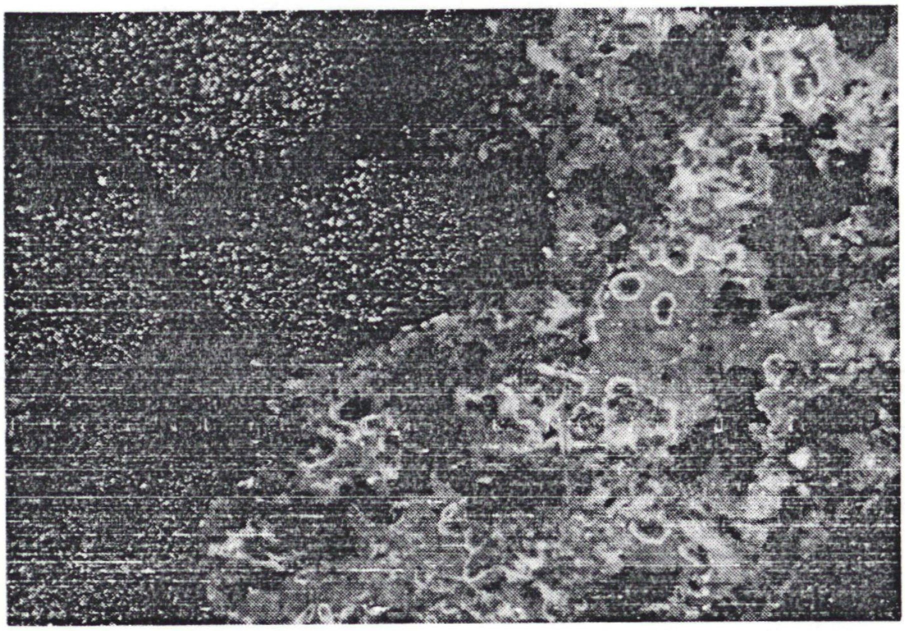

Fig. 32. Lanthanide-rich carbonatite composed of dolomite (black with white dots of calcite exolution blebs), zoned calcite (black to white due to outwards increase in Mn) and quartz (grey). The microphotograph is 2 mm vertically, cathodoluminescence. GGU 320443.

The *apatite* is generally found as rounded aggregates of acicular apatite crystals. In most late søvites the apatite aggregates consist of extremely fine-grained, acicular apatite in a fan pattern similar to what is described by Brögger (1921, p. 239) from the Fen Carbonatite Complex. These aggregates are in places concentrated to form an almost pure apatite rock. In other late søvites the apatite forms aggregates of radiating acicular apatite.

The *magnetite* forms large poikilitic grains with inclusions of apatite, amphibole and phlogopite. Almost massive accumulations of magnetite are locally found.

The *calcite* forms generally large platy crystals, which may be zoned both with respect to inclusions (of small dolomite exsolution blebs) and iron content. Where the late søvite is undeformed the calcite blades are perpendicular to the sheet orientation. Where deformed this calcite is characterised by abundant deformation twinning.

The *pyrochlore* is found as euhedral medium- to coarse-grained, zoned crystals often rich in fibrous amphibole and locally apatite inclusions. Both apatite and amphibole inclusions radiate from the centre of the pyrochlore. The pyrochlore is often zoned pale-brown to dark brown, and locally a brown, metamict, round core can be observed. This is the case in the northern late søvite, which can be traced with scintillometer due to the high uranium content. The late søvite is locally associated with pyrochlore enrichment of glimmerite wall rock. The *zircon* is found as euhedral crystals in the magnetite-apatite-pyrochlore-rich rock.

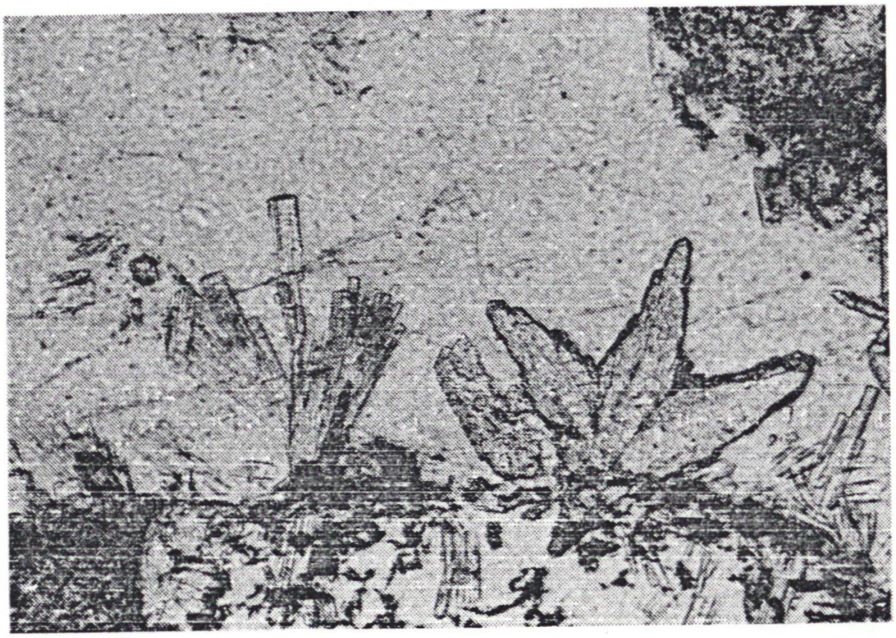

Fig. 33. Huanghoite (right) and strontianite (left) in quartz. Lanthanide-rich carbonatite vein. The microphotograph is 0.2 mm vertically. GGU 320160

5.4.2.8. *Lanthanide-rich carbonatite*

The lanthanide-rich carbonatite is found as veins varying in thickness from a few milimetres up to 4 metres, and they can be followed up to 100 m along strike. They are mainly localised in the core of the complex, although lanthanide enrichment has also been observed in the ankerite veins in the rim of the complex. The lanthanide-rich carbonatite is radioactive (mainly Th) and can be mapped with scintillometer beneath thin overburden.

The larger veins generally follow the two major trend directions parallel to the outline of the complex.

The lanthanide-rich carbonatites consist of calcite, dolomite, baryte, strontianite, quartz and aggregates of intergrown alstonite (Sr-Ba carbonate) and ancylite (Sr-lanthanide carbonate). Further huanghoite (Ba-lanthanide carbonate) (fig. 33) and burbankite (Na-,Ca-lanthanide carbonate) occur. The lanthanide-rich carbonatite further contains pyrrhotite, pyrite, chalcopyrite and minor hematite, galena and sphalerite. The sulphides are often concentrated near the margin of the veins. The calcite forms coarse fan-shaped crystals and aggregates of crystals up to 10 cm long, a size which also the alstonite-ancylite aggregates can reach.

Where carbonatite is cut by lanthanide-rich veins the carbonatite is stained red, the amount of exsolution blebs of dolomite in calcite increases, grain size decreases and magnetite is altered to pyrite or pyrrhotite.

The lanthanide-rich carbonatite veins are very often associated with apatite, pyrochlore and zircon mineralisation of the wall rock where this

TABLE 3

WHOLE ROCK ANALYSES OF TYPICAL ROCKS FROM QAQARSSUK

	320421	320424	320157
SiO_2	2.72	46.59	2.66
TiO_2	.15	.30	.11
Al_2O_3	.05	11.32	.57
Fe_2O_3	2.09	3.36	2.42
FeO	6.13	2.73	1.86
MnO	.37	.23	.38
MgO	14.73	5.22	2.42
CaO	30.86	8.67	47.62
Na_2O	.42	8.37	.20
K_2O	.08	.78	.50
Volatiles	37.86	10.29	36.10
P_2O_5	4.04	.85	2.82
Total	99.50	98.71	97.66

	320193	320172	320494	320437
SiO_2	35.01	13.37	7.14	6.90
TiO_2	.46	.29	.20	1.23
Al_2O_3	7.00	2.39	1.71	.42
Fe_2O_3	2.08	2.90	.40	32.35
FeO	6.65	4.07	2.41	16.52
MnO	.18	.21	.20	.14
MgO	13.36	8.13	3.83	2.56
CaO	15.35	34.75	44.85	13.87
Na2O	2.40	.65	.22	1.87
K_2O	3.70	2.24	1.47	.37
Volatile	8.97	26.19	36.62	.68
P_2O_5	2.66	3.74	.01	8.92
Total	97.82	98.93	99.06	85.83

320421	Rauhaugite
320424	Fenite (in rauhaugite)
320157	Søvite
320193	Hornblendite
320172	Silico-carbonatite
320494	Late søvite
320437	Apatite-magnetite-pyrochlore rock

is glimmerite, - the wall rock is then altered from black to brown glimmerite due to introduction of a tetraferri phlogopite rim on the phlogopite of the glimmerite.

5.4.2.5. *Lamprophyre*

In the northern part of the complex, a suite of 30 to 150 cm thick lamprophyre dykes were found striking perpendicular to the layering in the carbonatite and fenite, and dipping towards east. The lamprophyre dykes consist of more than 50% rounded inclusions of the various rocks in the complex ranging in size from 0.1 to 10 cm. The matrix is very fine-grained and consists of carbonate and mica. Further, apatite clinopyroxene, magnetite, hornblende and zoned phlogopite crystals are found in the matrix. Phlogopite phenocrysts in the lamprophyre are found to have the same age as the other rocks dated from the complex (Larsen et al., 1983).

5.5. GEOCHEMISTRY

5.5.1. *Distribution of phosphate*

The distribution of phosphate in the different rock types in Qaqarssuk is seen on fig. 34 and fig. 35.

The majority of rocks has less than 1% P_2O_5 with concentrations of individual samples ranging from 0.0 to 39 wt% P_2O_5 (pure apatite) (fig. 35).

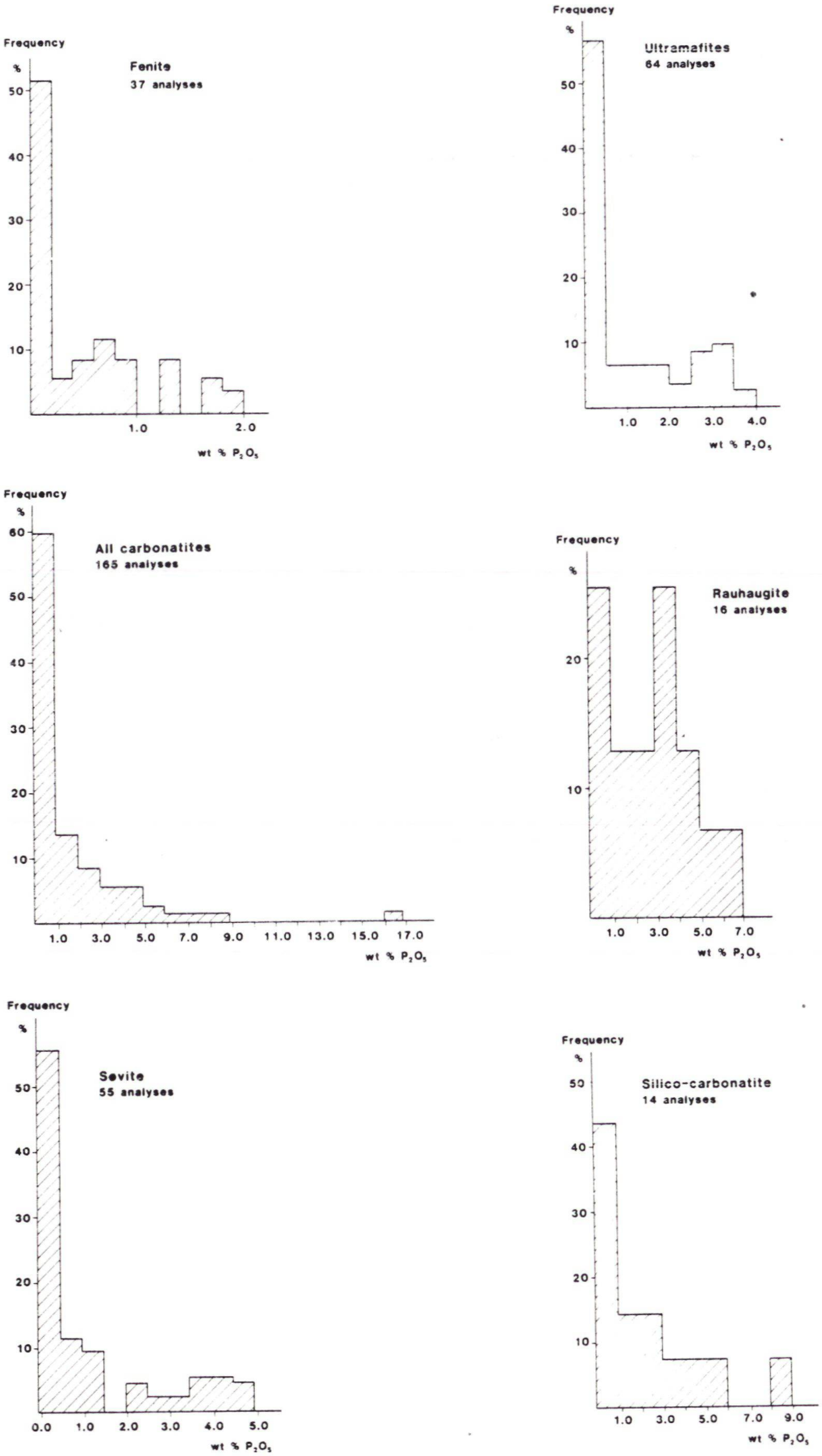

Fig. 34. Phosphorous distribution in rocks from Qaqarssuk (based on grab samples)

Fenite and ultramafic rocks

The phosphate analyses in *fenites* can roughly be divided into two populations - one with a phosphate content less than 0.2 wt% P_2O_5, and one with from 0.4 to 2% P_2O_5. The phosphate in these fenites is found as apatite crystals in veins together with carbonate, - and also as fine-grained, euhedral apatite crystals disseminated in the fenite.

The *ultramafic* rocks show a somewhat similar distribution, with a large population with less than 0.5 wt% P_2O_5 and a population with a normal distribution around 3 wt% P_2O_5. The apatite is either found together with calcite in the matrix between coarse-grained pyroxene, amphibole or biotite/phlogopite crystals, or enclosed in the silicate minerals.

Carbonatites

The major part of the carbonatites has less than 1 wt% P_2O_5. There is a smooth, skew frequency distribution of up to 9 wt% P_2O_5. The average content is 1.37 wt% P_2O_5, and the phosphate is found in rounded, medium- to coarse-grained apatite crystals, except in the late søvite where the apatite forms aggregates of acicular crystals.

The *søvite* has on average 1.03 wt% P_2O_5 and the phosphate analyses of the søvite can be divided into two populations: One consisting of pure søvite with P_2O_5 less than 1.5 wt% and one with 2 to 5 wt% P_2O_5. The latter consists of both "pure" søvite and søvite with a fairly large content of phlogopite/biotite, and hence transitional into

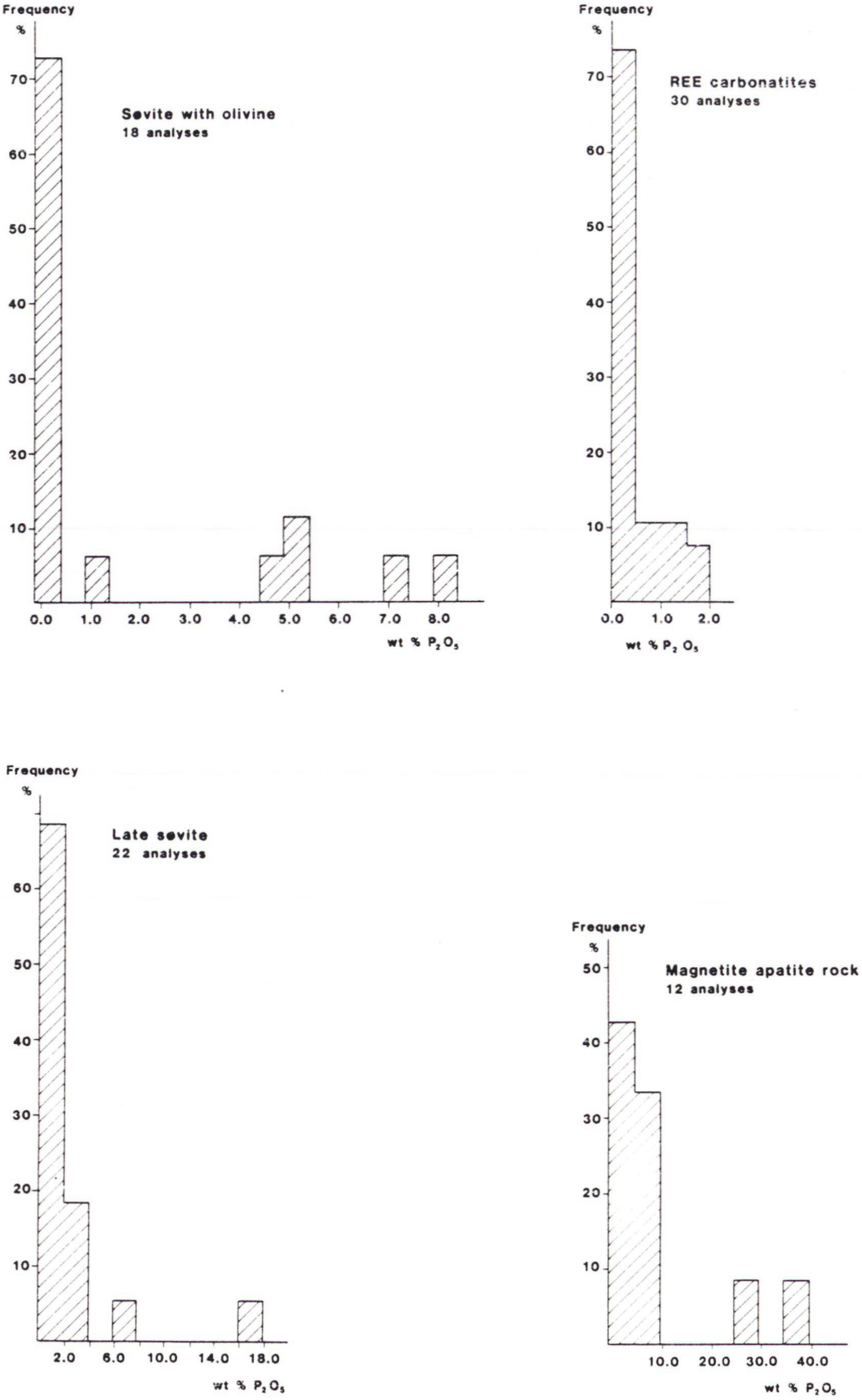

Fig. 35. Phosphorous distribution in rocks from Qaqarssuk
(based on grab samples)

the silico-carbonatites. The *søvite with olivine* associated with the søvite is either devoid in apatite or rich in apatite.

The *silico-carbonatite* contains on average 2.18 wt% P_2O_5, which is well over the average Qaqarssuk carbonatite.

The *rauhaugite* analyses has of average 2.66 wt% P_2O_5. The frequency distribution shows two overlapping populations, one skew with little phosphate and one approaching normal distribution around 3.5 wt% P_2O_5.

The *late søvite* contains on average 0.2% P_2O_5. It generally has a low apatite content, but the rock type is associated with the apatite-rich apatite-magnetite-pyrochlore-rich rock. The apatite in the late søvite as well as in the apatite-magnetite-pyrochlore-rich rock is generally found as rounded aggregates of acicular grains.

The *lanthanide-rich carbonatite* has on average less than 0.2 wt% P_2O_5.

5.5.2. *Lanthanides*

Carbonatites as well as ultramafic rocks and fenites show enrichment in the light lanthanides, and these rocks have smooth lanthanide distribution curves when normalised relative to chondrite. No Eu anomalies are found, but almost all rock types have a small negative Ce anomaly (fig. 36).

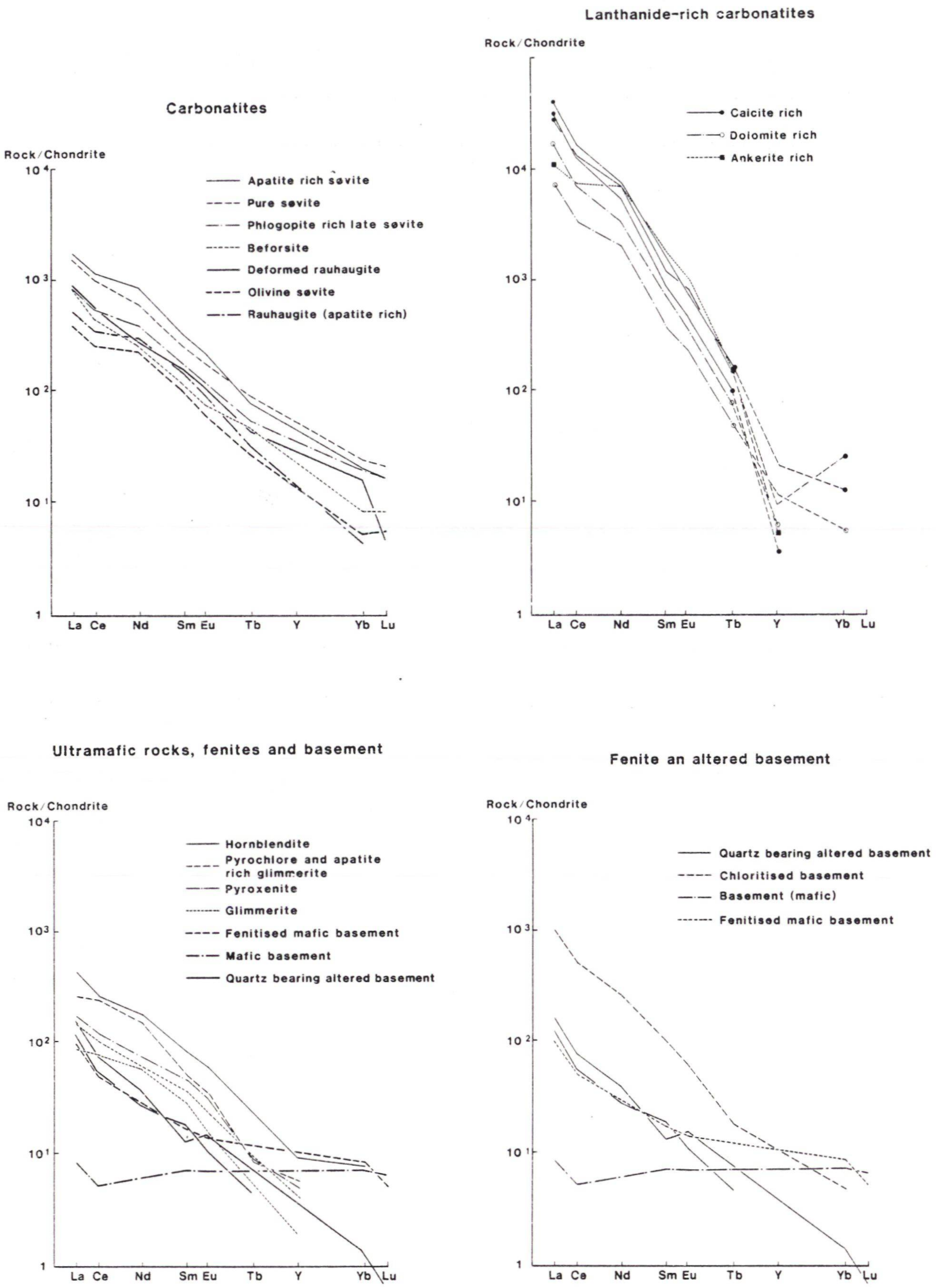

Analysed with INAA exept Y,
which is analysed with XRF

Fig. 36.

5.5.2.1. *Søvite and rauhaugite*

The lanthanide concentration increases from the olivine-søvite and rauhaugite to the søvite and silico-søvite, with constant slope of the curve (fig. 36) and constant La/Yb ratio. Apatite-rich rauhaugite and søvite have higher lanthanide contents relative to their apatite-poor counterparts. The lanthanides are concentrated in apatite, and ancylite, and locally in huanghoite, whereas the content in the carbonates is low.

5.5.2.2. *Lanthanide-rich carbonatites*

The concentration of light lanthanides is appr. ten times 10 higher than in the søvite, whereas the concentration of heavy lanthanides is similar to or even lower than in the other carbonatites, and consequently is the La/Yb ratio is much higher. The lanthanides are localised in the mineral ancylite with subordinate amounts in huanghoite, burbankite, alstenite, calcite and dolomite.

5.5.2.3. *Ultramafic rocks and fenite*

The mafic basement has a flat lanthanide distribution curve (around ten times chondrite) in contrast to fractionated felsic basement. The fenitisation of the basement is seen as an increase in the light lanthanide concentrations, whereas the heavy lanthanides are almost unaffected, and the felsic fenites can be recognised from the mafic fenite on their lower content of heavy lanthanides.

Ultramafic rocks often have a kink on the curve around Tb or Y from the steep slope in the light end to a more flat in the heavy lanthanide end. Some glimmerites have an upwards concave light lanthanide distribution curve.

5.5.2.4. *Interpretation of the lanthanide distribution*

- The rauhaugite and the olivine-søvite represent "primitive" carbonatites relative to (olivine-free) søvite, silico-søvite and late søvite.
- The general increase in lanthanide concentration from olivine-søvite and rauhaugite to søvite and late søvite is interpreted as due to precipitation of phases with low lanthanide content as dolomite, calcite, silicates and magnetite - and to loss of e.g. Mg^{+2} and CO_3^{2-} by metasomatism.
- The lanthanide-rich carbonatites with their discordant relations to the other carbonatites are regarded as the most evolved carbonatites. They probably represent a late residual fluid/liquid containing the most incompatible elements. The higher La/Yb ratio indicates that the intermediate and heavy lanthanides have been preferentially precipitated elsewhere. The lanthanide-rich carbonatites are often associated with apatite-pyrochlore-zircon mineralisation of the wall rock. The loss of intermediate and heavy lanthanides is explained by their increasing mobility with increasing field-strength (valency/ ionic radius), and hence these are likely to migrate into the wall

rock. Here they were precipitated in apatite and pyrochlore (the intermediate lanthanides and zircon (the heavy lanthanides).

- Increase in light lanthanides in fenites and ultramafic rocks shows that the lanthanides are mobile.
- The hornblendite can be recognised as altered mafic basement on the kink of the lanthanide distribution pattern (high inherent concentrations of heavy lanthanides relative to rocks derived from felsic basement with low initial heavy lanthanide content).
- The negative Ce anomaly could indicate that the carbonatite has been subjected to oxidising conditions prior to the intrusion. Such an oxidising event would increase the valency from Ce^{3+} to Ce^{4+}, and Ce^{4+} would be preferentially precipitated relative to the trivalent lanthanides.

5.5.3. *Other trace elements*

Th, Zn, Pb and Cu are enriched in the lanthanide-rich carbonatites, and these elements probably acted as incompatible elements during the evolution of the carbonatite.

Both the Sr and Ba concentration increases from rauhaugite over søvite and late søvite to the lanthanide-rich carbonatites indicating that these elements are concentrated in the residual melt/fluid. The Sr/Ba ratio is 4 to 8 in the rauhaugite and søvite and decreases to less than 1 on average in the lanthanide-rich carbonatites, indicating that Ba is less compatible than Sr.

In the fenites Sr and Ba concentrations are strongly elevated compared to the basement rocks, and the Sr/Ba ratio is considerably lower

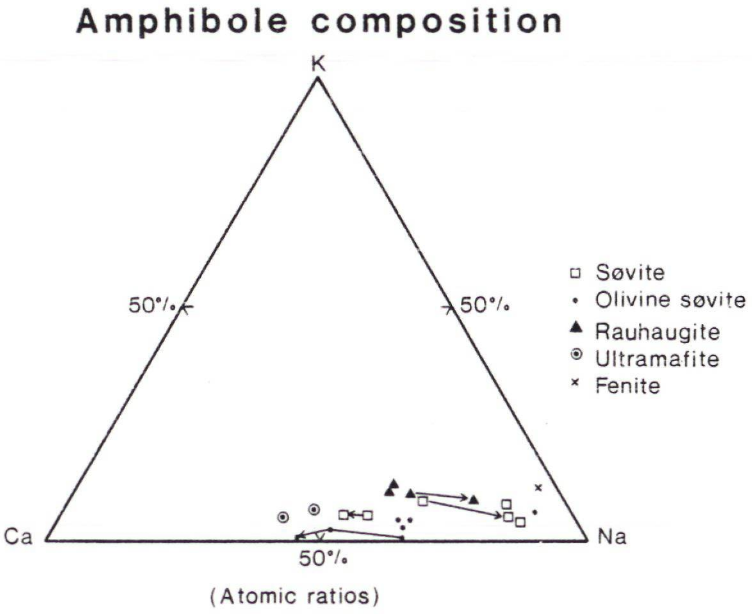
Amphibole composition
K
50°/.
50°/.
Ca
Na
50°/.
(Atomic ratios)
□ Søvite
• Olivine søvite
▲ Rauhaugite
◉ Ultramafite
× Fenite

Fig. 37

than in the adjacent carbonatites, indicating that Ba was more mobile than Sr.

Nb and Zr in concentration are high in late søvites, magnetite-apatite-pyrochlore-rich rocks and in metasomatic rocks adjacent to the late søvites and the lanthanide-rich carbonatites.

5.6. MINERAL CHEMISTRY AND EVOLUTION

5.6.1. *Silicates*

5.6.1.1. *Amphiboles*

The amphiboles fall in several groups:

1. The hornblendes occurring in the altered mafic basement, ultramafite and some silico-carbonatites.
2. The alkali amphiboles occurring in the fenite and in the carbonatites.
3. The fibrous orthoamphiboles found as alteration products of olivine.

The *hornblende* occurs as rims on pyroxene and as euhedral crystals. The hornblende is often zoned in silico-carbonatite and ranges in composition from edenitic hornblende to magnesian hastingsitic hornblende, where found in silico-carbonatite (no hornblende from altered mafic basement has been analysed).

The *alkali amphiboles* occur as fineto medium-grained, euhedral slender needles or as fibrous amphibole. The crystals are generally zoned

Fig. 38. Skeletal olivine crystals. Notice the abundant dolomite exolution blebs in the enclosed calcite. Olivine søvite. The microphotograph is 0.5 mm vertically. GGU 320168.

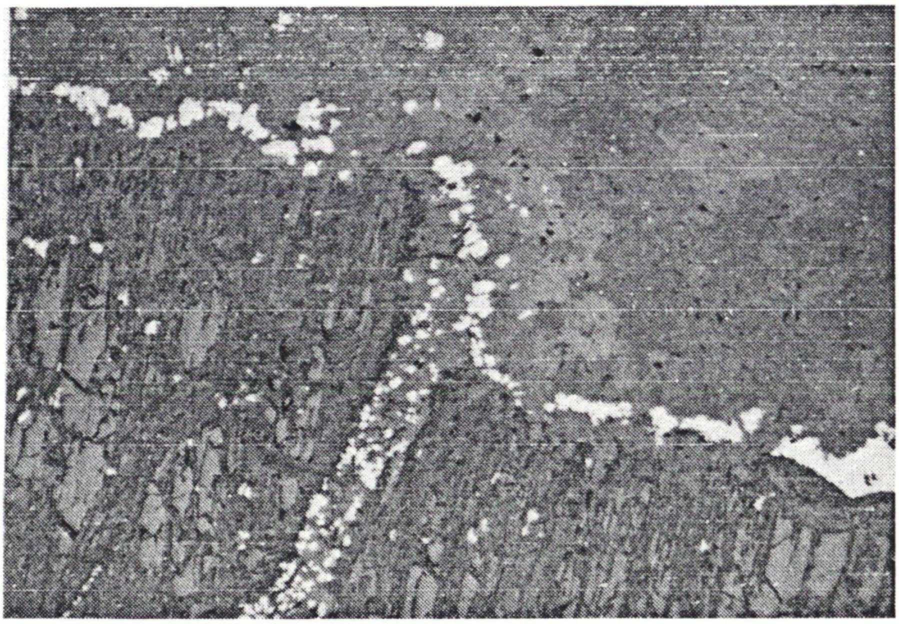

Fig. 39. Altered olivine with fine-grained magnetite along the former rim and along a crack. The microphotograph is 0.2 mm vertically, reflected light. GGU 320138.

with a colourless to pleochroic core (light brown green to green) and a pleochroic rim (green to blue) with a lower interference colour. This is chemically expressed by outwards increase in Fe and Na and decrease in Mg, Ca and K (fig. 37) and generally a transition from richterite in the core to magnesio-arfvedsonite in the rim.

5.6.1.2. *Mica*

Phlogopite is - by far - the dominant mica in the complex, and no biotite has been found. (Phlogopite is here defined as having Mg/Fe > 2 (atomic ratio).

Most phlogopite is normally pleochroic green to olive, but often zoned with a brown rim - often with reversed pleochroism.

In the carbonatites this reversely pleochroitic (brown to red) phlogopite is the type usually identified as *tetraferri-phlogopite*. The zoned phlogopite has outwards decrease in Al, Ti and Mg and an increase in Fe. The decrease in Al causes a lack of Al and Si in the tetrahedral site, which in the tetraferri-phlogopite variety is filled up with Fe^{3+}. Very fine-grained, red tetraferri-phlogopite is also seen as aggregates pseudomorphic after olivine, and in symplectite-like textures with calcite.

5.6.1.3. *Olivine*

The olivine is found as coarse, anhedral grains in the olivine magnetite rock. In søvite the olivine is found as euhedral crystals, or

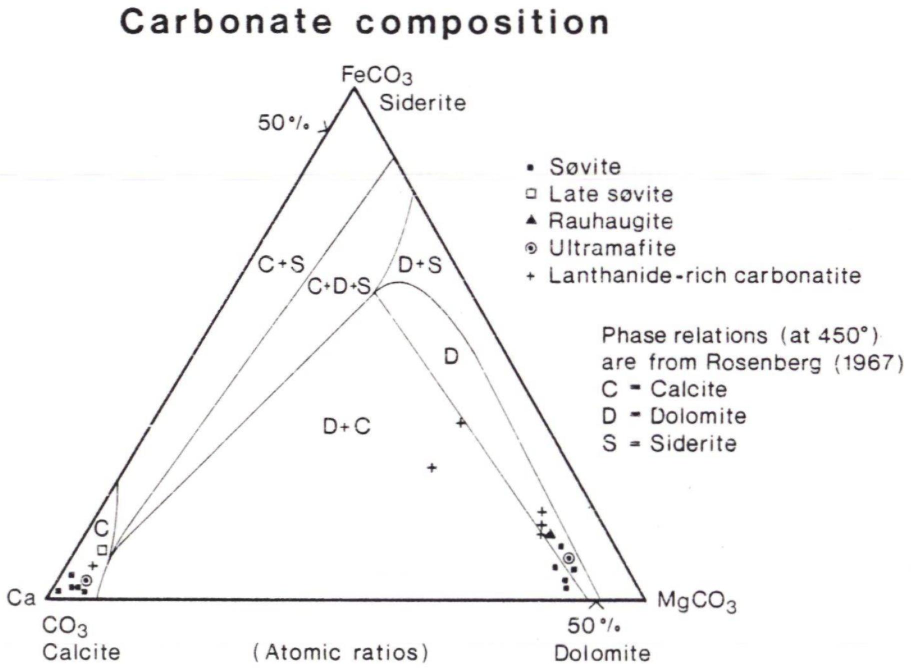

Carbonate composition

Fig. 40.

as hollow or skeletal crystals (fig. 38). Pseudomorphosed olivine may be recognised by magnetite rims, outlining the ghost shape of euhedral olivine (fig. 39).

Whatever morphology the olivine is found with, the composition is constant with a forsterite content from 78 to 80%.

5.6.2. *Carbonates*

5.6.2.1. *Ca, Mg and Fe carbonate*

In the søvite and the rauhaugite the carbonates have a rather uniform composition (fig. .40). The calcite is almost pure, but with slightly higher Mg and Fe in the late søvite. The dolomite generally has higher iron content than the calcite, and the iron content in the dolomite increases, the more peripherally in the complex the dolomite is situated, and the later the dolomite is formed. Ankerite (dolomite with more than 10 mol% siderite) is the dominating carbonate in many veins in the altered basement. Siderite is found 10 km from the core of the complex situated in highly altered basement. The Fe/Mn ratio is about 2 in the calcite, whereas the dolomite in the rauhaugite has Fe/Mn ratios from 8 to 20, and the dolomite in late lanthanide-rich veins has Fe/Mn ratios around 4.

The amount of Ca and Mg which can be dissolved in dolomite and calcite, respectively, decreases with decreasing temperature. The exsolution blebs in the carbonates hence indicate that the carbonates were formed at higher temperatures, and that dolomite exsolved calcite

TABLE 5

LANTHANIDE-, Sr- AND Ba-RICH CARBONATES

	Ancylite				Huanghoite		
GGU	320031	320149	320443	252561	320149	320160	320411
F	ud	ud	ud	.3	ud	3.25	3.36
Na_2O	ud	0.1	ud	.03	0.7	-	-
SiO_2	ud	-	ud	-	ud	0.2	0.1
CaO	ud	1.4	ud	2.9	1.2	3.4	3.7
SrO	14.8	16.6	14.78	21.0	3.4	5.1	2.4
BaO	0.8	0.3	2.09	ud	28.0	32.2	30.0
La_2O3	15.8	13.6	15.4	20.2	11.5	11.0	15.9
Ce_2O3	25.2	23.0	26.6	20.8	14.6	18.3	18.8
Pr_2O_3	2.05	ud	1.83	ud	ud	ud	ud
Nd_2O_3	6.8	6.3	5.04	3.3	5.1	4.3	4.5
Sm_2O_3	0.7	ud	.35	ud	ud	ud	ud
Y_2O_3	0.02	ud	-	-	ud	0.15	-
Total	66.17	61.3	66.09	68.53	64.5	77.9	78.76

	Burbankite	Strontianite to alstonite				
GGU	252561	320160	320411	252561	320149	320141
F	.17	0.06	-	-	ud	ud
Na_2O	7.41	0.08	-	0.1	0.7	0.8
SiO_2	-	0.1	-	0.05	ud	ud
CaO	14.4	4.08	2.6	15.1	13.0	16.4
SrO	17.7	56.4	52.0	29.3	18.2	5.0
BaO	8.1	5.6	11.0	29.7	38.8	48.6
La_2O_3	7.2	ud	0.4	ud	0.1	-
Ce_2O_3	9.3	ud	ud	ud	0.3	-
Pr_2O_3	0.5	ud	ud	ud	ud	ud
Nd_2O_3	1.2	ud	ud	ud	0.3	0.4
Sm_2O_3	0.1	ud	ud	ud	ud	ud
Y_2O_3	0.03	ud	ud	ud	ud	ud
Total	66.11	66.32	66.0	74.25	71.4	71.2

GGU	Rock type
252561	Lanthanide-rich carbonatite
320031	Mafic fenite
320141	Rauhaugite
320149	Lanthanide-rich carbonatite
320160	Lanthanide-rich carbonatite
320411	Rauhaugite
320443	Lanthanide-rich carbonatite

ud: undetermined

and vice versa at decreasing temperature. In the coarse and deformed carbonatites no exsolution blebs are seen, and the carbonates are interpreted as recrystallised at relatively low temperatures during the deformation of the rock.

The amount of dolomite blebs in calcite enclosed in hollow olivine is appr. 20%, which is equivalent to the Mg content of a calcite formed at appr. 700° C. (Rosenberg, 1967).

5.6.2.2. *Lanthanide-, Ba- and Sr-rich carbonates*

Ancylite $Sr(La,Ce,Nd)(CO_3)_2(OH)H_2O$ is by far the most dominating lanthanide-rich carbonate mineral. Ancylite is concentrated in the late lanthanide-rich carbonatite veins where it is intimately intergrown with *alstonite* $CaBa(CO_3)_2$. Small amounts of ancylite are also found disseminated in the silico-søvite, the rauhaugite and as exsolutions in calcite in some late søvites. The alstonite and ancylite are identified with X-ray diffraction (XRD) and microprobe analysis (Table 5).

Huanghoite $Ba(La,Ce,Nd)(CO_3)_2F$ is found as a common accessory mineral in the lanthanide-rich carbonatite veins, but minor amounts are found in søvite and rauhaugite. Identified with microprobe analysis. (Table 5).

Burbankite $(Na,Ca)_3(Ca,Sr,Ba,La,Ce,Nd)_3(CO_3)_5$ was found at one locality as aggregates of coarse (up to 1 cm long), radiating greenish-yellow crystals. Identified with XRD and microprobe analysis (Table 5.)

Strontianite $SrCO_3$ is a common mineral in the late lanthanide-

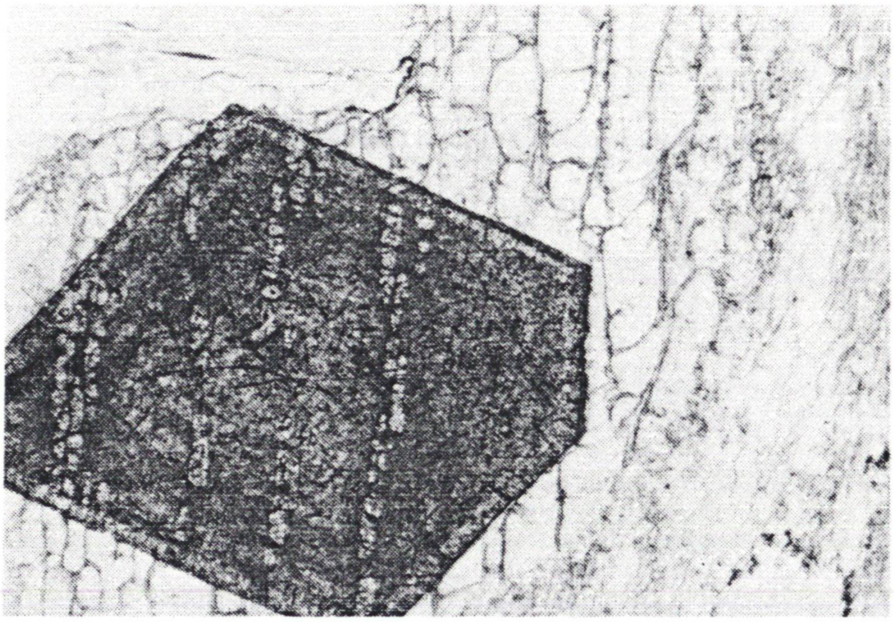

Fig. 41. Euhedral, light brown, slightly zoned pyrochlore. Late søvite. The microphotograph is 0.5 mm vertically. GGU 320410.

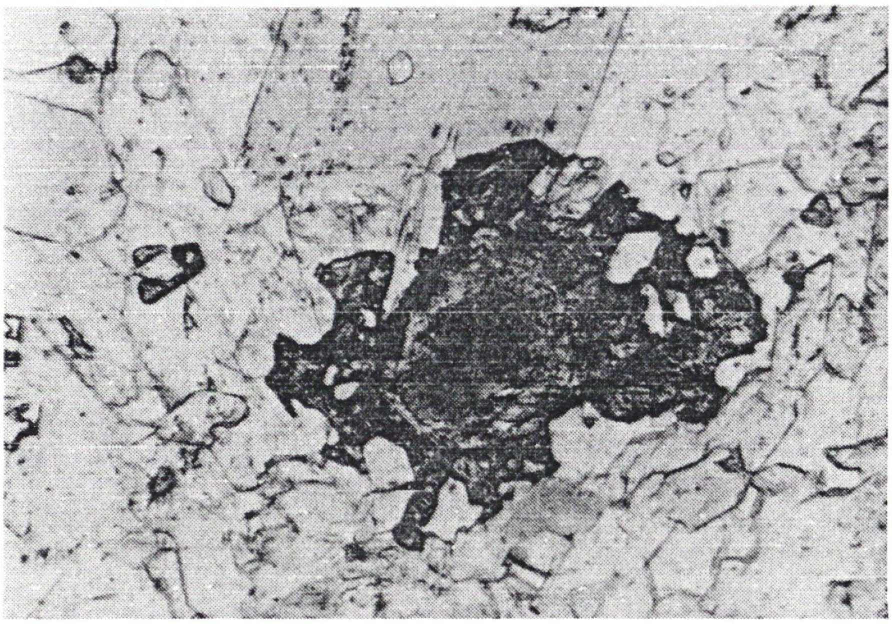

Fig. 42. Zoned pyrochlore with straw yellow, round, metamict core, light yellow intermediate part and light brown to colourless rim rich in inclusions. Late søvite. The microphotograph is 0.2 mm vertically. GGU 320407.

rich carbonatites, but is also found in søvite and rauhaugite. The strontianite contains appreciable amounts of Ca and Ba. (Table 5).

Baryte $BaSO_4$ is also common in the lanthanide-rich carbonatites.

5.6.3. *Magnetite*

The magnetite is found with many morphologies ranging from fine octahedral crystals in some late søvites, to skeletal, dendritic or symplectic magnetite-calcite intergrowth, coarse poikilitic grains in rauhaugite and as schlieren in glimmerite.

One feature which is found in almost all magnetite is exsolution of ilmenite - either as fine lamellae or as patches. An exception is magnetite from the magnetite-apatite-pyrochlore-rich rocks (Gothenborg and Pedersen, 1976).

Magnetite grains (including ilmenite exolutions) were analysed with XRF and have about 3.5 to 5.5 wt% TiO_2 and 0.3 wt% V_2O_5.

The magnetite itself has varying TiO_2 content (from 0.4 to 4 wt%) with a decrease towards the ilmenite exsolutions. Magnetite found as rims around and veins in altered olivine has almost no TiO_2 (0.01 wt%) and no ilmenite. The MgO content of the magnetite varies from almost nil in the pure søvite over about 0.2 wt% in rauhaugite to 0.8 wt% in olivine søvite (up to 1.6 wt% MgO in magnetite veins within and around altered olivine).

The Al_2O_3 content in the magnetite is low - about 0.01 to 0.2 wt%. MnO and SiO_2 contents are on a similar level.

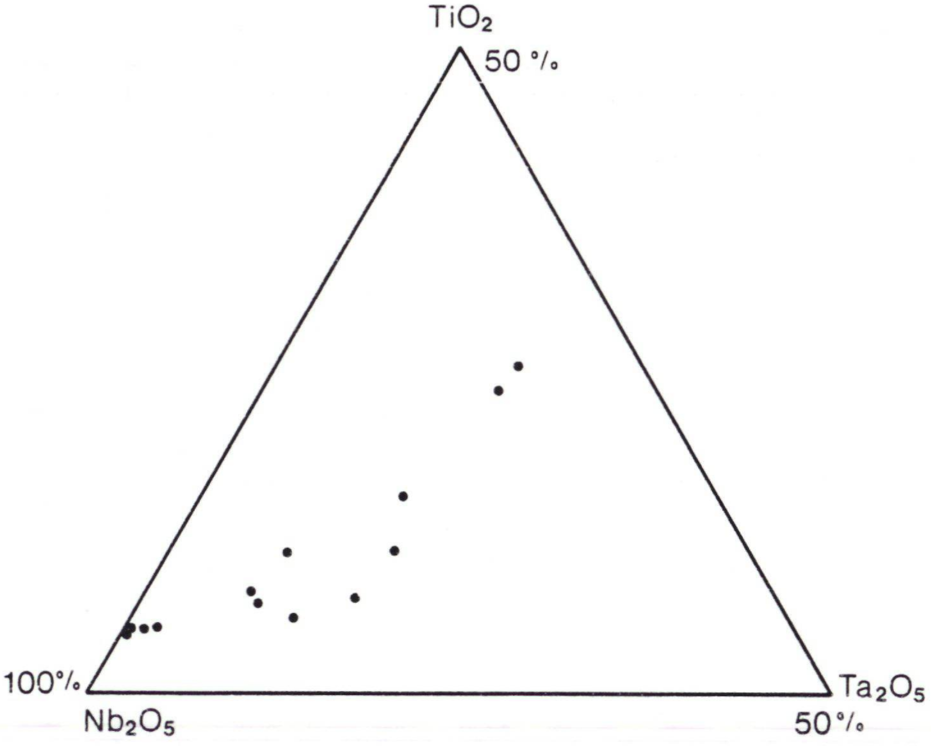

Relative proportions of oxides in pyrochlore

Fig. 43

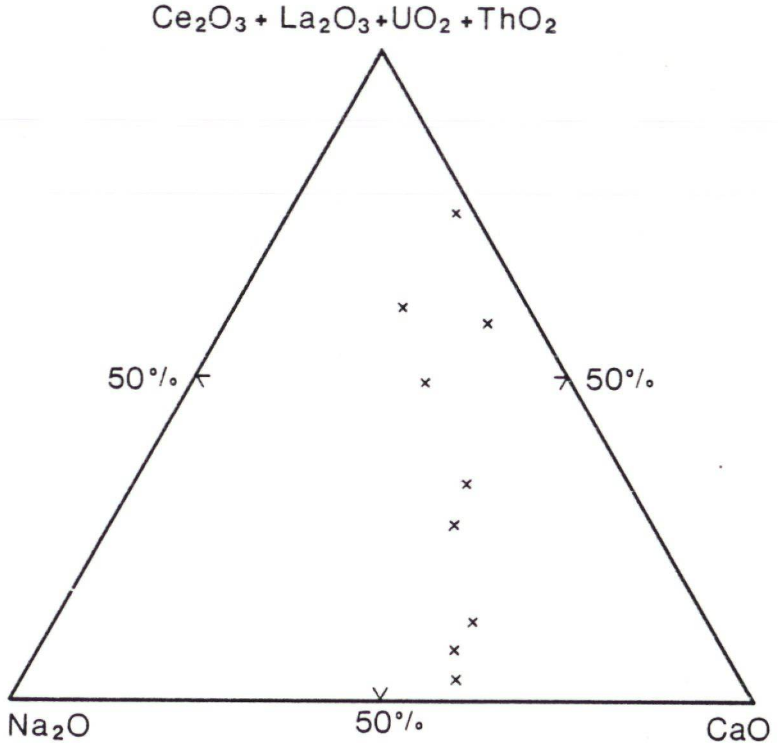

Relative proportions of oxides in pyrochlore

Fig. 44

5.6.4. *Pyrochlore*

Attention has been paid to the pyrochlore group minerals during this investigation because:

- Some late søvite dykes, the associated magnetite-apatite-pyrochlore rock and some apatite-rich glimmerites contain appreciable amounts of pyrochlore.
- The pyrochlore is radioactive, and thus possible to trace by radiometric measurements, and hence can be used as a pathfinder for apatite. (A radiometric survey in selected areas was carried out in 1985.)
- As a carrier of lanthanides, the pyrochlore may play a role in the lanthanide budget, which is a key to understanding apatite genesis.
- The pyrochlore may enhance the economic potential of the complex.

In the Qaqarssuk area pyrochlore occurs in different rock types, and both the morphology and composition varies widely. In the following the pyrochlore from the different environments is briefly described.

5.6.4.1. *Pyrochlore distribution, texture and composition*

The bulk of the pyrochlore is located in the magnetite-apatite-pyrochlore rock and the glimmerite (approximately 60% and 30% in these two rock types, respectively, and the remaining 10% in carbonatites and fenites).

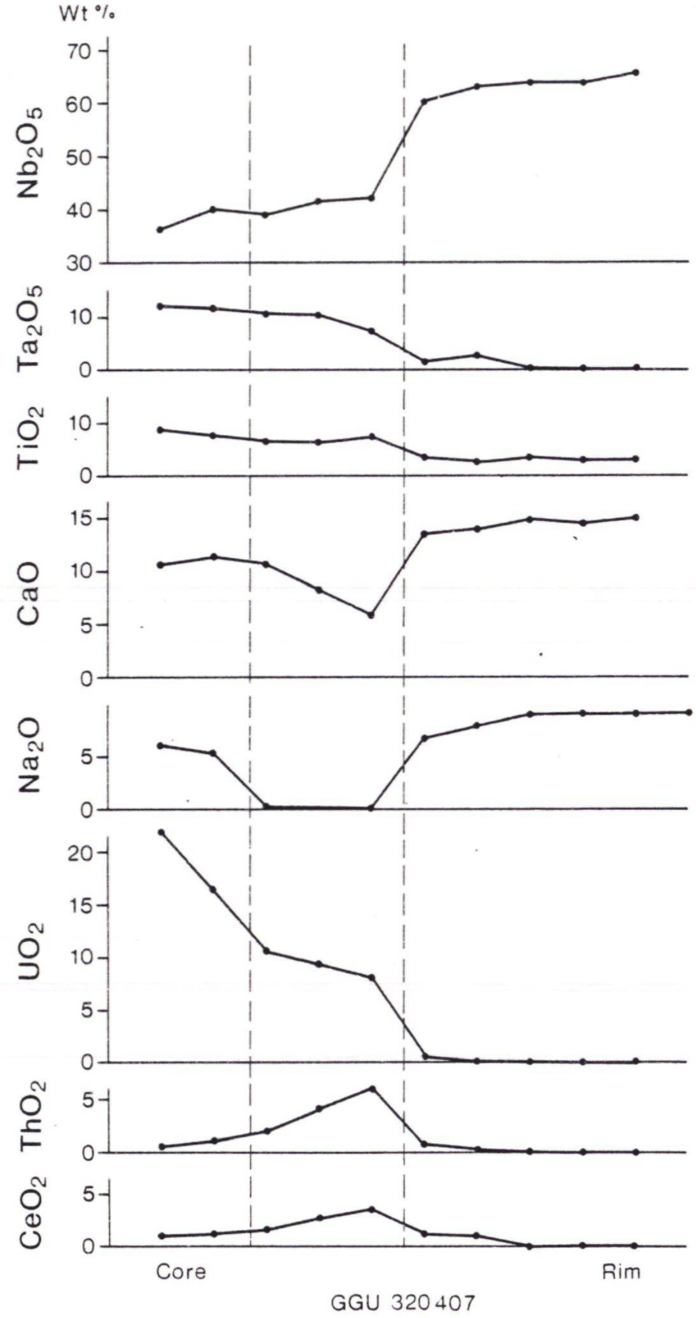

Fig. 45. Zoning in pyrochlore from søvite
The core is straw yellow, the intermediate zone is light yellow and the rim is colourless.

In *late søvite* and the *magnetite-apatite-pyrochlore-rich rock* the pyrochlore mainly occurs as transparent, colourless, euhedral crystals, rich in amphibole and apatite inclusions. These inclusions often radiate from the centre of the pyrochlore, and variation of inclusion density may form a zoning in the pyrochlore. This pyrochlore is generally pure with a formula approaching $(Na,Ca)_2Nb_2O_6(O,OH,F)$. It may be zoned with alternating colourless and dark bands (fig. 41). Locally an orange to straw yellow, transparent betafite core overgrown by a light yellow middle zone and a colourless rim can be observed (fig. 42). (Betafite is defined as a pyrochlore group mineral with more than 15% U). The straw-yellow core is rich in Ta, Ti and U (fig. 45). The core is transitional to the pure rim via the light yellow Th and lanthanide-rich band.

The pyrochlore in the *fine-grained rauhaugite* generally has a straw-yellow, metamict, rounded core enriched in uranium-tantalum-titanium which is overgrown with colourless pure pyrochlore.

The pyrochlore in the *ultramafic* rocks has slightly elevated U, Ta and lantanide contents relative to pyrochlore from the magnetite-apatite-pyrochlore rock, and pleochroic haloes can be observed in the surrounding phlogopite. The pyrochlore occurs as fine euhedral brown, dirty (poorly transparent) crystals disseminated in the ultramafite or in small carbonate veinlets in the ultramafite.

The pyrochlore in the *fenite* is localised either in small phosphate-, carbonate and lanthanide-rich veins, or disseminated in the fenite. The pyrochlore in the veins has a straw-yellow U-, Ta- and Ti-rich round core (266078) and a weakly coloured rim. The disseminated pyrochlore is rounded, a brown to yellow, metamict betafite (320056). This betafite occurs here together with apatite and a lanthanide-rich

TABLE 4

PYROCHLORE GROUP MINERALS IN QAQARSSUK

	266078		320056		320023	320488		320407			320438
	Core	Rim	Core	Rim		Core	Rim	Core	Int.	Rim	
Nb_2O_5	60.0	64.1	32.6	29.2	64.8	51.9	62.6	39.5	54.8	66.5	67.6
Ta_2O_5	5.0	2.7	7.6	8.2	.9	3.4	.4	7.7	5.1	.1	.0
TiO_2	2.7	2.7	12.3	11.2	3.8	4.1	3.0	8.6	4.2	3.6	4.3
Fe_2O_3	.4	.4	1.1	1.0	.6	2.3	.7	.3	.5	.0	
La_2O_3	.3	.3	.0	.0	1.2	.4	.6	.4	.3	.0	.1
Ce_2O_3	1.9	1.7	.9	3.2	4.2	1.2	2.2	1.4	2.5	.6	.5
Nd_2O_3	.5	.5	.4	.5	.6	.1	.3	.2	.6	.1	.2
Na_2O	1.9	2.9	1.7	.3	5.4	2.0	8.1	5.6	5.4	7.9	7.9
CaO	12.9	13.4	12.4	7.7	12.2	7.0	13.3	8.0	8.6	12.2	16.6
UO_2	2.8	2.7	25.2	22.8	.6	2.8	.3	17.1	5.3	.1	.3
ThO_2	.2	.2	.4	.4	1.6	.3	.1	1.8	4.0	.0	.2
ZrO_2	.3	.4	0.0	.2	.8	.3	.0	.0	.0	.1	.0
SiO_2	.4	.2	.5	.6	.4	7.2	.3	1.0	1.0	1.1	.1
Total	89.3	92.2	95.1	85.3	97.1	83.0	91.9	91.6	92.3	92.3	98.0

266078	Pyrochlore in vein in fenite
320056	Betafite disseminated in fenite
320023	Pyrochlore in glimmerite
320488	Pyrochlore in fine-grained rauhaugite
320407	Pyrochlore in søvite
320438	Pyrochlore in apatite-magnetite-pyrochlore rock

silicate mineral.

The variation in the pyrochlore composition reflects lanthanide, U and Th substitution for Na and Ca (fig. 43), and Ti and Ta substitution for Nb (fig. 44). When the pyrochlore is zoned, the U and Ta contents are highest in the core and decreasing outwards. This may be coupled with an increase in lanthanides and Th in a band intermediate between the core and the generally pure rim (fig.45).

This compositional variation in the pyrochlore can be summarised as follows:

- On a large scale - as a function of the enclosing rock type, ranging from "pure" in the carbonatite (at least in the rim), intermediate at the carbonatite-ultramafite interface and in ultramafite, to "dirty" and rich in substituting elements like Ta and U when located in narrow veins in, or disseminated in, fenite.
- On a small scale - as a zoning in individual pyrochlore crystals. This is most pronounced in carbonatite where the pyrochlore crystals have betafite cores, intermediate zones with high lanthanide and Th content, and "pure" rims.

5.6.4.2. *Interpretation of the varying pyrochlore composition*

Most of the elements substituting for Nb, Na and Ca in the pyrochlore are large, heavy ions. In alkaline environment these elements are soluble as carbonate (fluorine and sulphate) complexes (Møller and Morteani, 1983, Poty et al., 1974 and Kosterin, 1959), which explains that the

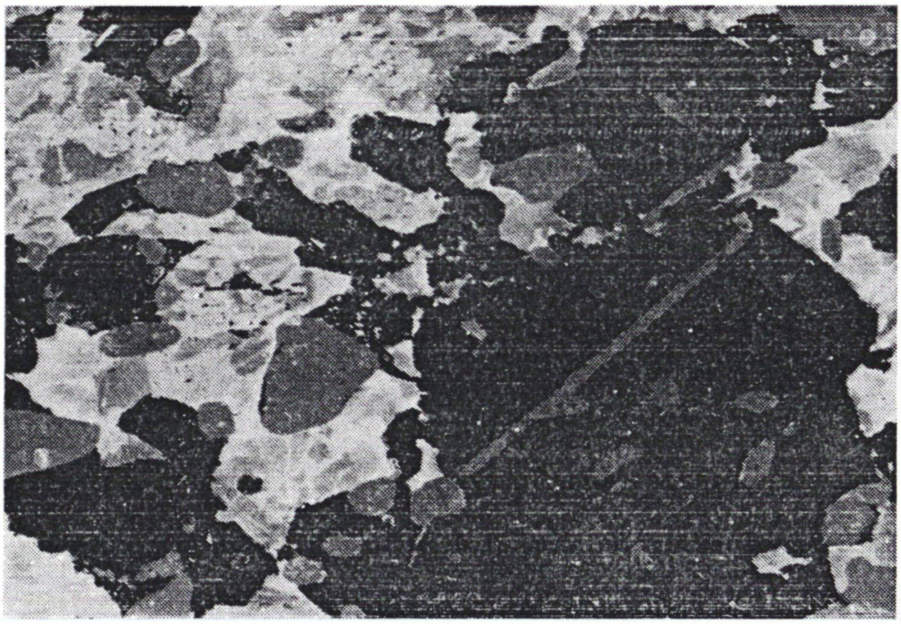

Fig. 46. Euhedral and very elongate apatite (grey) enclosed in olivine (black), whereas the apatite in the calcite (bright) is rounded. Olivine søvite. The microphotograph is 1 mm vertically, cathodoluminescence. GGU 252510.

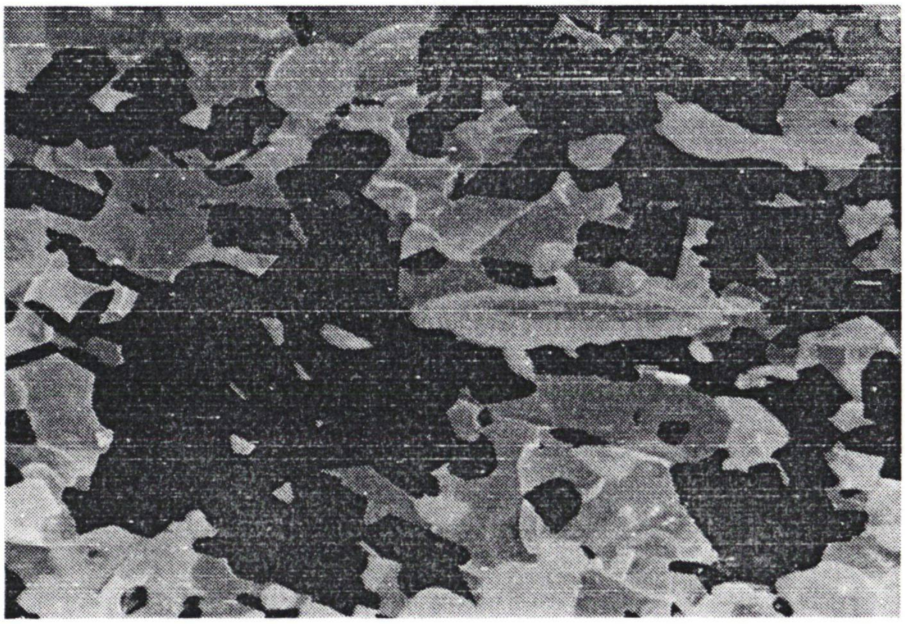

Fig. 47. Zoned and unzoned apatite (grey) in glimmerite (phlogopite is black). The dark core and bright rim indicate increasing lanthanide concentration outwards. The microphotograph is 1 mm vertically, cathodoluminescence. GGU 320040.

pyrochlore in the carbonatites is pure, - at least the rims, which must have crystallised in the carbonate-rich environment.

The mobility and solubility of lanthanides, Th, Ta and U is dependent on their ability to form and maintain these complexes, i. e. their field strength, which increases from lanthanides over Th to Ta and U. Where the complexes are broken, the elements will be precipitated, i.e. in a rock such as fenite (320056). If the carbonate concentration is increased gradually the elements with the highest field strength (U and Ta) will be the first to be soluble - followed by Th and lanthanides. This sequence can be observed on a small scale in the zoned pyrochlore (fig. 45) and on a large scale from the carbonatite to ultramafite to fenite. This suggests that pyrochlore with the highest Ta concentration is likely to be formed in relatively carbonate-poor environment and localised in the fenite.

5.6.5. *Apatite*

The phosphate in the rocks of the Qaqarssuk Complex is almost entirely contained in fluor-apatite and only traces of phosphorus are observed in silicates and other minerals. A few monazite grains were found intergrown with magnetite in rauhaugite (320141).

The apatite in the Qaqarssuk Carbonatite Complex can roughly be divided into four types based groups on texture, composition and nature of the host rock.

Type 1: Medium- to coarse-grained, subhedral apatite with an outward increase in lanthanide and Sr content is found in søvite, silico-søvite, rauhaugite and in carbonate matrix of

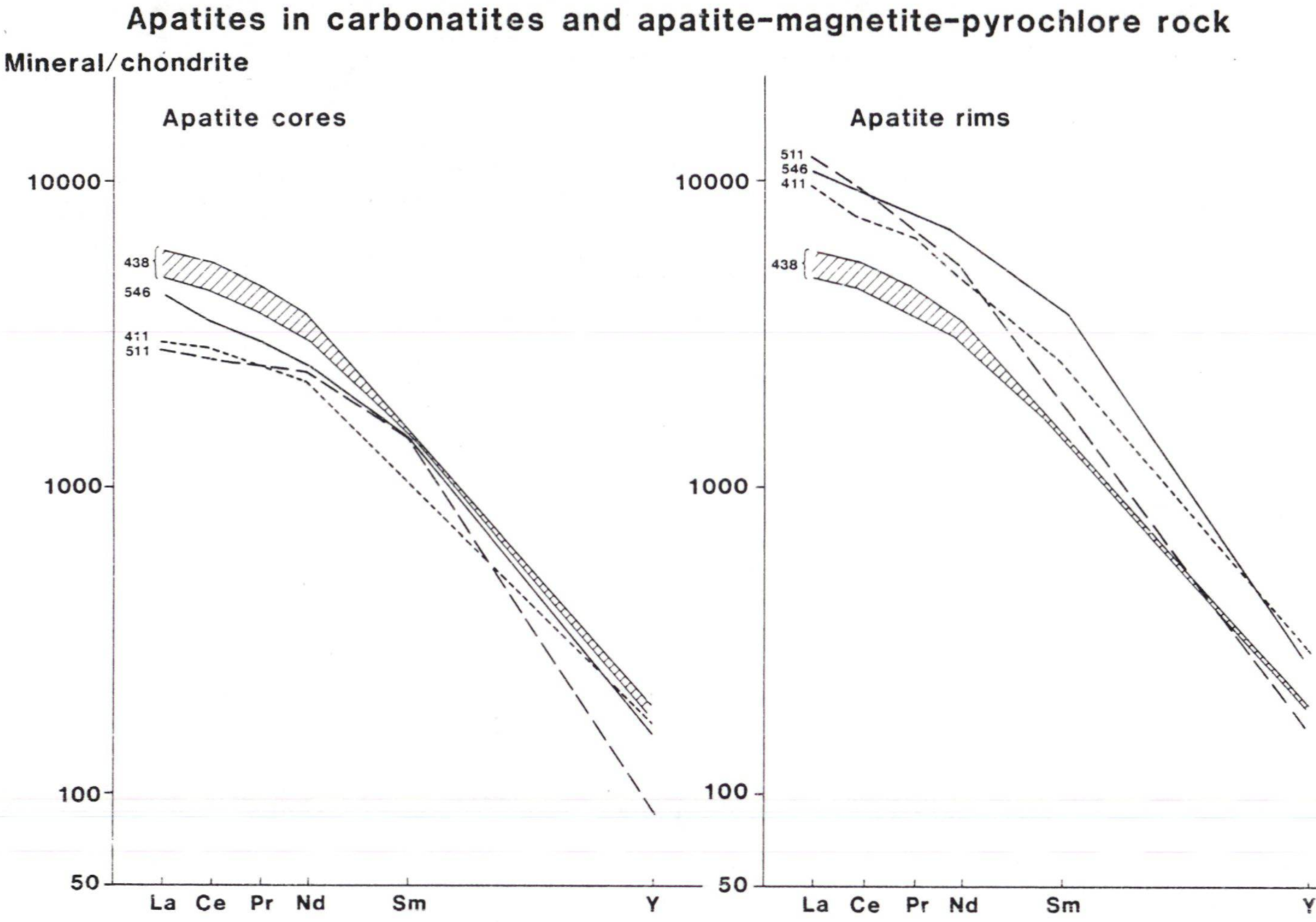

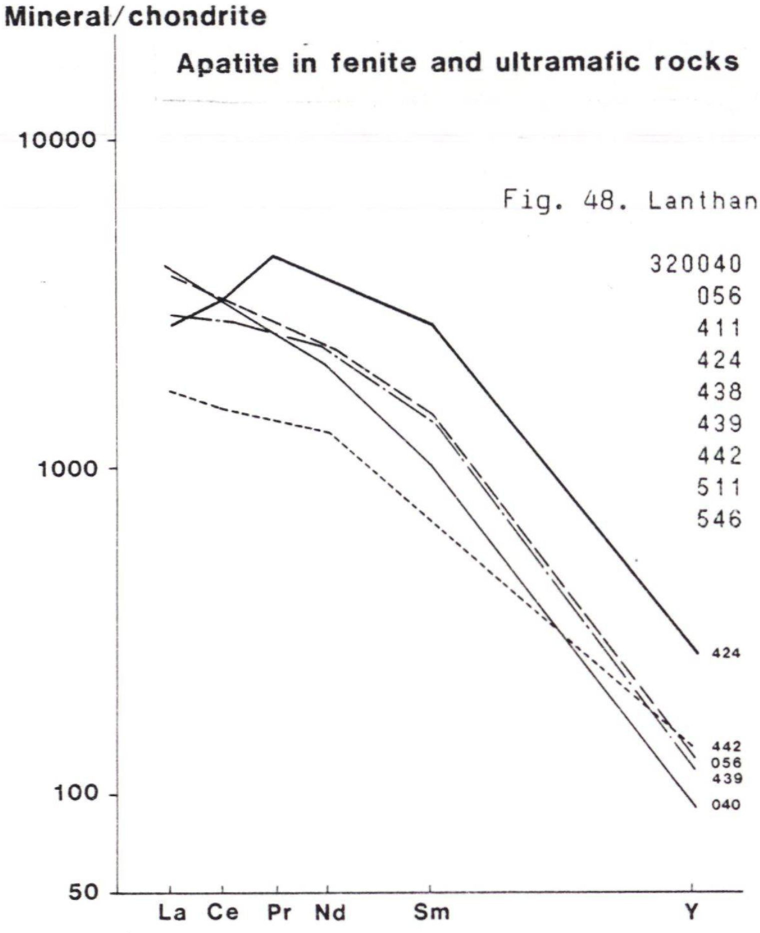

Fig. 48. Lanthanide distribution in apatite from Qaqarss

320040	in glimmerite
056	in fenite together with betafite
411	in rauhaugite
424	in fenite
438	in apatite-magnetite-pyrochlore rock
439	in mafic fenite
442	in quartz-bearing altered basement
511	in silico-søvite
546	in søvite

carbonate-rich ultramafic rocks.

Type 2: Fine- to medium-grained, eu- to anhedral apatite, generally with lower lanthanide and Sr content (relative to the above mentioned), is found as veins or disseminated in fenite and ultramafic low rocks with carbonate content.

Type 3: Acicular apatite crystals in rounded aggregates with high lanthanide and Sr contents are found in late søvite and apatite-magnetitepyrochlore-rich rocks.

Type 4: Very fine-grained apatite characterised by high lanthanide, Sr and locally rim, Ba and Mn contents is found in some lanthanide-rich carbonatite veins.

The distribution of lanthanides (normalised relative to chondrite) is characterised by strong enrichment in the light lanthanides. The distribution pattern is not linear, as is the case with the whole-rock lanthanide distribution patterns, but upwards concave with relative over representation of the intermediate lanthanides as Nd and Sm.

The lanthanide content in the apatite is proportional to the Na content.

5.6.5.1. Type 1: apatite in *Søvite, silico-søvite, rauhaugite and ultramafic rocks*

In these rocks the apatite has a compositional zoning which can be studied with cathodoluminescence. The core is then dark blue with a sharp contact to a bright blue rim. This difference is due to higher lanthanide contents in the rim. The same picture - the bright rim - is seen on the microprobe backscattered electron image due to a higher portion of heavy

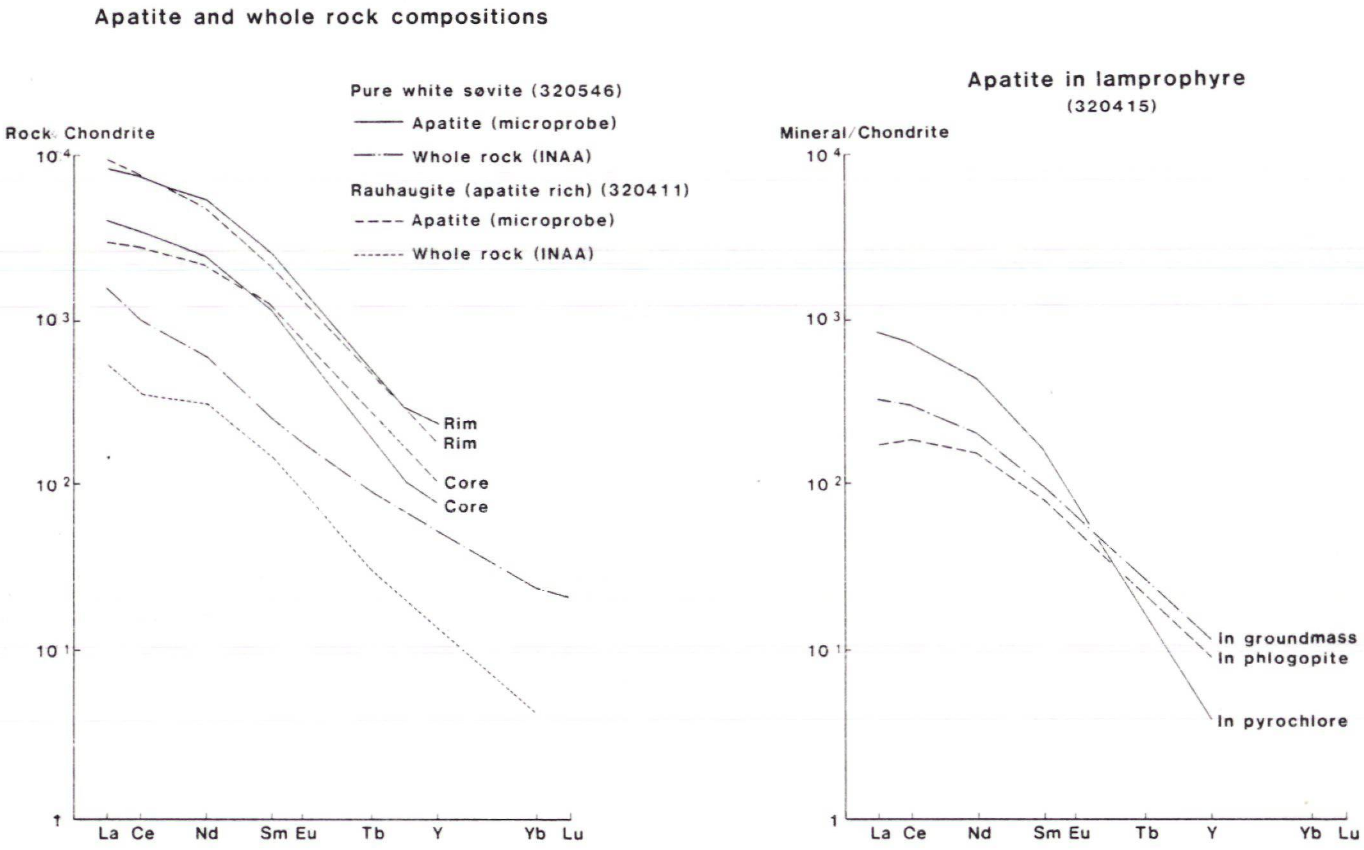
Apatite and whole rock compositions
Pure white søvite (320546)
Apatite (microprobe)
Whole rock (INAA)
Rauhaugite (apatite rich) (320411)
Apatite (microprobe)
Whole rock (INAA)
Rock/Chondrite
10 4
10 3
10 2
10 1
1
Rim
Rim
Core
Core
La Ce Nd Sm Eu Tb Y Yb Lu
Apatite in lamprophyre
(320415)
Mineral/Chondrite
10 4
10 3
10 2
10 1
1
In groundmass
In phlogopite
In pyrochlore
La Ce Nd Sm Eu Tb Y Yb Lu

Fig. 49

elements (lanthanides and Sr). The core is rounded indicating that crystals were partly resorbed in a period between precipitation of the core and the rim. The apatite has embayments in the crystal surfaces which cut the chemical zonation) and indicate a second period of resorption. The factor 2 to 3 increase in lanthanide concentration from core to rim is illustrated on fig. 48 and 49. The SrO concentration is increased with a similar factor (fig. 50). The apatite is rich in carbonate inclusions (dolomite dominating over calcite) and fluid inclusions.

The apatite in the ultramafic rocks are locally compositionally zoned, but in general, they are characterised by a low lanthanide and Sr content, similar to the concentrations found in the core of apatite in søvite and rauhaugite.

5.6.5.2. *Type 2: apatite in fenite and ultramafite*

The apatite in fenite is characterised by low Sr/lanthanide ratios compared to apatite from ultramafic rocks and carbonatite. Three types of apatite compositions have been found in the fenite.

- In the quartz-bearing, altered basement, apatite with very low Sr and low lanthanide contents is found (fig. 50), locally overgrown with apatite with lanthanide and Sr contents similar to what is found in other fenites.
- In fenite adjacent to rauhaugite, apatite with strong enrichment of intermediate lanthanide is found.
- In apatite near the fenite-carbonatite interface and in apatite veins in the fenite, the apatite has a lanthanide distribution similar to what is found in the apatite in ultramafite.

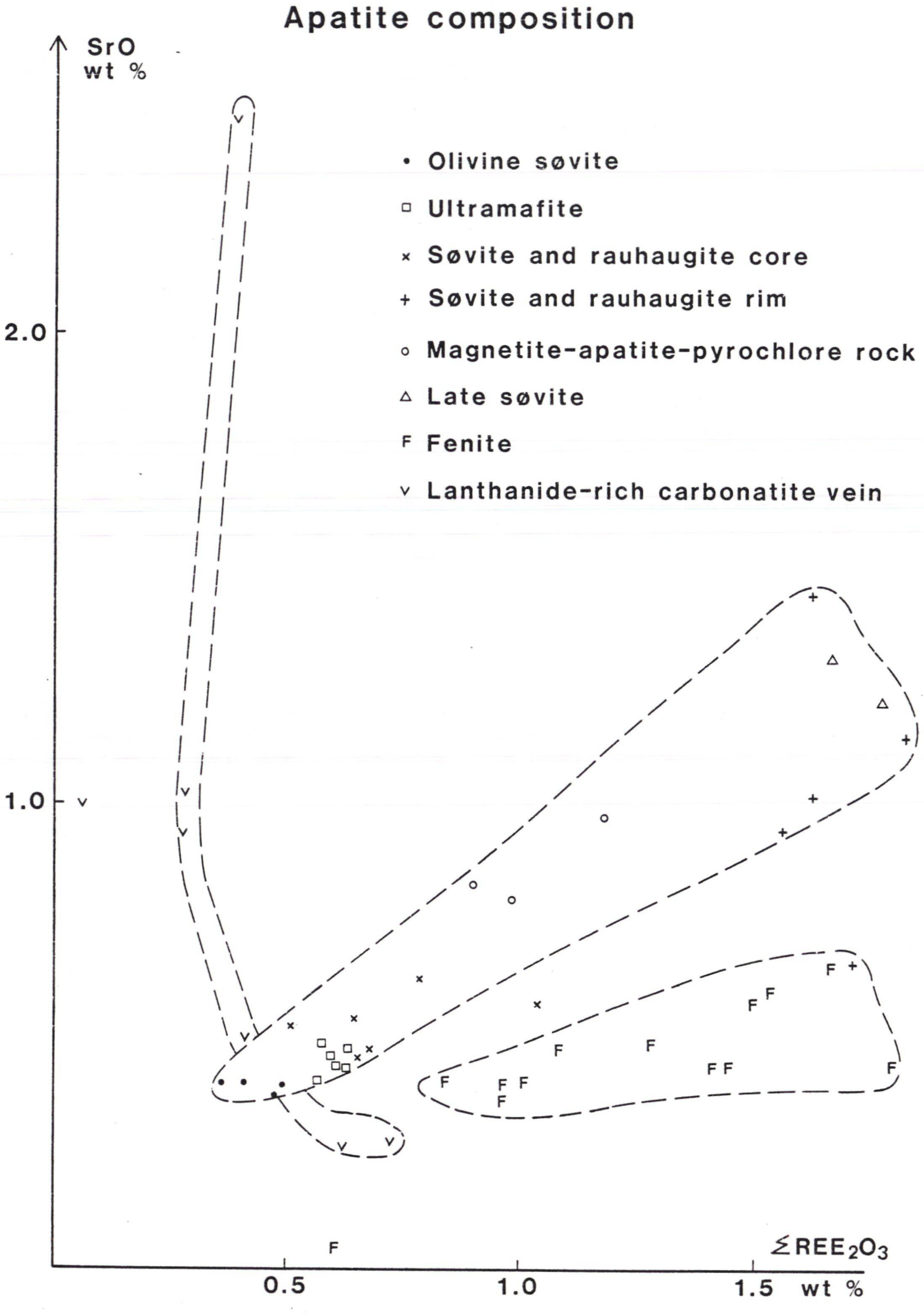
Apatite composition
SrO wt %
2.0
1.0
• Olivine søvite
□ Ultramafite
× Søvite and rauhaugite core
+ Søvite and rauhaugite rim
○ Magnetite-apatite-pyrochlore rock
△ Late søvite
F Fenite
V Lanthanide-rich carbonatite vein
0.5
1.0
1.5
ΣREE₂O₃ wt %

Fig. 50.

5.6.5.3. *Type 3: apatite in late søvite and magnetite-apatite-pyrochlore-rich rock*

The lanthanide and Sr concentration in the acicular apatite is intermediate to the concentrations found in the core and the rim of apatite from the other carbonatites (fig. 50). The lanthanide and Sr content in the aggregates of radiating apatite needles is high and similar to the concentration in the rim of apatite from the other carbonatites.

5.6.5.4. *Type 4: apatite in Lanthanide-rich carbonatite veins*

The apatite in the lanthanide-rich carbonatite veins shows a wide range of compositions and textures, from compositions similar to what is found in the other carbonatites, to Sr, Ba, Mn, Na and lanthanide-rich apatite. Apatite with "usual" composition occurs as rounded grains whereas the Sr, Ba, Mn, Na and lanthanide rich apatite is very fine-grained.

5.7. REGOLITH/OVERBURDEN

The carbonatite and especially the ultramafic rocks associated with it are generally located in depressions in the landscape, owing to their low resistance to weathering.

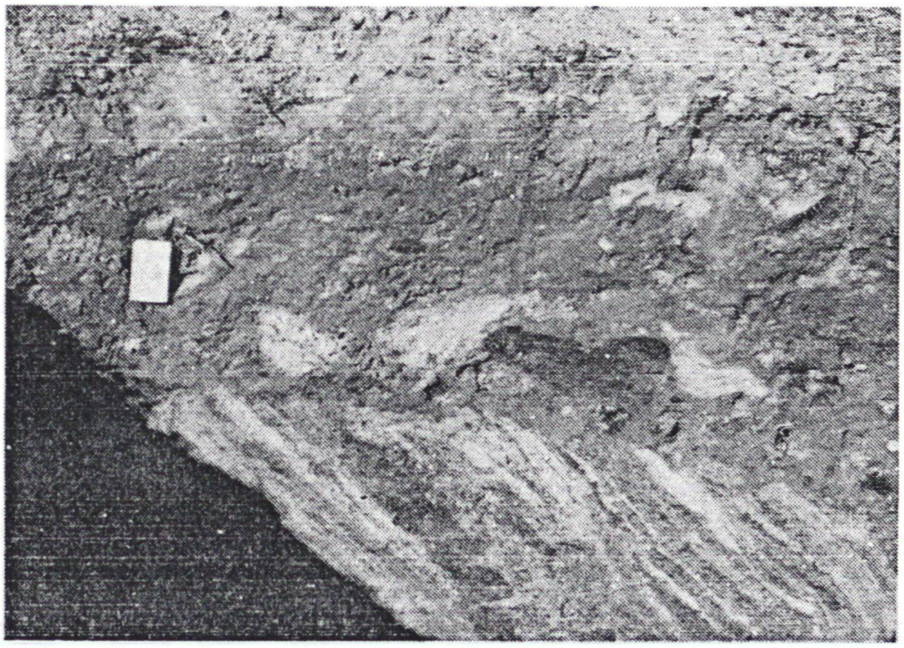

Fig. 51. Regolith with preserved original layering (B horizon at bottom) overlain by soil (A horizon) with deformed regolith clasts.

The amount of glacial deposits is generally low in the area (less than .5 m), and the low frequency of outcrops in the areas with carbonatite and ultramafic rocks is caused by the presence of a layer of weathered bedrock. Apart from this, alluvial and solifluction deposits are found in the lowermost parts of the landscape.

5.7.1. *Soil geochemistry*

Residual soil enriched in phosphorus and niobium overlying carbonatite complexes is well-known from many other parts of the world - mainly in low latitudes, e.g. Araxa in Brazil and Sukulu in Uganda (Reedman, 1984), but also in the high latitudes as Sokli in Finland (Vartiainen & Paarma, 1979). In these localities, large quantities of residual soil have accumulated on top of the carbonatite where leaching of the carbonate, has left a P, Nb and often iron-rich residium, characterised by secondary hydrous iron oxides, iron-rich clay minerals and locally secondary phosphate (francolite).

In 1984, 300 soil samples were collected in soil presumably overlying carbonatite and ultramafic rocks in the Qaqarssuk Carbonatite Complex. The purpose of this was:

1. To evaluate the soil as a source for P and Nb.
2. To trace possible deposits of P, Nb or lanthanides beneath the soil cover.

A typical soil profile over carbonatite or glimmerite in the Qaqarssuk Carbonatite Complex is as follows:

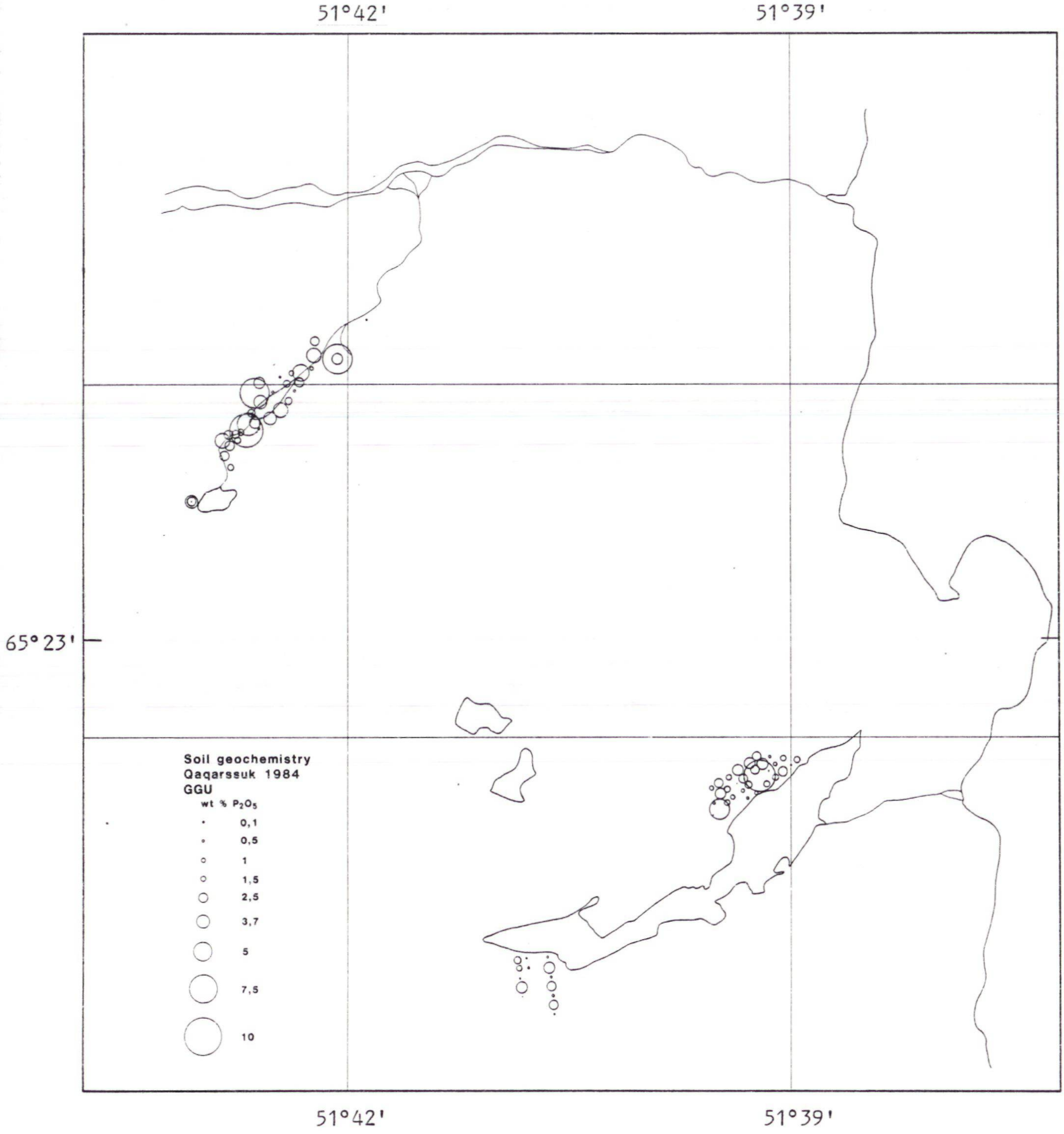
51°42'
51°39'
65°23'
Soil geochemistry
Qaqarssuk 1984
GGU
wt % P_2O_5
0,1
0,5
1
1,5
2,5
3,7
5
7,5
10
51°42'
51°39'

Fig. 52.

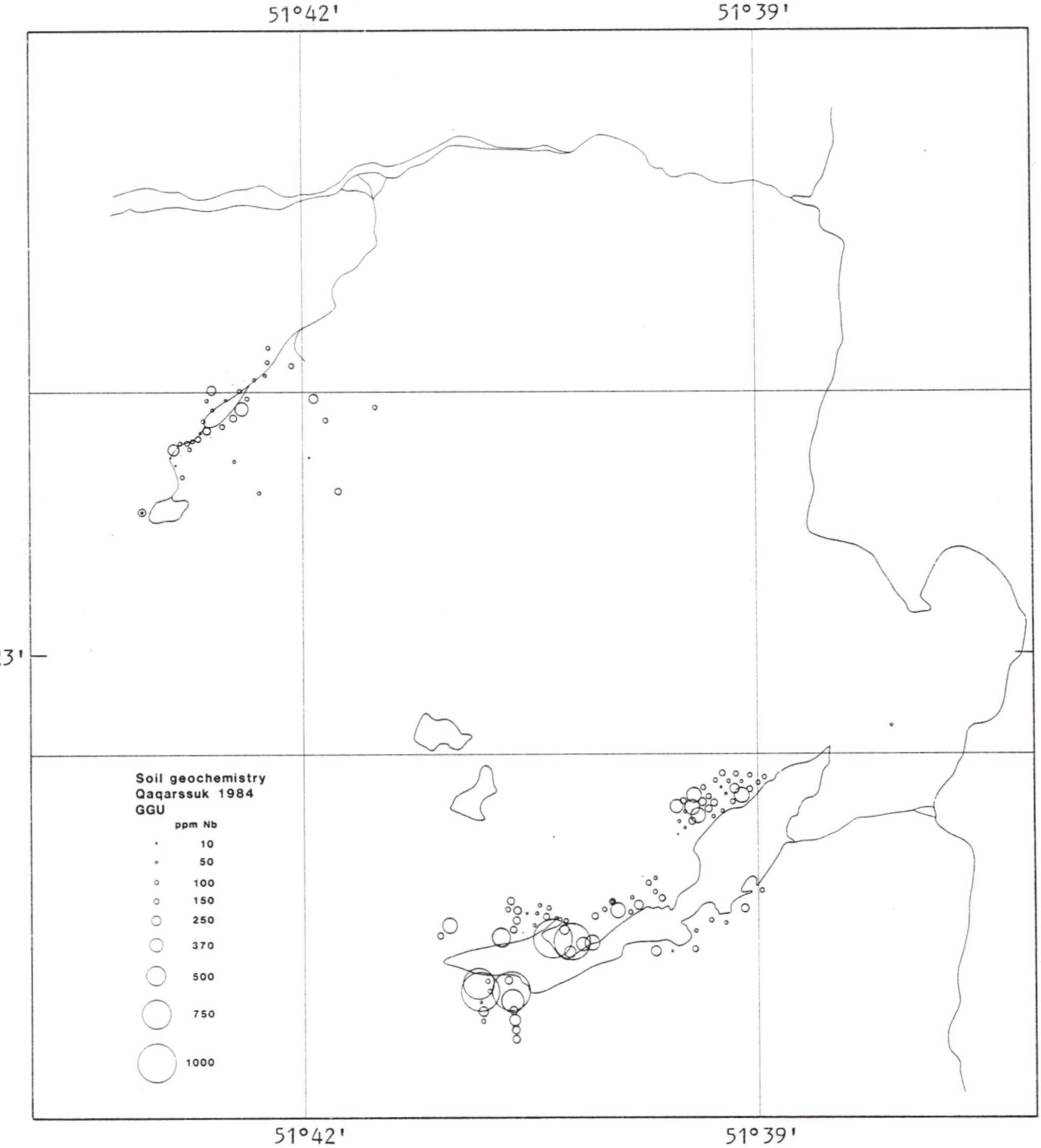
51°42'
51°39'
3'
Soil geochemistry
Qaqarssuk 1984
GGU
ppm Nb
10
50
100
150
250
370
500
750
1000
51°42'
51°39'

Fig 53.

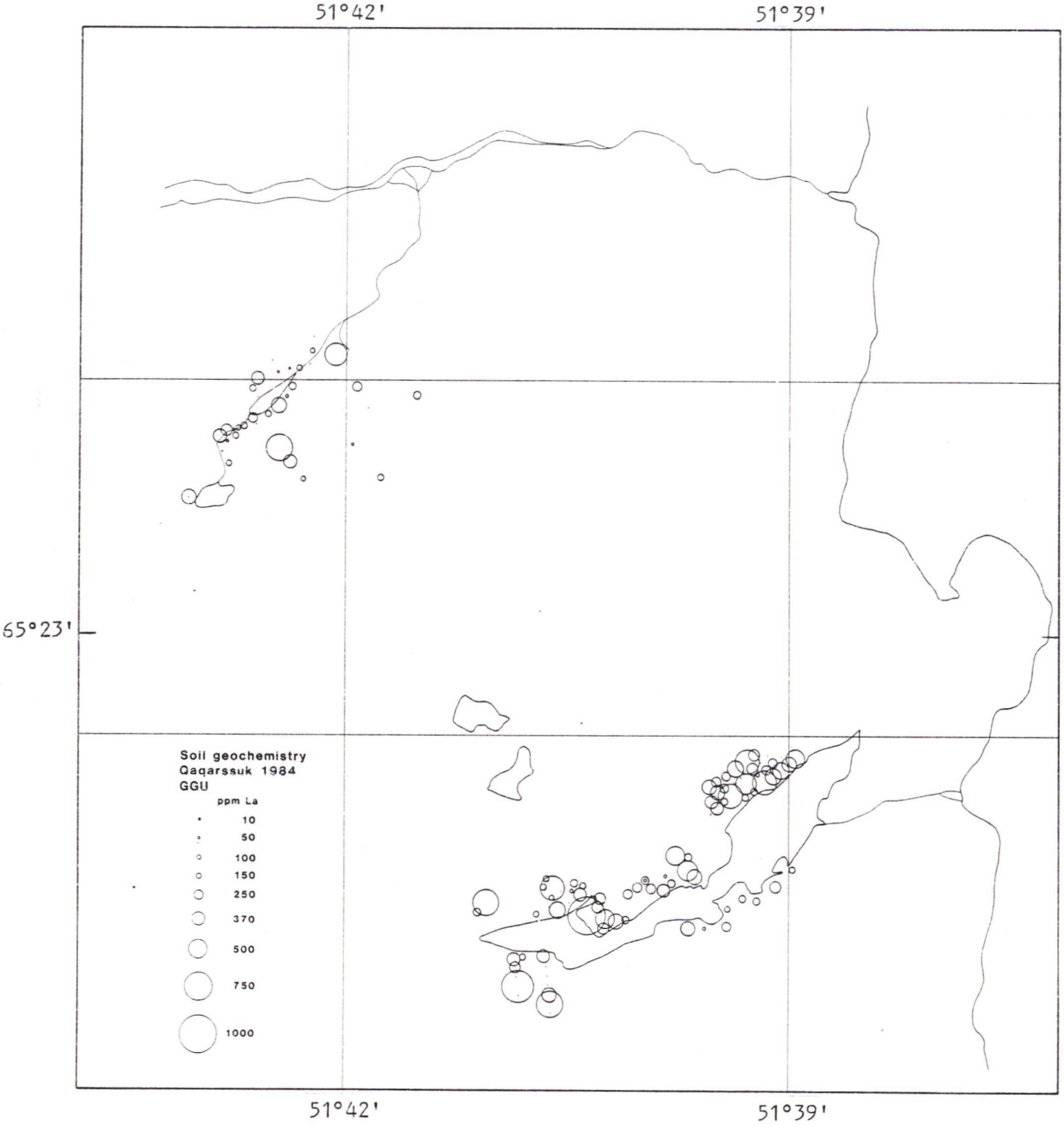

51°42'
51°39'
65°23'
Soil geochemistry
Qaqarssuk 1984
GGU
ppm La
10
50
100
150
250
370
500
750
1000
51°42'
51°39'

Fig. 54.

Depth	Horizon	
2- 0 cm	L or H	Leaves or humus.
0-10 cm	A	Reddish-brown clay loam rich in humus and roots and with patches of B horizon.
10-60 cm	B	Black to light yellowish-brown, sandy loam with single grain structure and with preserved primary bedrock structure.
60-80 cm		Disintegrated glimmerite or carbonatite bedrock.
80 cm	C	Glimmerite or carbonatite bedrock.

Hydrous iron oxide and clay minerals are abundant in the A horizon and are, with a few exceptions fairly rare in the B horizon. No secondary phosphate has been found.

Analyses of the residual soil (B horizon sampled in 1984) have indicated

1. intensive leaching of the carbonatite has taken place, yielding a soil with up to 8 wt% P_2O_5, down to at least 2 m beneath the surface. This leached residual soil is locally preserved.
   As can be seen on fig. 52 and 53 P and Nb enriched soils are not common in the area.
2. strong Nb and REE anomalies are present in areas not investigated by Kryolitselskabet Øresund A/S. The anomalous areas were revisited in 1985 and a detailed radiometric survey was carried out to illuminate the bedrock geology.

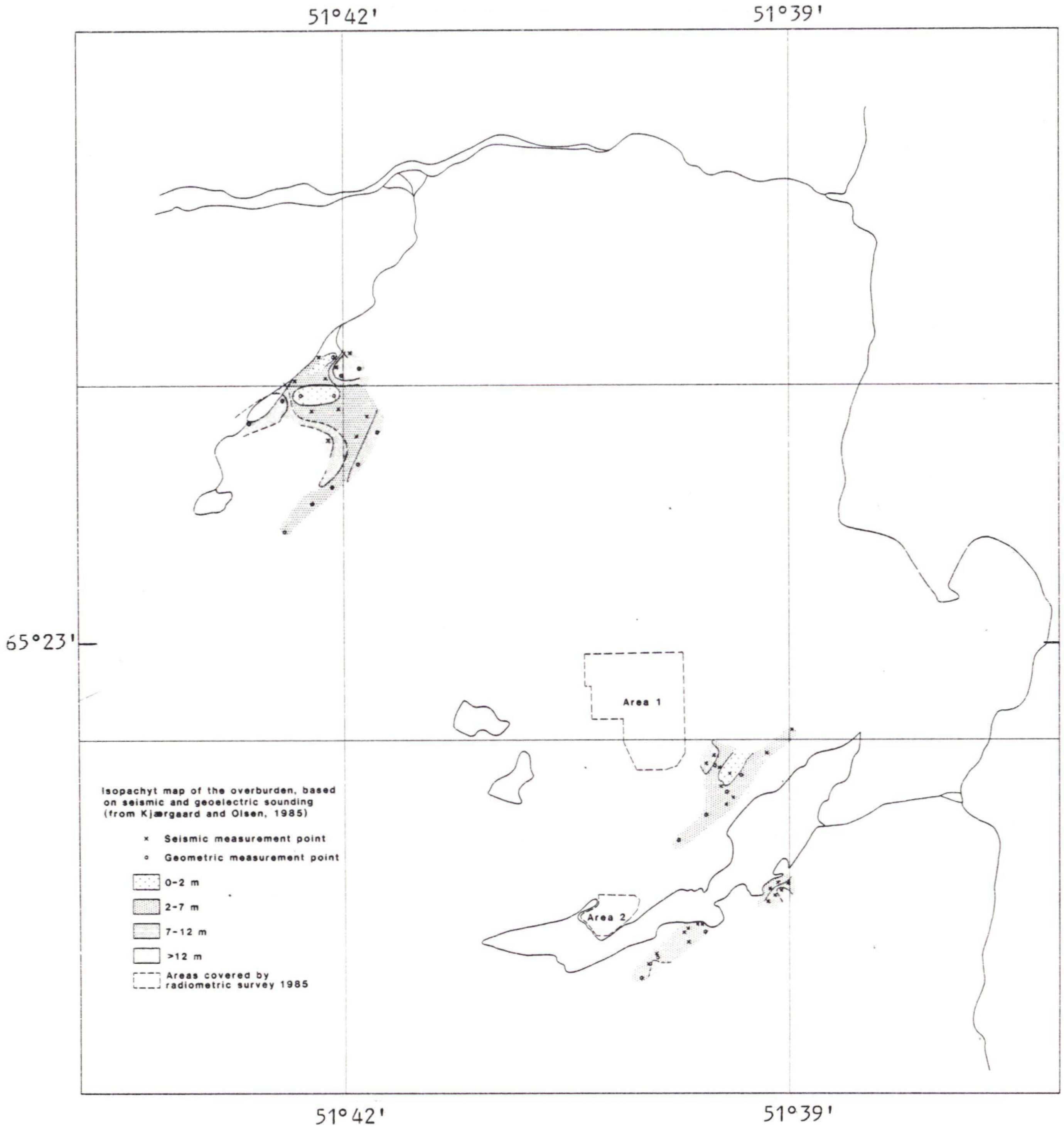
51°42'
51°39'
65°23'
Area 1
Area 2
Isopachyt map of the overburden, based on seismic and geoelectric sounding (from Kjærgaard and Olsen, 1985)
× Seismic measurement point
∘ Geometric measurement point
0-2 m
2-7 m
7-12 m
>12 m
Areas covered by radiometric survey 1985
51°42'
51°39'

Fig. 55.

5.7.2. *Seismic and geoelectric investigations*

The seismic and geoelectric investigations showed that:

- It was possible to map the thickness of the overburden (fig. 55), and locally to differ between alluvial and more solid (regolitic) deposit on top of the bedrock.
- It was possible roughly to determine the character of the bedrock beneath the overburden.
- Ice lenses are abundant in the overburden. As resistivities and seismic velocities are much higher in the ice lenses, they obscured observations, where present.

  The geoelectric method was the most powerful method for mapping overburden thicknesses in the range 2 to 20 m, in this terrain.

5.8. MAGNETIC INVESTIGATIONS

The magnetic maps on fig. 56 and fig. 57 are made by Morten Kjærgaard (1985), on the basis of measurements carried out by Kryolitselskabet Øresund A/S in 1970 and 1971 (vertical field) and in 1975 (total field), respectively. The interpretation of the magnetic map is carried out in cooperation with Morten Kjærgaard.

Qaqarssuk Carbonatite Complex

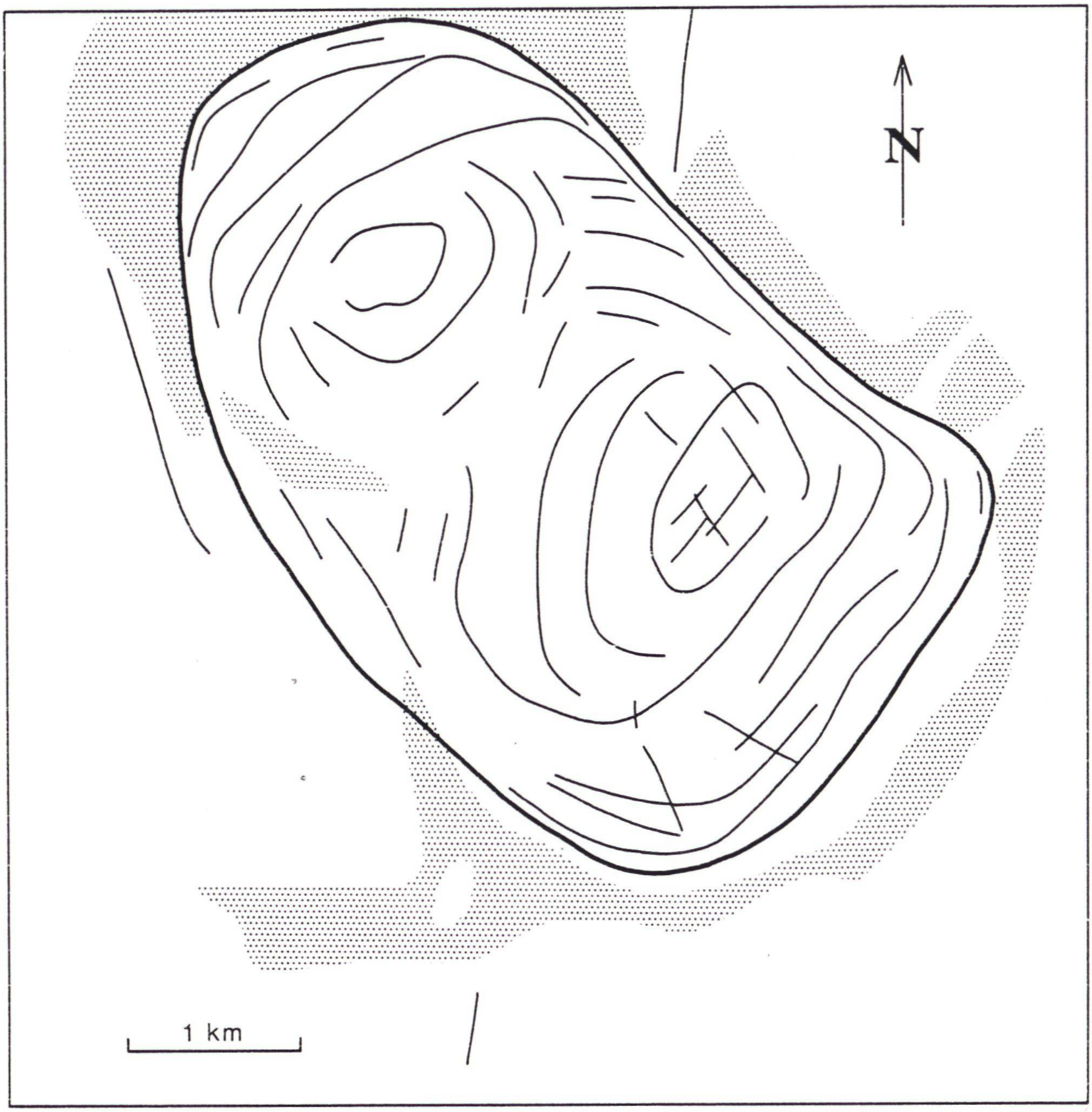

Interpretation of magnetic (vertical field) anomaly map

Fig. 56 A.

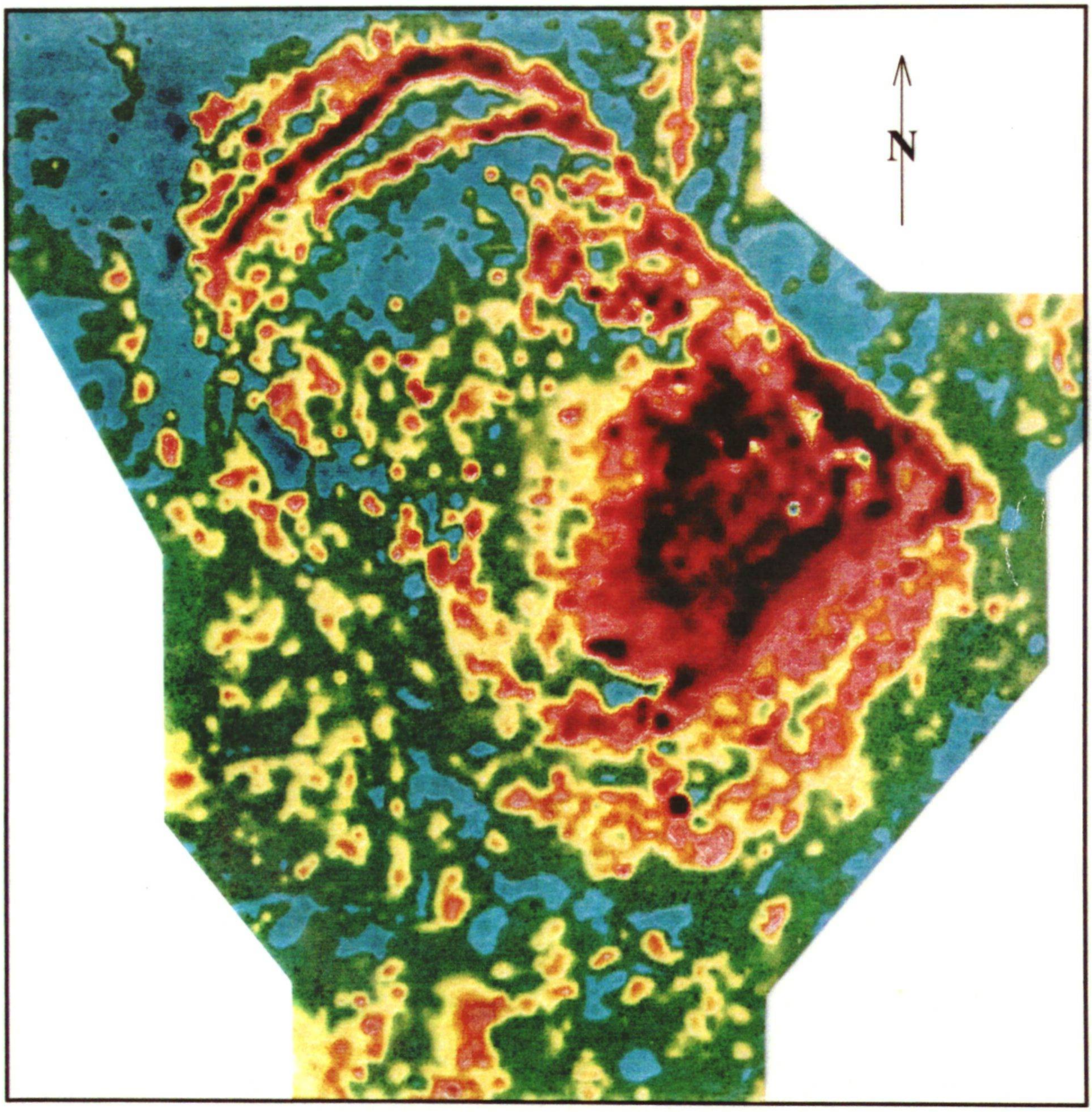

Vertical (residual) magnetic field
Nanotesla

⬛ Over 4200
⬛ 4200 - 3800
🟫 3800 - 3400
🟫 3400 - 3100
🟥 3100 - 2800
🟥 2800 - 2500
🟥 2500 - 2300
🟥 2300 - 2100
🟥 2100 - 1900
🟥 1900 - 1700
🟥 1700 - 1500

🟧 1500 - 1400
🟧 1400 - 1300
🟨 1300 - 1200
🟨 1200 - 1100
🟨 1100 - 1050
🟨 1050 - 1000
🟨 1000 - 950
🟨 950 - 900
🟩 900 - 850
🟩 850 - 800
🟩 800 - 750

🟩 750 - 700
🟩 700 - 600
🟩 600 - 500
🟩 500 - 400
🟦 400 - 300
🟦 300 - 100
🟦 100 - -100
🟦 -100 - -300
⬛ -300 - -500
⬛ -500 - -700
⬛ -700 - -900

Fig. 56 B.

The most striking features on the map (fig. 56) are the semi-rectangular, ring-shaped or curved, strong positive anomalies. These can be correlated to the occurrence of major steeply dipping søvite sheets. The anomalies are caused by the high magnetite content or magnetite accumulations in these søvites and the associated glimmerites. The rauhaugite and the silico-søvite are only associated with weak magnetic anomalies.

Another striking feature is the subcircular positive anomaly in the south eastern part of the core. This can be ascribed to the high frequency of søvite rich in magnetite, and glimmerite rich in magnetite in this area. The positive anomaly covers a larger area than the carbonatite, which is due to the shallow outwards dip of the søvites in this inner core, indicating that the søvites and associated rocks are shaped like a cone with outwards dipping sides.

This core in the SE part of the complex is surrounded by a number of concentric more or less continuous positive anomalies, which can be correlated to søvite ring dykes around the core.

Arcuate anomalies in the north-western area of the inner part of the complex support field data, indicating the presence of a minor cone-shaped set of carbonatite dykes - and hence another inner core.

A suite of magnetic anomalies in the southern part of the complex can be correlated with late søvite containing accumulations of magnetite and of magnetite-apatite-pyrochlore.

The complex is surrounded by a negative magnetic anomaly. This is caused by the high degree of hydrothermal alteration of the basement, in which the magnetite has been altered to hematite. This negative magnetic anomaly coincides with the radiometric anomaly surrounding the complex, and caused by Th enrichment.

South eastern part of Qaqarssuk Carbonatite Complex

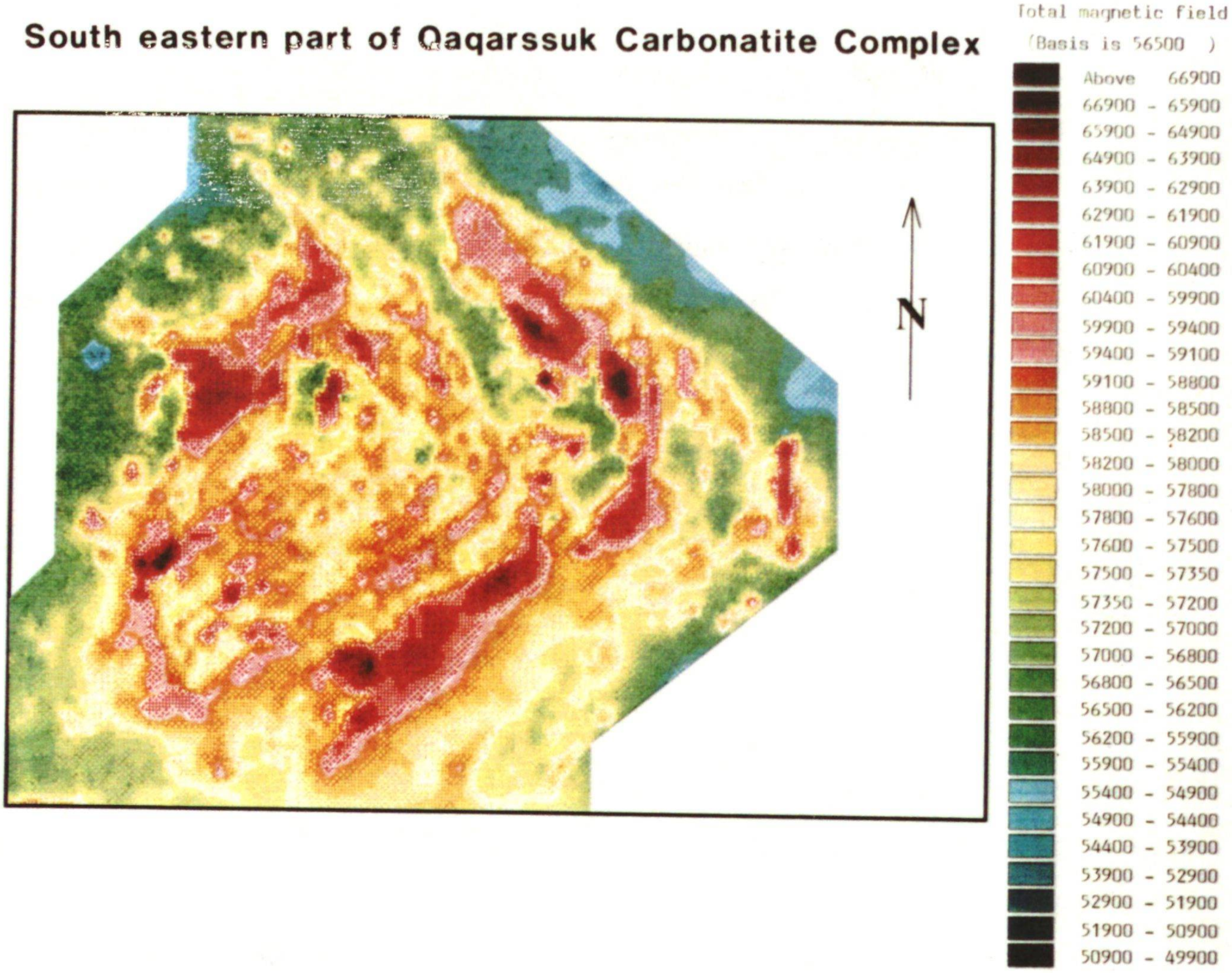

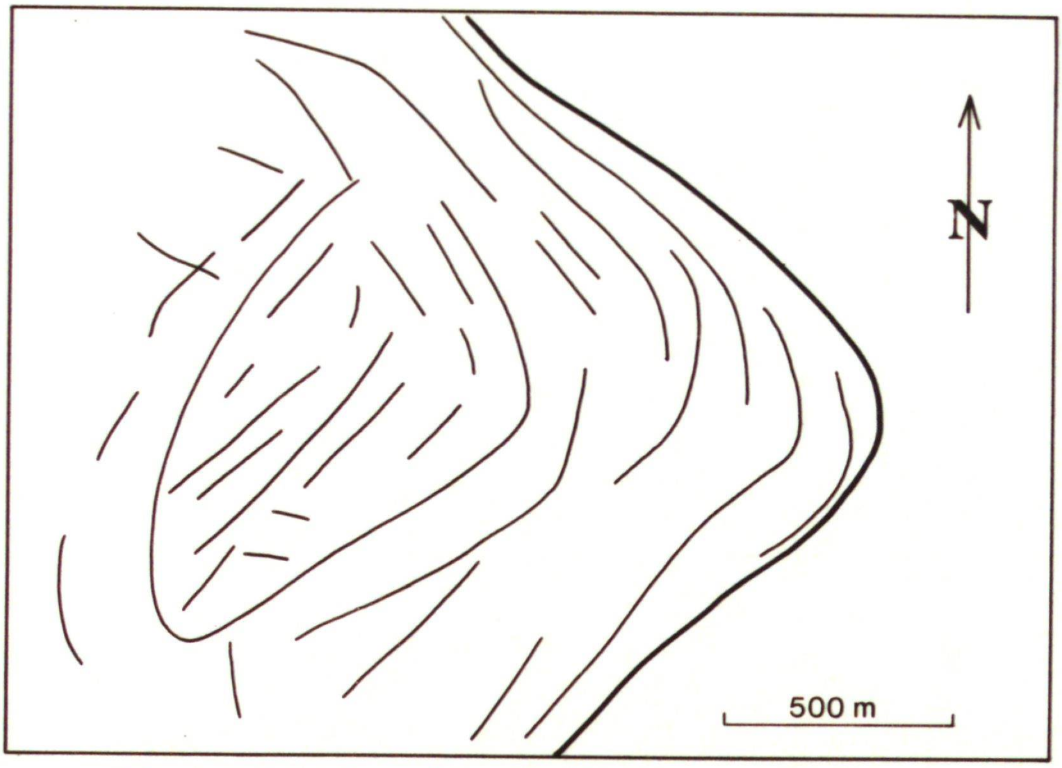

Interpretation of the (total field) magnetic anomaly map

Trends in positive magnetic anomalies

Margin

Fig. 57.

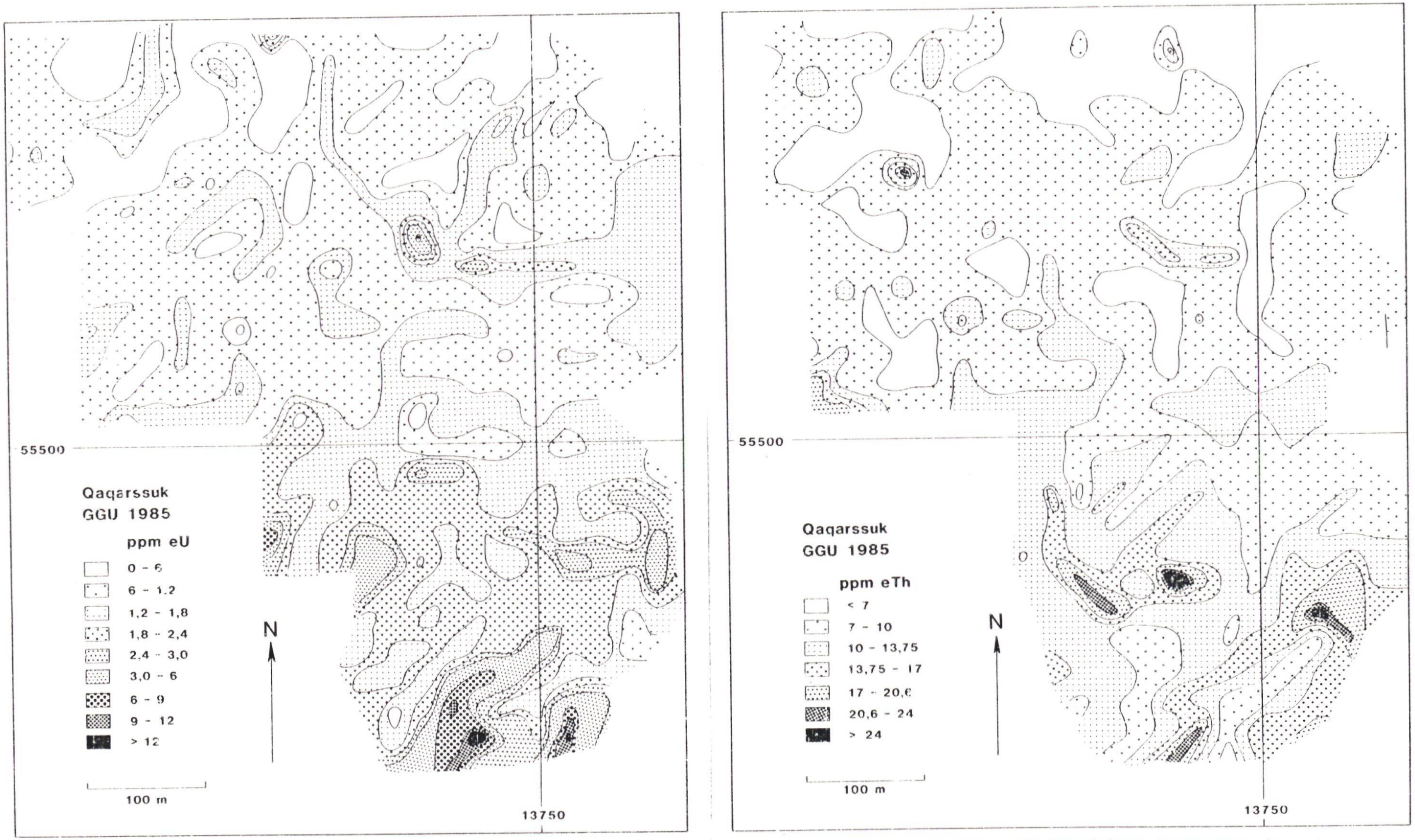

(Concentrations calculated from measurements by portable 4 channel scintilometer)

(Concentrations calculated from measurements by portable 4 channel scintilometer)

Fig. 58. Area 1.
The area can be divided into a northern area with relatively low background and a southern with higher background which can be correlated to carbonatite (and ultramafite) and fenite, respectively. Lanthanide-rich carbonatites are localised where eU 〉 6 ppm or eTh 〉 13.75 ppm.

The radiating carbonatite veins and shear zones can only be seen on the magnetic map in the SE'ern part of the complex, where two small positive anomalies radiating out from the complex can be correlated to carbonatite veins.

The large N-S trending dolerite dyke, cut by the rocks of the carbonatite complex, can clearly be seen on the magnetic map in the NE part, whereas the less well-defined N-S trending positive anomaly in the SW part of the map is interpreted as the continuation of the dolerite dyke. The dextral offset of the dyke over the complex is consistent with the interpretation of the emplacement of the complex, in an area of tension associated with dextral movement (fig. 6).

The well-defined eastern margin of the complex is very well-defined relative to the western margin. This is due to

1. the higher frequency of carbonatite sheets along the eastern and
2. to the less frequent overburden at the eastern margin compared to the western.

The negative magnetic anomaly cutting the structure of the carbonatite in the north-western part of the complex coincides with a steep valley, and is interpreted as a topographic effect.

5.9. RADIOMETRIC INVESTIGATIONS

A radiometric survey carried out by Kryolitselskabet Øresund A/S in 1970 and 1971 showed that the major part of the radioactive elements (mainly Th) is located in the marginal part of the complex. As mentioned above, the radioactive zones can be correlated with highly altered rocks with low susceptibility. The Th is located in ankerite veins together

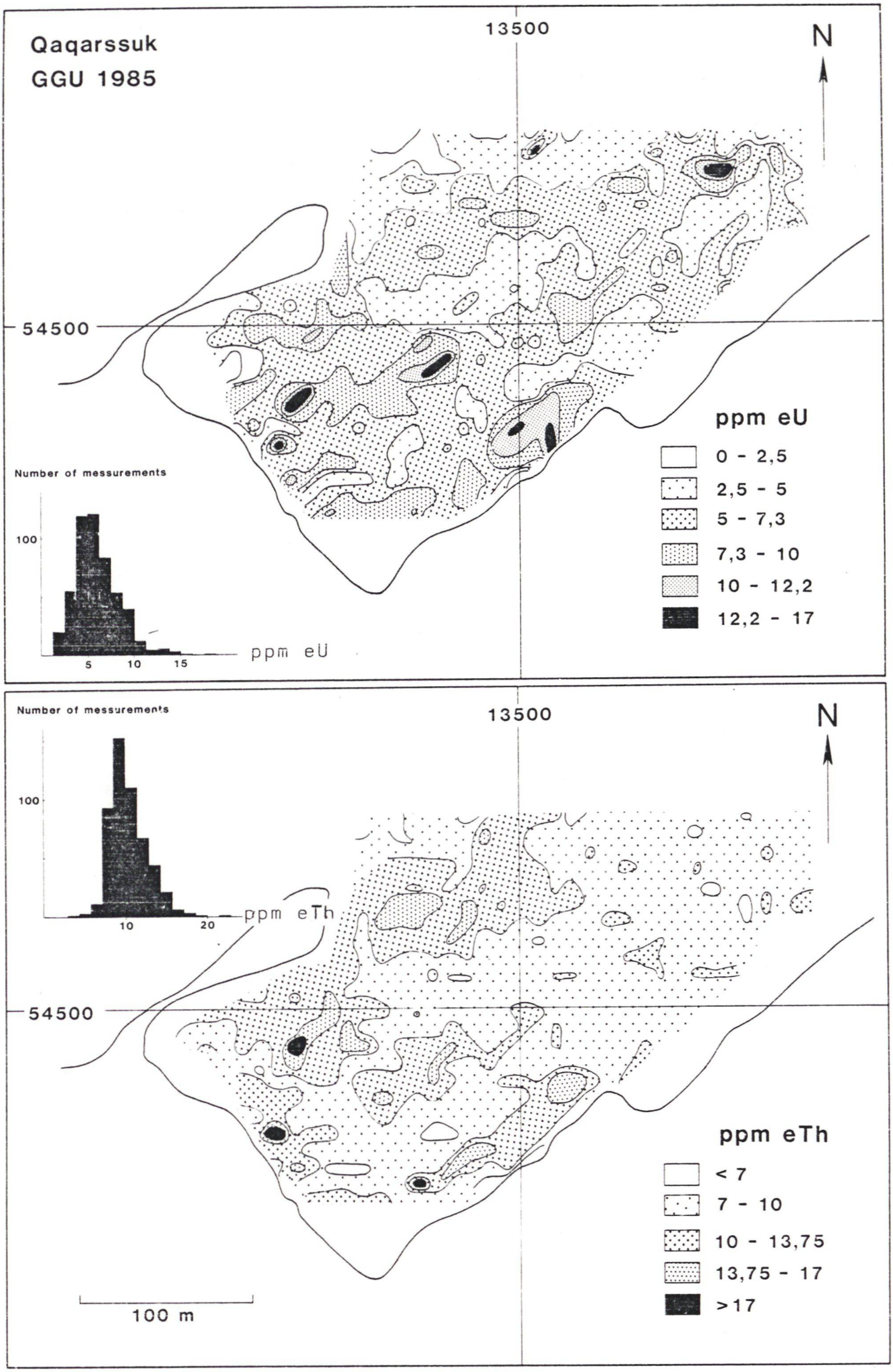
Qaqarssuk
GGU 1985
13500
N
54500
Number of messurements
100
5
10
15
ppm eU
ppm eU
0 - 2,5
2,5 - 5
5 - 7,3
7,3 - 10
10 - 12,2
12,2 - 17
Number of messurements
100
10
20
ppm eTh
13500
N
54500
ppm eTh
< 7
7 - 10
10 - 13,75
13,75 - 17
>17
100 m

Fig. 59.

with lanthanides, but with a low lanthanide/Th ratio compared to the lanthanide-rich carbonatites in the core of the complex.

In 1985, a four channel radiometric survey was carried out in the central parts of the complex. Two areas were selected (fig. 55).

1. The first area was located where outcropping lanthanide carbonatite was abundant. The area was investigated in a 25 m x 25 m grid to test whether it was possible to map the major lanthanide-rich carbonatites and the boundary between the fenite (with relatively high radiometric background) and the ultramafites and carbonatite (with relatively low radiometric background).
   The result of this survey was that the grid point frequency was too low to pick up all major lanthanide-rich carbonatites. However, the anomaly pattern (fig. 58) reflects the orientation of the lanthanide-rich carbonatites. Apart from this, the boundary between fenite on the one side and the carbonatite-ultramafic rocks on the other was mappable with the radiometric survey.
2. The second area was located over Nb and La anomalies in soil, an area without outcrops. Distance between measuring points was 10 m x 10 m. This survey showed that the Nb and La-rich soil samples were located over radiometric anomalies (fig. 53, 54 and 59). As seen on fig. 59 both eTh and eU anomalies trend NE-SW, parallel to the major part of the late søvites in the area, and to many lanthanide-rich carbonatites in the core of the complex. The presence of both late søvite and lanthanide-rich carbonatite was verified by digging in the soil at the radiometric anomalies.
   As can be seen on fig. 59 the eU and eTh anomalies are not located on top of each other, but rather on strike with each other. This is taken to indicate that the Th-rich rocks (the lanthanide-rich

carbonatites) and the U-rich rocks - (pyrochlore-rich rocks) are located in the same fractures or veins, but that the lanthanide-rich carbonates and the pyrochlore are precipitated at different locations/facies in the same vein.

5.10. SUMMARY AND CONCLUSION

5.10.1. *Summary of the geological evolution of the Qagarssuk Carbonatite Complex*

5.10.1.1. *Age and structural control of the intrusion*

The carbonatites were intruded into the Archaean basement 173 my ago. The semirectangular outline of the complex and the outer carbonatite sheets are controlled by preexisting fault and fracture zones, which probably were reactivated during large scale tectonic events as the opening of the North Atlantic. The space for the intrusion is likely to have been be provided with en échelon offset in an appr. 50° trending dextral fault.

The fenite as well as the carbonatite are generally highly strained, and the textures indicate that the fenite and the major part of the carbonatites have been deformed by solid state ductile deformation. The late søvite is generally less deformed and the lanthanide-rich carbonatites are undeformed, indicating that these rocks were emplaced late and after deformation in the complex. The onion-like shape of the complex and the outwards dipping foliations and plunging lineations indicate that the core of the complex got its shape by diapiritic rise of hot, volatile-rich fenites and carbonatites.

5.10.1.2. *Alteration of basement rocks*

During the intrusion, the mafic and felsic basement rocks adjacent to the carbonatite were altered by extensive metasomatism. The early fenitisation is characterised by alkali-pyroxenes and albite, whereas later fenitisation is characterised by alkali-amphiboles and albite, indicating an increase in the H_2O pressure during the evolution of the fenite. The degree of alteration of the basement decreases with decreasing distance from the carbonatite causing the alteration, and the thickness of the metasomatic aureole further depends on the thickness of the carbonatite. The sequence of metasomatic rocks with increasing distance from a carbonatite is (in felsic rocks): Ultramafite, fenite, quartz-bearing basement, (where plagioclase is altered to albite and plagioclase content is increased), basement with aegirine-augite and alkali-amphibole veins or joint surfaces. In the carbonatite there may be an increase in the amount of fenite inclusions and silicate minerals towards the contact.

The complex is surrounded by a hydrothermal aureole, within which the plagioclase is partly altered, whereas the mafic minerals is wholely transformed into mica. The magnetite has been altered to hematite, and the zone appears as a magnetic low on the magnetic anomaly map. This zone is radioactive due to Th mineralisation, mainly localised in narrow ankerite-calcite veins. Beforsite intrusions are mainly localised in this

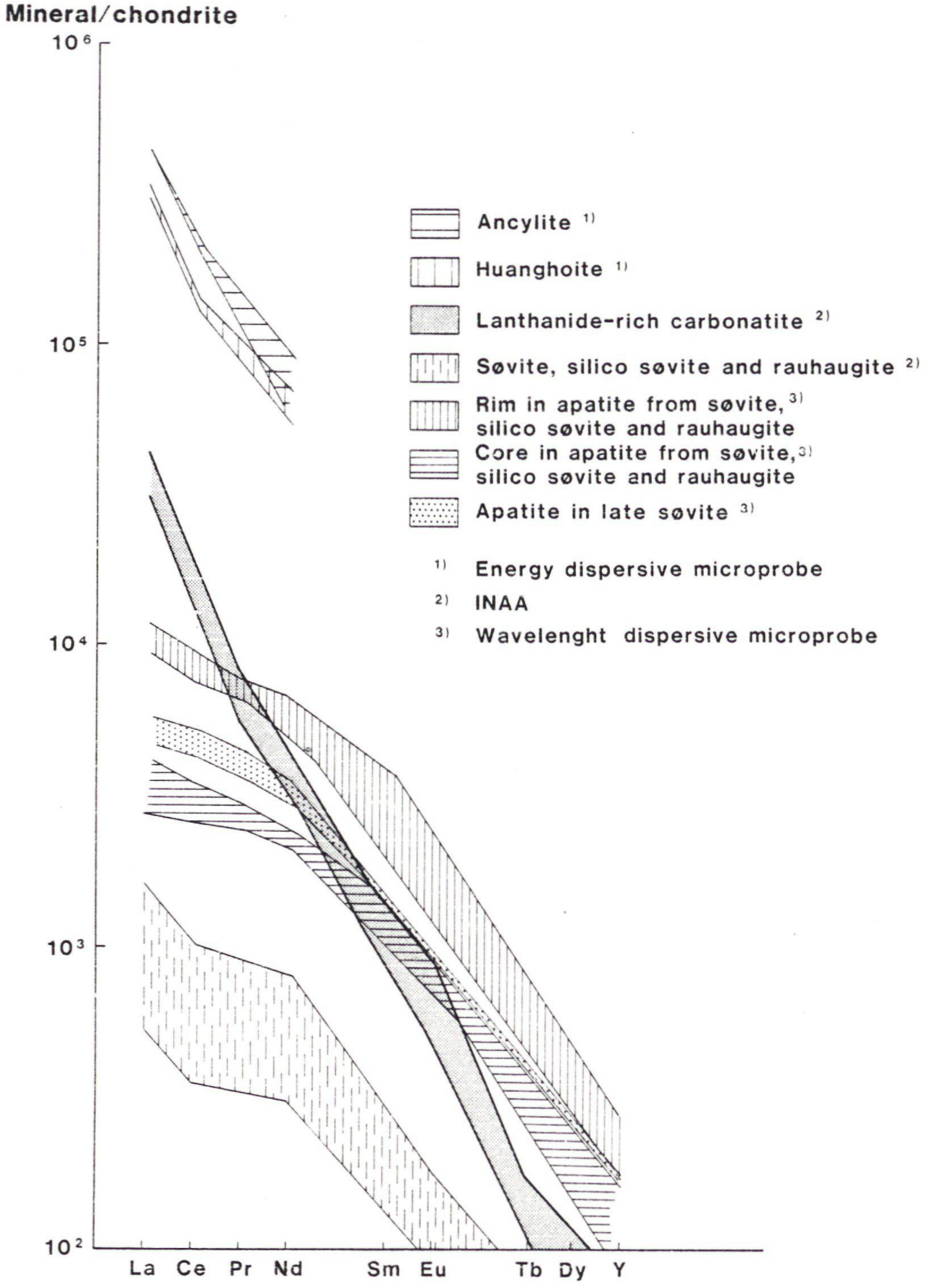

Chondrite normalised lanthanide and Y distribution for rocks and minerals from Qaqarssuk

Fig. 60.

zone, often associated with shear zones. The energy for the hydrothermal alteration must be derived from cooling of the hot diapir.

5.10.1.3. *Evolution of the carbonatites*

Rauhaugite and olivine-søvite are the carbonatites with the lowest content of e.g. lanthanides, and they are regarded as the most primitive carbonatites in the complex. The rauhaugite and the olivine-søvite have similar compositions. Where the olivine in søvite is hydrated, it is transformed to amphibole, phlogopite and magnetite, and the adjacent calcite is altered to dolomite. Aggregates of amphibole, phlogopite and magnetite are abundant in the rauhaugite, and the rauhaugite is likely to be the equivalent to the olivine-søvite, where this primitive carbonatite was intruded as minor dykes and veins and the olivine was hydrated.

Where larger sheets of carbonatite or closely spaced carbonatite sheets exceed appr. 20 m, the composition of the carbonatite is søvitic, and the adjacent basement is altered to ultramafic rocks as glimmerite, pyroxenite or hornblendite. These altered basement rocks are strongly enriched in Mg and locally P and Fe. Koster van Groos (1975) noticed that $MgCO_3$ in carbonatite melt dissociates more easily than $CaCO_3$, whereafter the Mg associates with the silicates. The thick søvitic carbonate sheets with their adjacent Mg-rich ultramafites are interpreted as formed by such a process. The loss of Mg^{2+} coupled with loss of $CO_3{}^{2-}$ explain the increase in lanthanides and other trace elements in the søvite and silico-søvite relative to rauhaugite and olivine søvite.

The concentration of elements as Nb, Ta, U, Th, Zr, base metals,

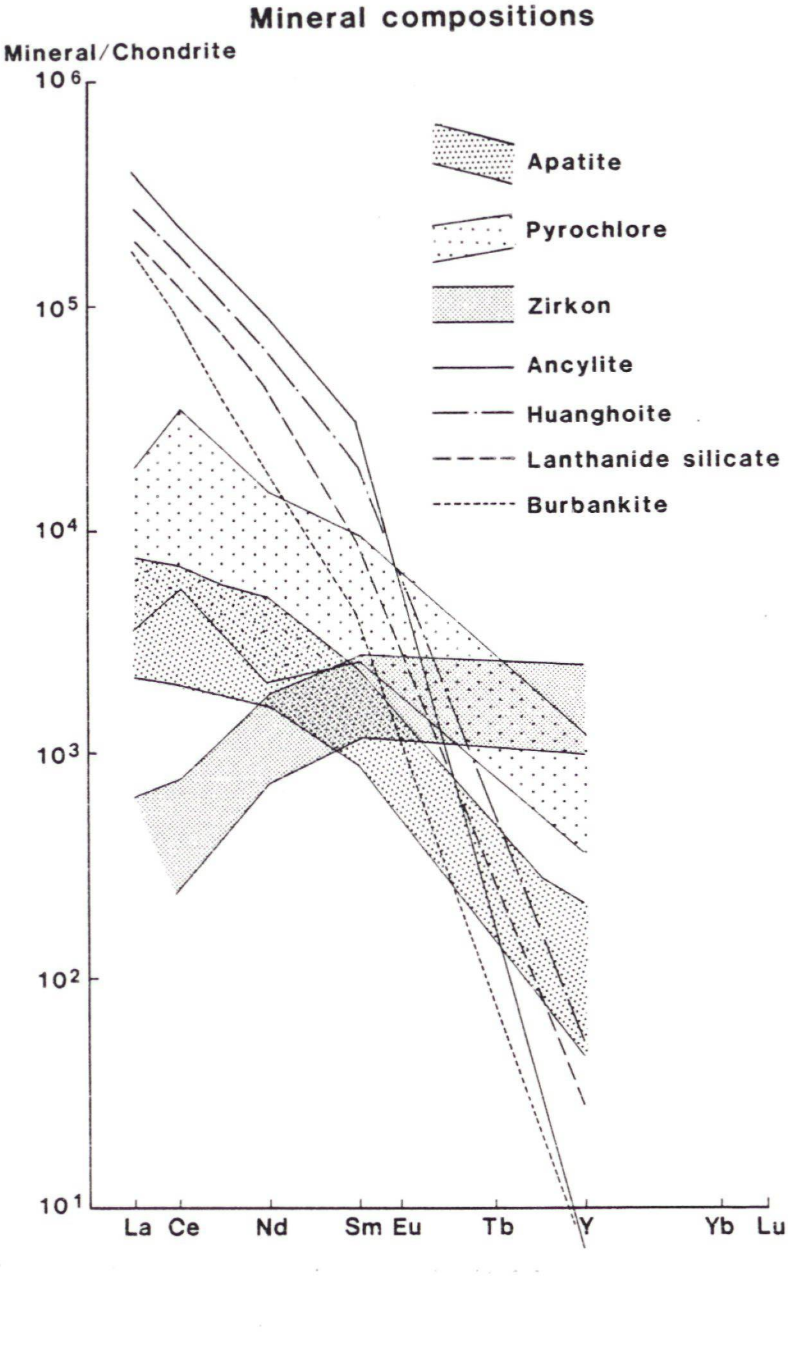
Mineral compositions
Mineral/Chondrite
10⁶
10⁵
10⁴
10³
10²
10¹
La
Ce
Nd
Sm
Eu
Tb
Y
Yb
Lu
Apatite
Pyrochlore
Zirkon
Ancylite
Huanghoite
Lanthanide silicate
Burbankite

Fig. 61.

lanthanides, Sr, Ba and P increases with decreasing age of the carbonatite, indicating that these elements are concentrated in the residual melt/fluid and precipitated in late dykes and veins. These elements are localised in different rock types/facies.

The late søvite contains elevated concentrations of the incompatible elements listed above, and the presence of blebs of acicular apatite indicates that the phosphate concentration in the melt exceeded the solubility limit and that immiscible droplets of phosphate melt were generated and quenched. The presence of such quenched, immiscible phosphate melts have been described by Sommerauer and Katz-Lehnert (1985) from the Kaiserstuhl carbonatites. The magnetite-apatite-pyrochlore-rich rocks are found as cumulates in late søvites and hence likely to be generated by settling of magnetite, pyrochlore and phosphate melt blebs often together with phlogopite, amphibole and zircon.

The lanthanides reach the highest concentrations in veins with abundant cavities and this indicates deposition from a fluid/gas phase, together with Sr and Ba. These veins are often associated with P, Nb, Zr and Fe mineralisation of the wall rock, contemporaneous with alteration of the wall rock into brown (tetraferri-phlogopite) glimmerite. The lanthanide-rich carbonatite veins are depleted in intermediate and heavy lanthanides (fig. 60) indicating that these were more mobile than the light. The intermediate lanthanides were precipitated in apatite and pyrochlore and the heavy lanthanides in zircon and pyrochlore (fig. 61). wall rock.

Table 6

Composition pf typical apatites from Qaqarssuk

GGU	320411		320438		320056	249866	320042	320439
No of anal.	9	7	9	8	7	14	2	5
	Core	Rim	Coarse	Acicular				
F	3.68	3.55	2.33	2.63	3.17	3.70	3.72	2.88
Na_2O	0.19	.31	0.25	0.23	0.32	.45	1.29	0.23
SiO_2	0.03	.02	0.04	0.04	0.25	.07	0.02	0.11
P_2O_5	41.68	41.70	41.00	40.21	40.79	40.18	31.45	40.74
CaO	54.60	53.33	53.51	53.91	54.21	52.58	45.40	55.37
SrO	0.52	.99	0.97	0.82	0.36	1.30	2.46	0.47
BaO	-	0.01	-	.01	-	0.01	2.38	0.02
MnO	0.05	0.01	-	-	-	0.05	nd	-
La_2O_3	0.11	0.35	0.22	0.19	0.19	0.37	.16	0.11
Ce_2O_3	0.29	0.73	.51	0.45	0.44	0.81	nd	0.28
Nd_2O_3	0.15	0.32	.41	0.22	0.22	0.37	0.04	0.13
Sm_2O_3	0.03	0.05	-	0.03	.04	0.04	nd	0.02
Dy_2O_3	0.01	-	-	0.01	.01	0.01	nd	0.01
Y_2O_3	0.03	0.05	.05	0.03	0.05	0.04	nd	0.03
Total	101.37	101.42	99.29	98.78	100.05	99.98	86.92	100.60

320411	Rauhaugite
320438	Apatite-magnetite-pyrochlore-rich rock
320056	Fenite
249866	Late søvite
320042	Lanthanide-rich vein
320439	Pyroxenite

nd: not determined

5.10.1.4. *Chemical evolution of the apatite*

The correlation of Na and lanthanide contents in the apatite indicates substitution of the endmember vitusite $Na_3(La,Ce)(PO_4)_2$ in the apatite. The over-representation of the intermediate lanthanides as Nd and Sm in the apatite relative to host carbonatite (fig. 49 and 62) is consistent with the higher partition coefficients for these elements relatively to the other lanthanides. (Watson and Green, 1981).

The zoning of the apatite (fig. 48, 49, 50 and 62) indicates that the apatite crystallised at two stages, an early stage - possibly before the carbonates, and then again (after a period of apatite dissolution) a later stage when carbonate had been crystallising for a while, thereby raising the lanthanide and Sr concentration in the residual melt.

The apatite in the ultramafic rocks has a composition similar to the early carbonatite, indicating that the apatite in these rocks was formed early - before the final solidification of the carbonatite.

The K_{Ap}^{REE} increases with decreasing temperature whereas the K_{Ap}^{Sr} is constant, which is the probable explanation for the lower Sr/lanthanide ratio in the - presumably colder - fenite.

The strong enrichment in intermediate lanthanides in apatite from some fenites is likely to be generated by precipitation of apatite from a solution already enriched in these elements, probably derived from dissolved apatite.

5.10.1.5. *Summary of processes responsible for apatite accumulation.*

Metasomatism.

The bimodal distribution of P_2O_5 in the fenite indicates that there was an influx of phosphate into some of the basement rocks during the fenitisation. This process is of limited economic importance as no fenites with more than 2 wt% P_2O_5 were found.

The apatite enrichment in the ultramafic rocks is due to metasomatic influx of phosphorus. The most extreme enrichment is seen where ultramafic rocks (glimmerites) are cut by lanthanide-rich carbonatite veins. The wall glimmerite may contain as much as 10 wt% P_2O_5 and often pyrochlore as well (Interim report 3, fig. 4). The precipitation of phosphate in the ultramafic rocks is caused by decrease in temperature and pressure and increased silica activity causing a decrease in phosphate solubility.

Crystal accumulation

The morphology of the skeletal olivine and the skeletal magnetite in søvite and olivine søvite indicates that these minerals may have formed in a (carbonatitic) melt undergoing rapid solidification. The concentration of these minerals in certain layers suggests that these minerals locally were accumulated by a crystal sorting process, in a melt with sufficiently low viscosity. Following this line, the most likely explanation of the bimodal distribution of phosphorus in the søvite and olivine søvite, is that the apatite was accumulated in a similar process, as soon as it crystallised. The very elongated apatite inclusions in olivine indicate that the early apatite was formed as slender needles - i.e. crystallised from a cooling liquid (Wyllie et al., 1962).

Wall-rock contamination

The apatite content in the silico-søvites is higher than the average søvite, which is likely to be explained as precipitation of apatite due to increased silica activity in the carbonatite (Watson, 1979) by incorporation of wallrock.

Liquid immiscibility

The rounded bleb-like shape of the apatite in the late søvite and magnetite-apatite-pyrochlore rock together with the very fine-grained apatite in these aggregates is interpreted as quenching of phosphate droplets derived by liquid immiscibility of phosphate in carbonatite.

5.10.2. *Phosphate potential of the Qagarssuk Carbonatite Complex*

The average phosphate content in the carbonatite is 1.37wt% P_2O_5 (mean of 165 grab samples), and thus the carbonatite can be regarded as a large, but very low grade deposit. However, there are locally high apatite contents in silico-søvite, ultramafite, rauhaugite and in magnetite-apatite-pyrochlore rock associated with the discordant søvites.

5.10.2.1. *The resources*

At several localities, thick apatite-rich layers of *silico-søvite* with an average of 3.5 to 6 wt% P_2O_5 are found, in the core of the complex. One of these layers is 12 m thick and can be followed over 100 m along the strike before it disappears under overburden. This locality contains at least 0.75 million ton of ore with 3,85 wt% P_2O_5 calculated to a depth of 200 m. Three occurrences of apatite-rich silico-søvite more than 10 m thick, found by drilling carried out by Kryolitselskabet Øresund A/S, could not be followed along the strike, due to the relatively low density of drill holes. They are, however, likely to have similar dimensions as the above-mentioned. The apatite-rich ultramafites are often found associated with the apatite-rich silico-søvites.

Apatite-rich *rauhaugites* are found as sheets up to 13 m thick in the marginal parts of the complex where they can be followed more or less continuously parallel to the margin of the complex. The rauhaugite contains 1 to 6 wt% P_2O_5 with an average of 2.66 wt% P_2O_5 (average of 16 grab samples). A 13 m thick rauhaugite sheet was chip sampled (including fenite inclusions) and yielded 3.40 wt% P_2O_5. This sheet could be followed over appr. 200 m, which gives 0.75 mill t of ore, calculated to a depth of 200 m.

The *apatite-magnetite-pyrochlore rock* is found as sheets up to 10 thick with an average P_2O_5 concentration of 8.59 wt%. In one area, the apatite-magnetite-pyrochlore rock is abundant (west of the camp), and causes a strong magnetic anomaly indicating the presence of the rock at least 100 m along the strike, which - with an assumed average thickness of 10 m and depth of 200 m - gives .8 mill t of ore with an average of 8.6 wt% P_2O_5 and 0.8 wt% Nb.

The surface *soil* covering the carbonatite and ultramafite has an elevated P_2O_5 content relative to the bedrock (Kunzendorf & Secher, in press). Below this, there is a *residual soil* (a regolith) in which the structure in the carbonatite and ultramafite locally is preserved. The thickness of this regolith is very variable up to 25 m and with an estimated average of 3 m in the floors of the valleys (Kjærgaard & Olsen, 1985). The P_2O_5 content in the residual soil is generally less than 2 wt% P_2O_5, but in the northern part of the complex residual soil with 6 - 8 wt% is found to a depth of at least 3 m. However, this regolith occurs only over an area of appr. 10,000 m^2.

The four occurrences of silico-søvite with appr. 3.5 wt% P_2O_5 and and estimated tonnage of 0.75 mill. t (each), one occurrence of rauhaugite with 3.4 wt% P_2O_5 and estimated 0.75 mill. t and one occurrence with 0.8 mill. t of apatite-magnetite-pyrochlore rock with 8.6 wt% P_2O_5 gives a total of 4.55 mill. t of ore with average 4.4 wt% P_2O_5 .

Further exploration in the area is likely to increase the tonnage with a factor 2 or 3. The "theoretical" maximum amount of phosphate which may be concentrated in rock types with elevated P_2O_5 content can be calculated as follows: The søvite is assumed to be derived from rauhaugite by loss of mainly Mg, CO_2 and P. The average rauhaugite has appr. 2.5 wt% P_2O_5 , the average søvite has appr. 1 wt% P_2O_5 . The søvite covers an area of appr. 1.2 mill. m^2. Calculated down to a depth of 200 m this gives a total of 720 mill. t søvite which in average has lost 1.5 wt% P_2O_5, i.e. 10.8 mill. t of P_2O_5.

The lanthanide content in the apatite is approximately 0.6 to 0.7 wt% (oxide), which is similar to or slightly higher than Kola phosphate from which the lanthanides has been recovered.

The *cadmium content* of the apatite varies from 0.1 to 0.2 ppm, table 2, which is low compared to sedimentary phosphate but similar to that found in other igneous apatites. The apatite from Qaqarssuk (and Sarfartoq) must from this point of view be regarded as an attractive raw material for use in the fertilizer production.

5.10.2.2. *Infrastructure*

The Qaqarssuk Carbonatite Complex is situated 20 km from the coast, close to the Kangia valley, giving easy access to the coast. The area has presently no infrastructure. Sukkertoppen, which is the nearest city with helicopter facilities and harbour, is situated 55 km west of Qaqarssuk. Søndre Strømfjord airport is situated 180 km north of Qaqarssuk, but an old airship is located in the Kangia Valley 20 km from the core of the complex.

5.11. SELECTED REFERENCES:

Gothenborg, J. & Pedersen J. L. 1976: Exploration of the Qaqarssuk carbonatite complex, 1975, Part II, Kryolitselskabet Øresund A/S, unpubl. company report.

Gothenborg, J., Keto, L. & Pedersen, J. L. 1977: Exploration of the Qaqarssuk carbonatite complex 1976. Kryolitselskabet Øresund A/S. Unpubl. company report.

Kjærgaard, M. & Olsen, K. B. 1985a: Shallow-seismic, geoelectric and magnetitc investigation of the the Qaqarssuk carbonatite complex, West Greenland. Rapp. Grønlands geol. Unders. **125**, 140-144.

Kjærgaard, M. & Olsen, K. B. 1985: Geoelectric and seismic investigations at Qaqarssuk. Lab. for Geophysics, University of Aarhus, Unpubl. report 64 p.

Knudsen, C. 1985: Investigation of the Qaqarssuk carbonatite complex, southern West Greenland, Rapp. Grønlands geol. Unders. 125, 35-40.

Knudsen, C. In press: Apatite accumulation in the Qaqarssuk Carbonatite Complex, southern West Greenland. *In* R. P. Sheldon and A. J. G. Notholt (eds), Phosphate deposits of the world (Vol. 2).

Kunzendorf, H. & Secher, K. In press: Dispersion of niobium and phosphorus in soil overlying the carbonatite complex Qaqarssuk, southern West Greenland. J. geochem. Explor.

Kurki, I. & Juhava, R. 1971: Report on the exploration work in Søndre Isortoq Area, 1970: Unpubl. company report.

Vuotovesi, T. 1974: Qaqarssuk carbonatite complex. Unpubl. MSc thesis (in Finnish - translated to English by T. Tukiainen).

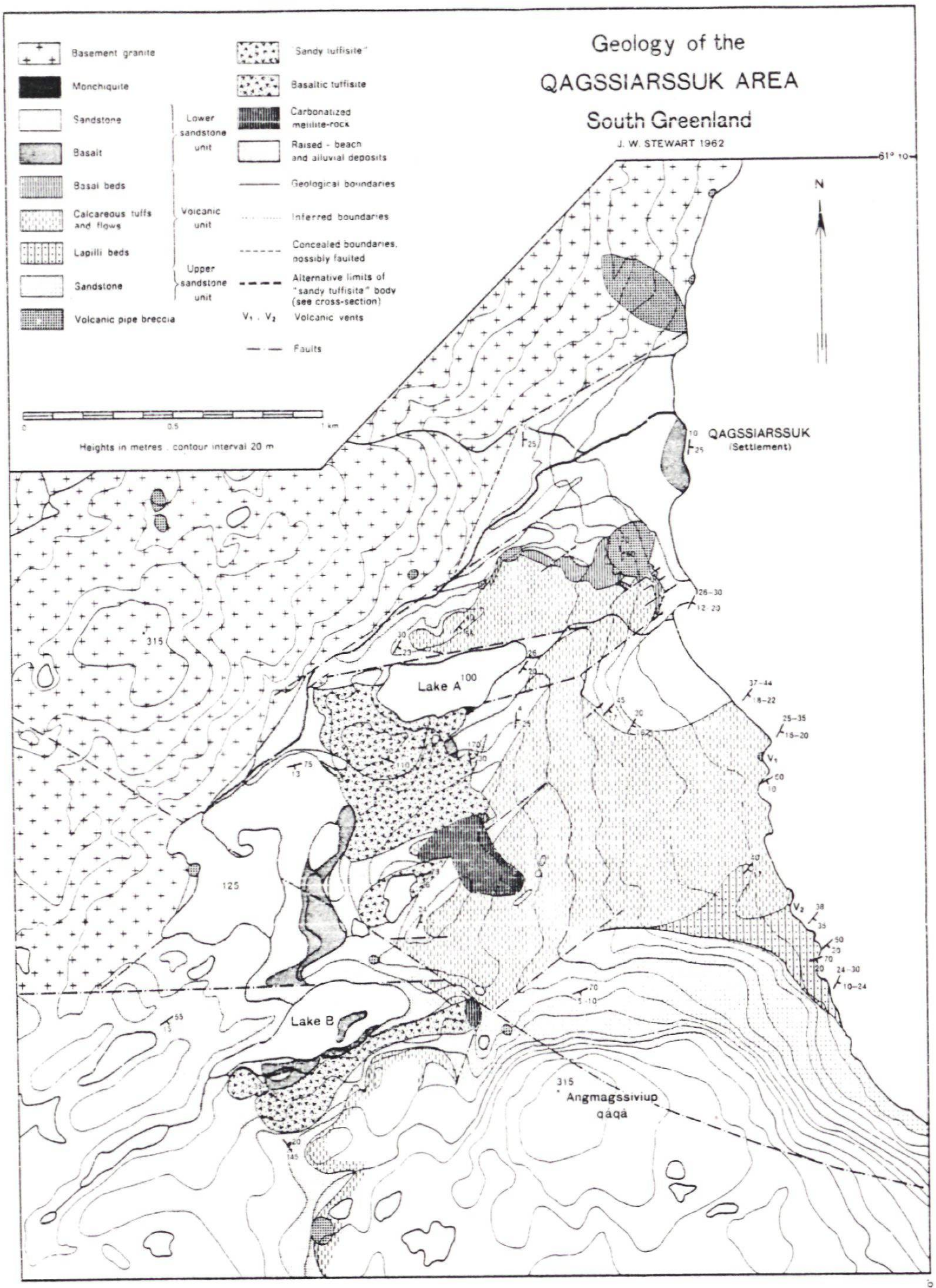

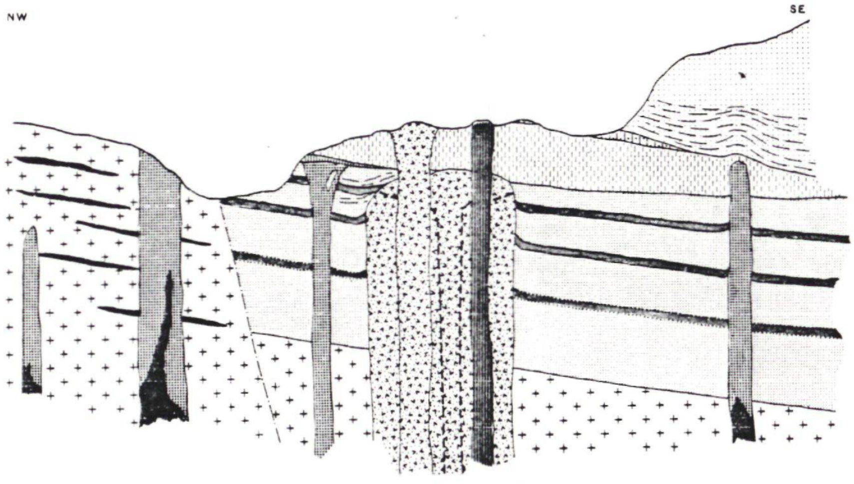

Schematic cross-section through the Qagssiarssuk area in a roughly north-west — south-east direction. Overall length ca. 3 km; vertical component of relief exaggerated ca. 2½ times.

Fig. 62. From Stewart (1970).

6. PHOSPHATE POTENTIAL OF THE INTRUSIVE AND EXTRUSIVE CARBONATITES AND ALKALINE SILICIC ROCKS IN THE GARDAR IGNEOUS PROVINCE, SOUTH GREENLAND

6.1. INTRUSIVE AND EXTRUSIVE CARBONATITE AT QASSIARSUK

6.1.1. *General geology*

In the Qassiarsuk area, situated just across the fiord from the Narsarsuaq airport, a series of continental clastic sediments, lavas and pyroclastic rocks of the Eriksfjord Formation unconformably overlie the pre 1600 m.y. crystalline basement (fig. 62). These rocks are about 1300 m.y old and formed early in the evolution of the Gardar igneous alkaline province (Stewart, 1970). The sequence contains an approximately 30 m thick volcanic unit consisting of thin layers of carbonated vesicular lava overlain by bedded calcereous tuffs and agglomerates.

The basement as well as this volcanic unit are cut by tuffisite diatremes and vents, containing blocks of søvite, orthoclasite and country rocks in a matrix that is either monchiquite, carbonatite or mica-peridotite. The basement is cut by numerous carbonatite and lamprophyre dykes and sills. These strongly alkaline intrusions are associated with K metasomatism of the adjacent basement, and often surrounded by K-fenite.

TABLE 7

Whole rock analyses of rocks from Qassiarssuk.

GGU No	320207	320211	320209	320256	320216	320231	320257
SI02	19.10	24.06	2.60	8.14	24.52	5.09	7.71
TI02	0.17	3.48	0.40	1.72	3.39	0.02	0.25
AL203	0.28	3.33	0.90	2.59	3.00	0.05	1.17
FE203	2.51	10.38	2.60	8.81	12.89	6.08	12.95
FE0	0.29	1.20	1.52	0.15	0.00	0.18	0.00
MN0	0.25	0.27	0.67	0.44	0.24	0.11	14.20
MG0	1.04	10.95	15.97	1.49	10.90	-0.02	0.68
CA0	40.91	18.59	31.06	41.77	18.54	47.56	27.43
NA20	0.02	0.08	0.02	0.04	0.00	0.07	0.14
K20	0.04	0.96	0.03	0.92	0.17	0.01	0.03
H20	30.10	22.23	36.80	29.89	23.41	0.74	3.13
P205	3.13	3.12	3.81	3.51	1.89	35.18	20.23
Sum	97.88	98.65	96.38	99.47	98.95	95.07	87.92

320207	Sovite dyke
320209	Rauhaugite lava
320211	Sandy tuffisite
320216	Lapilli tuff
320231	Apatite rich lamprophyre-margin
320256	Carbonatitic lava with relict melilite or nyerereite
320257	Black apatite-manganese rock

6.1.2. *Distribution of apatite*

The apatite-rich rocks in the Qassiarsuk area can roughly be divided into the following groups:

a. Intrusive carbonatites and carbonated ultramafic rocks.
b. Extrusive carbonatites and calcareous tuffs.
c. Hydrothermally altered margins of carbonatite and lamprophyre intrusions.

6.1.2.1. *Intrusive carbonatites and carbonated ultramafic rocks*

Samples of two *søvite dykes* have been analysed (3.10 and 3.04 wt% P_2O_5, respectively). The apatite is found as needles with abundant fluid and solid inclusions near the rim (fig. 65).

Samples of three *rauhaugite dykes* have been analysed (3.67, 3.16 and 0.30 wt% P_2O_5, respectively.) The phosphate-rich carbonatite is coarser and more iron-rich than the phosphate-poor variety. The most phosphate-rich carbonatite occurs as a composite sheet intrusion cutting mica-peridotite (Stewart, 1970).

Six samples of *carbonated ultramafite* have been analysed (0.18 to 3.10 wt% P_2O_5). The highest values are found in samples with pseudomorphosed melilite or nyererite. These rocks are also characterised by a relatively high TiO_2 content varying from 1.6 to 3.8 wt%. The apatite is found as radiating clusters of euhedral crystals. The higher

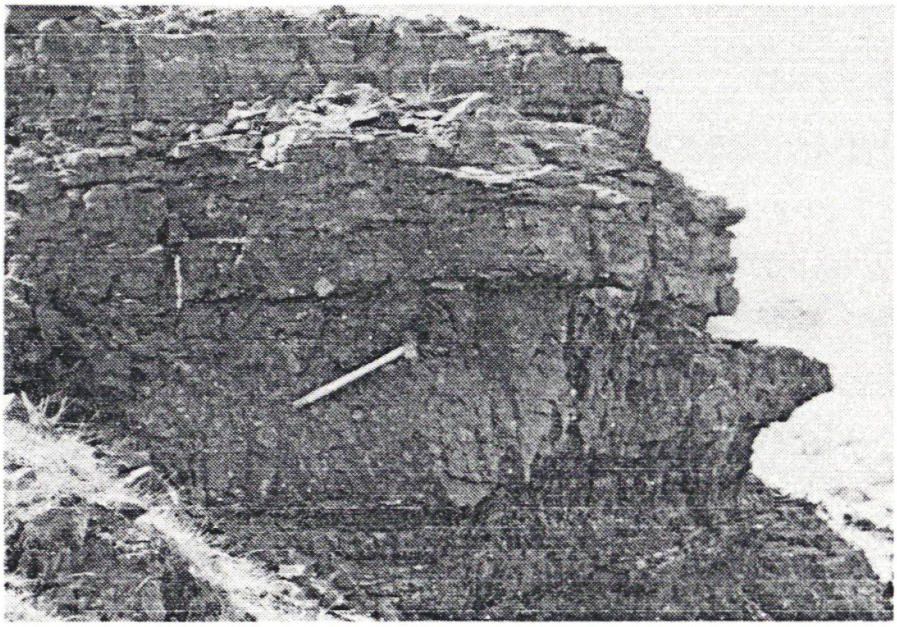

Fig. 63. Vesicular carbonatite lava sheet (at the hammer) on top of a calcareous tuff.

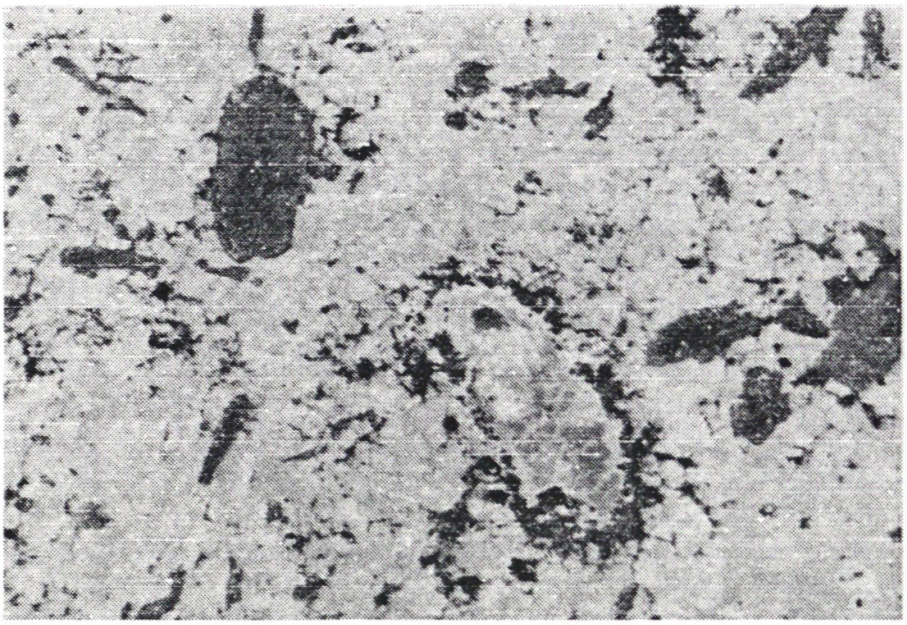

Fig. 64. Zoned apatite (A) in carbonatite (søvite) lava. The core of the apatite is dark and has low lanthanide content, whereas the rim has a higher lanthanide content. The rim is rich in calcite inclusions. The microphotograph is 2 mm vertically, cathodoluminescence. GGU 320209.

P_2O_5 values were found in a rock mapped as "sandy tuffisite" by Stewart (1970). This has the shape of a vertical cylinder with a horizontal area of approximately 0.25 km^2. A chip sample of this rock type collected (by A. Jones) in 1985 gives 2.14 wt% P_2O_5.

6.1.2.2. *Extrusive carbonatites and calcareous tuffs*

Five samples from *carbonatite lava* flows (fig. 63), varying from .5 to 2 m in thickness, have been studied. One fine-grained, vesicular carbonatite lava (GGU 320209) has a P_2O_5 content of 3.78 wt%. Both søvite and rauhaugite have elevated phosphate content and the apatite is found as slightly resorbed needles with inclusion-rich rims. This is similar to what is seen in the intrusive carbonatites, and these rocks are probably the extrusive equivalent to the rauhaugite and søvite dykes, respectively.

Four carbonated lavas rich in pseudomorphs of the nyererite or melilite have been analysed and have P_2O_5 content ranging from 1.84 to 3.48 wt%. (GGU 320256 has 3.48 wt%). The apatite is similar to the above described.

During the field season 1985 chip samples were collected to test whether the P_2O_5 content in GGU 320209 and 320256 was representative for the rock units, - which they are. (The chip samples yielded 3.79 wt% P_2O_5 for GGU 320209 and 3.48% P_2O_5 for GGU 320256.)

The extrusive carbonatites at Qassiarsuk cover an area of approximately 2 km^2.

Seven samples of *lapilli tuff* and *fine-grained calcareous tuff* have been analysed and have P_2O_5 contents varying from .11 to

TABLE 8

	COMPOSITION OF APATITE FROM QASSIARSSUK								MOTZFELDT	GRØNNEDAL-IKA
GGU	320209			320211	320216	320231	320233	320251	58111	320268
N	4	3	3	4	1	2	5	2	11	8
	Core	Int.	Rim							
F	3.70	3.10	4.40	2.15	ud	4.85	3.1	ud	2.95	3.68
Na_2O	0.05	0.06	0.05	0.05	0.35	-	.04	-	0.12	0.13
SiO_2	0.03	0.09	0.02	1.01	0.2	-	.3	-	0.54	0.06
P_2O_5	41.08	40.71	41.43	38.4	41.0	40.9	41.0	41.4	39.41	41.85
CaO	53.31	54.05	54.52	54.2	53.7	54.6	55.4	54.3	53.24	54.28
SrO	1.29	0.97	0.44	2.25	1.12	1.23	0.09	1.17	1.64	0.93
BaO	ud	ud	ud	0.18	0.02	.01	ud	0.02	0.02	-
La_2O_3	0.07	0.06	0.03	0.018	0.06	0.025	0.13	0.08	0.40	0.09
Ce_2O_3	0.13	0.13	0.11	0.016	0.13	0.038	0.29	0.17	0.68	0.29
Nd_2O_3	0.03	0.03	0.14	0.012	0.09	0.014	0.09	0.08	0.25	0.18
Sm_2O_3	ud	ud	ud	-	0.006	0.011	-	0.02	0.02	0.03
Dy_2O_3	ud	ud	ud	-	0.02	0.016	ud	0.003	-	0.04
Y_2O_3	0.05	0.02	0.01	0.019	0.034	0.076	ud	0.03	0.08	0.11
Total	99.74	99.22	101.24	98.305	96.73	101.77	100.44	96.883	99.35	101.67

320209	Carbonatite lava	320231	Apatite rich rock adjacent to lamprophyre
320211	Sandy tuffisite	320233	K-fenite
320216	Lapillituff	320251	Martite tuff

ud: undetermined

3.31 wt%. It has not been possible to confirm earlier reported high P_2O_5 values in tuff (Interim report No. 3), and the phosphate mineralisation of tuff mentioned in interim report No. 3 must be of minor importance.

6.1.2.3. *Hydrothermally altered margins of carbonatite and lamprophyre intrusions*

The highest P_2O_5 values are found in fenites around carbonatite and lamprophyre intrusions in the region from Igaliko in the south to Qassiarsuk in the north. The apatite is very fine-grained and intergrown with iron and/or manganese oxides. The width of these alteration zones rarely exeeds a few metres, and even though the P_2O_5 content may be as high as 29 wt%, the total amount of phosphate in these zones is low.

6.1.3. *Apatite composition.*

The apatite from Qassiarsuk is fluor-apatite characterised by a fairly low lanthanide content and less fractionated lanthanide distribution (fig. 65) relative to apatite from other carbonatites in Greenland. The Sr content is 0.5 - 2.5 wt% (fig. 66).

The low lanthanide content of the apatite from Qassiarsuk may indicate a low lanthanide partition coefficient compared to apatite from Qaqarssuk, found in rocks with similar lanthanide contents.

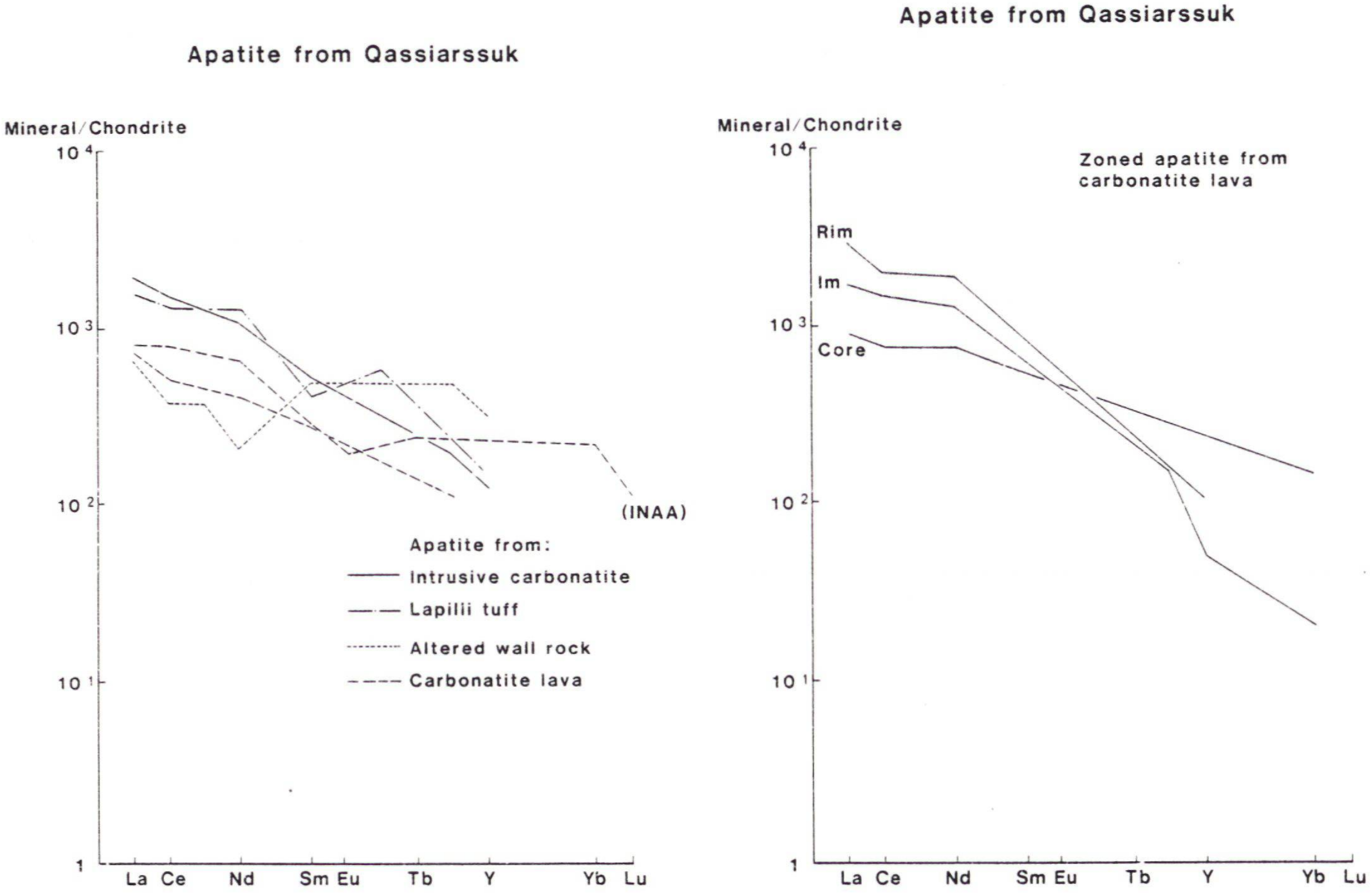
Apatite from Qassiarssuk
Mineral/Chondrite
10^4
10^3
10^2
10^1
1
La Ce Nd Sm Eu Tb Y Yb Lu
(INAA)
Apatite from:
Intrusive carbonatite
Lapilli tuff
Altered wall rock
Carbonatite lava
Apatite from Qassiarssuk
Mineral/Chondrite
Zoned apatite from carbonatite lava
Rim
Im
Core
10^4
10^3
10^2
10^1
1
La Ce Nd Sm Eu Tb Y Yb Lu

Fig. 65.

6.2. APATITE-ENRICHED SYENO-GABBRO ASSOCIATED WITH ALKALINE SILICIC ROCKS IN THE GARDAR IGNEOUS PROVINCE

Apatite-enriched syeno-gabbro has been reported from several alkaline igneous complexes in the Gardar Province, South Greenland. Recently apatite-rich rocks from a dyke are reported by Upton et al (in press). This is a 20 km long and 0.5 km wide dyke (1154 +/- 16 my), composed of a mafic border group and a salic central zone. The highest apatite concentrations are found in the syeno-gabbro of the border zone, where apatite has accumulated by crystal fractionation from a P_2O_5-rich magma. The P_2O_5-content ranges from 1.5 to 3.5 wt%. The salic central zone is related to the border zone, but injected later - after further differentiation by crystal fractionation. The presence of presumably apatite-rich cumulates generated by this crystal fractionation is indicated by a gravity anomaly parallel to the giant dyke.

Similar apatite-rich syeno-gabbro is reported from the Narssaq intrusion (D. Olsen, pers. comm.) and the Kûngnât igneous complex (Upton, 1960). The P_2O_5 ranges from 1.5 to 3.5 wt% in the syenogabbro, which further contains 3 to 5 modal% vanadium-rich magnetite (0.3 to 1.9 wt% V).

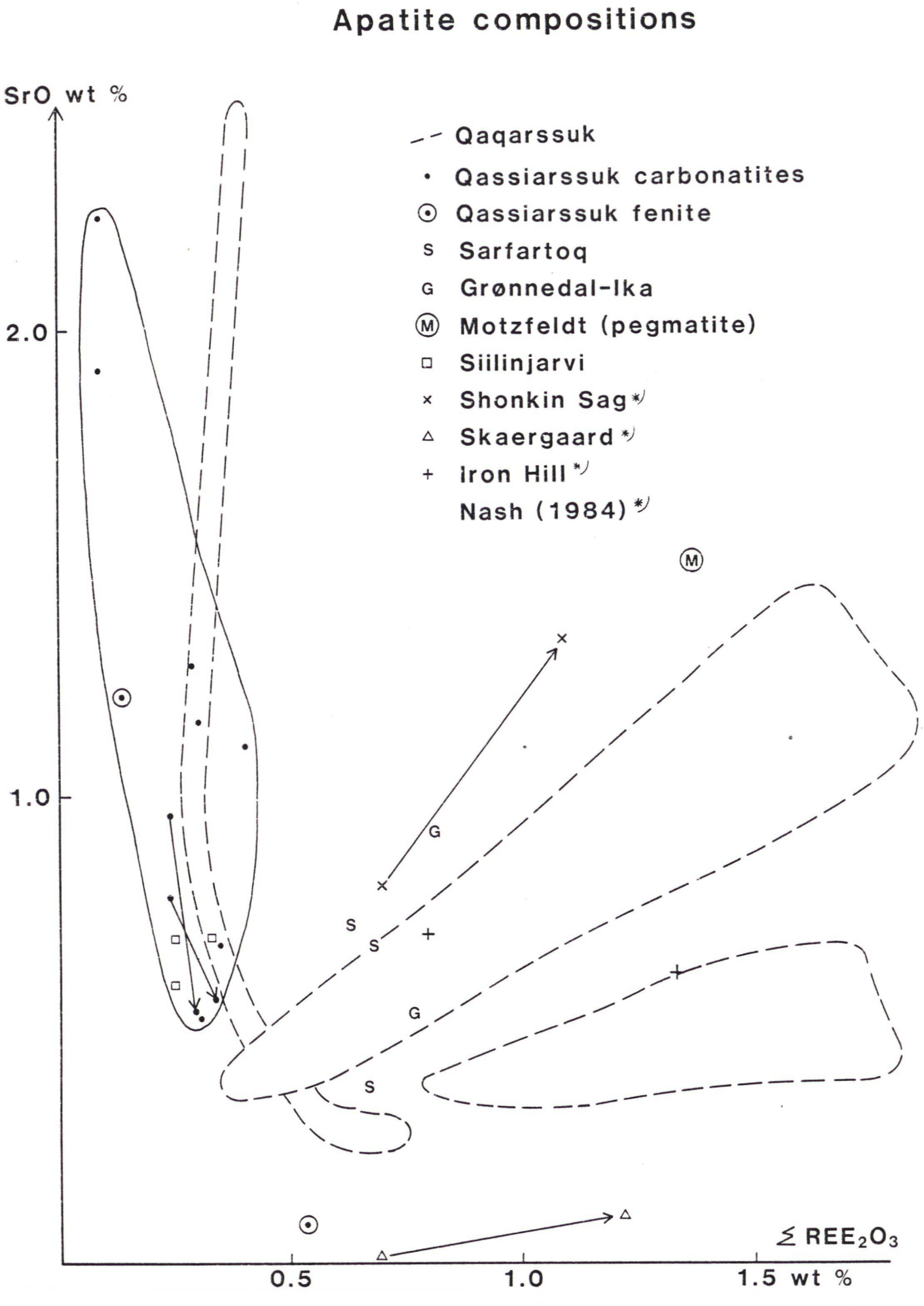
Apatite compositions
SrO wt %
2.0
1.0
0.5
1.0
1.5 wt %
Σ REE$_2$O$_3$
Qaqarssuk
Qassiarssuk carbonatites
Qassiarssuk fenite
S Sarfartoq
G Grønnedal-Ika
M Motzfeldt (pegmatite)
Siilinjarvi
× Shonkin Sag *)
△ Skaergaard *)
+ Iron Hill *)
Nash (1984) *)
M
G
S
S
S
G
S

Fig. 66.

6.3. CONCLUSION

The extrusive carbonatites at Qassiarsuk must be regarded as an interesting prospecting target/source for igneous phosphate because

1. The phosphate content is relatively high.
2. The phosphate-enriched rocks occur as horizontal layers near the surface.
3. The area has an existing infrastructure, and the extrusive carbonatites are situated within 2 km from the small harbour in Qassiarsuk. (The Narsarsuaq airport is situated just across the fiord.)

The apatite carrying syeno-gabbro must also be regarded as interesting from an economical point of view, as it is situated near the coast, it is associated with vanadium-rich magnetite, and the feldspar may find use as an industrial mineral.

6.4. SELECTED REFERENCES

Stewart, J. W. 1970: Precambrian alkaline-ultramafic/karbonatite volcanism at Qaqssiarssuk, South Greeland. Bull. Grønlands Geol. Unders., **84**. pp

Upton B. G. J. 1960: The alkaline igneous complex of Kûngnât Fjeld. South Greenland. Bull. Grønlands Geol. Unders. **27**, 145 pp

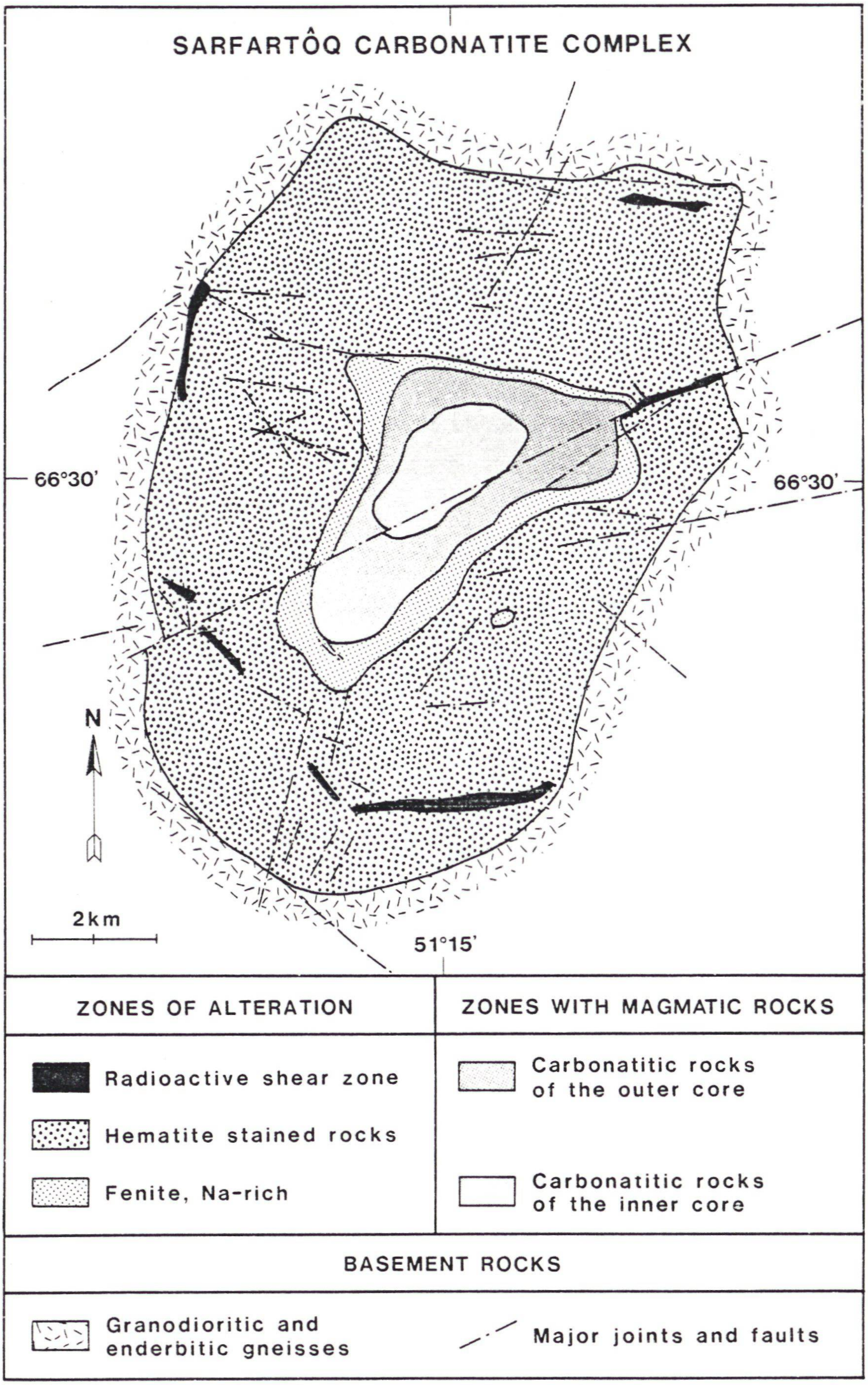

Fig. 67. From Secher (in press,a)

Upton, B. G. J., Stephenson, D. & Martin, A. R. 1985: The Tugtutôq older giant complex: mineralogy and geochemistry of an alkali gabbro-augite syenite-foyaite association in the Gardar Province of South Greenland. Mineralog. Mag.

7. THE SARFARTÔQ CARBONATITE COMPLEX

The complex is located in southern west Greenland (66°30'N, 51° 15'W), covering an area of 90 km^2. The complex is well exposed in the steep sides of the Sarfartôq valley although the central part is covered by glaciofluvial deposits in the bottom of the valley.

The following description is based on the work by Secher and Larsen (1980), Secher (in press, a) and on microprobe work by the author.

7.1. GENERAL GEOLOGY

The Sarfartôq Carbonatite Complex is located in the transition zone between the Archaean granulite facies; gneiss complex to the south and the Proterozoic, amphibolite facies Nagssugtoqidian mobile belt to the north. Dolomitic magma was intruded in two major stages of activity, approximately 600 my ago. During the first stage a suite of steeply inwards dipping carbonatite sheets was intruded. During the second stage several batches of magma were emplaced into a zone surrounding the rocks of the first stage, as concentric and radial dykes and agglomerates. The complex is divided into a core consisting of carbonatite and Na-fenite

TABLE 9

COMPOSITION OF APATITE

	Sarfartôq				Siilinjarvi		Kola
GGU	254335	254215	254267	254328	Fenite	Selico søvite	
N	5 & 21	2	5	12	16	14	4
F	2.71	2.49	ud	2.27	2.37	2.22	3.92
Na_2O	0.29	0.13	ud	0.18	0.1	0.13	0.12
SiO_2	0.08	0.03	ud	0.02	0.05	0.02	0.20
P_2O_5	40.44	39.77	ud	41.28	41.18	41.36	41.13
CaO	54.18	54.89	ud	54.77	55.38	54.75	52.77
SrO	0.74	0.38	0.54	0.68	0.70	0.64	3.35
BaO	-	-	0.01	0.01	ud	ud	-
La_2O_3	0.12	0.06	0.09	0.12	0.06	0.06	0.06
Ce_2O_3	0.33	0.17	0.23	0.28	0.12	0.19	0.30
Nd_2O_3	0.17	0.09	0.12	0.13	0.07	0.08	0.12
Sm_2O_3	0.02	0.01	0.02	0.02	ud	ud	ud
Y_2O_3	0.03	0.02	0.01	0.02	-	-	-
Sum	99.11	97.98		99.78	100.03	99.45	102.97

ud: undetermined

and a wide marginal zone as a rim consisting of altered basement rocks.

The *core* is divided into 3 zones based on the proportion of carbonatite to fenite (fig. 67). The inner core is dominated by carbonatite and covers an area of approximately 2 - 3 km^2. The poorly exposed inner core is supposed to be dominated by søvite. Locally lenses of glimmerite and bands in which magnetite constitutes up to 80% of the rock volume are found, but in general the amount of ultramafic rocks is low compared to e.g. Qaqarssuk Carbonatite Complex. The outer core is dominated by fenite and forms a 1 to 3 km wide ring occupying approximately 9 km^2. The fenite of the outer core is cut by rauhaugite sheets varying from 2 to 30 m in thickness and rauhaugite is the dominating carbonatite type and søvite only occurs sporadically. The outer core is surrounded by a narrow rim of fenite, - approximately 5 km^2.

The marginal *zone* is characterised by hematite staining, due to alteration of magnetite, and the complex occurs as a magnetic depression on the regional aeromagnetic anomaly map (Secher and Thorning, 1982). The rim contains mineralised veins and shear zones, rich in Nb, U and light lanthanides (in pyrochlore) or rich in Th and heavy lanthanides. The pyrochlore mineralisation is locally almost massive, and mineralised zones, several metres wide with 10 to 15 wt% Nb_2O_5 are found.

7.2. APATITE

Apatite is the only important phosphate-bearing mineral in the complex. Apatite occurs as euhedral to subhedral crystals in textures from disseminated via clusters and rosettes to large single crystals,

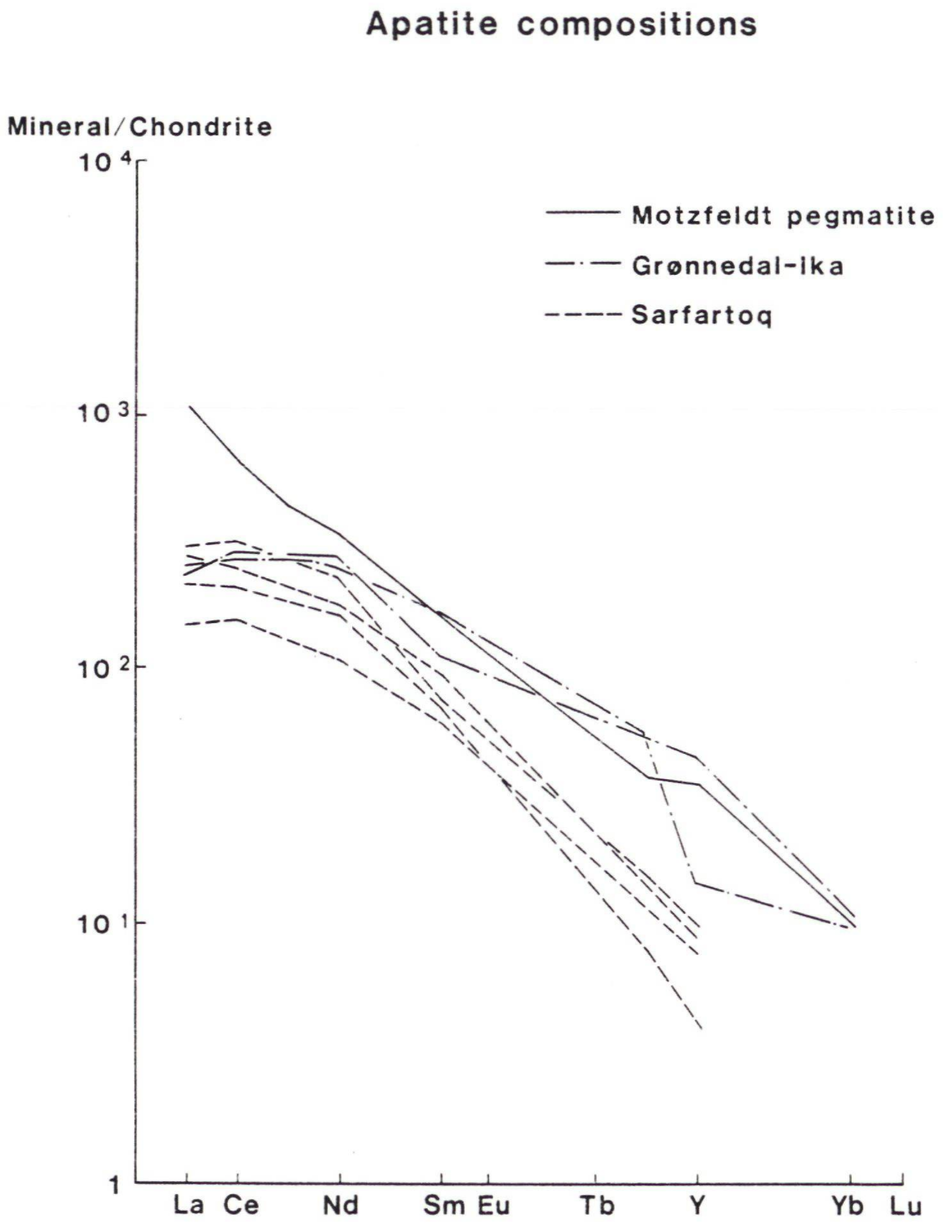
Apatite compositions

Fig. 68.

often rich in inclusions of dolomite. The apatite is fluor-apatite, and the colour is generally light yellowish green, but brown and pink apatite is found. The lanthanide distribution patterns (fig. 68) in the apatite is similar to what is found in the apatite from Qaqarssuk but the zoning in the apatite is not as common and lanthanide- and Sr-rich rims have not been observed (fig. 66).

The rauhaugite contains the major part of the phosphate, with a P_2O_5 content varying from 0.5 to 8.0 wt% and a mean of approximately 3.5 wt%. The phosphate content decreases with increasing CaO/MgO ratio, and the søvitic carbonatite is almost devoid of apatite (0.1 to 2 wt% P_2O_5). There is a tendency of increased phosphate content in the outer parts of the core.

7.3. THE PHOSPHATE POTENTIAL

As mentioned above, the rauhaugite in the outer core is the most interesting as a source for igneous phosphate. The rauhaugite occurs as 2 to 30 m thick sheets in the fenite and these sheets can be followed up to 500 m along strike. The rauhaugite with average 3.5 wt% P_2O_5 is estimated to comprise approximately 20% of the total rock volume in the 9 km^2 large outer core. This gives a total volume of rauhaugite of 180 to 350 mill m^3 calculated to a depth of 100 and 200 m respectively and hence 500 and 1000 mill t of rauhaugite. As only the larger sheets (>10 m thick) can be regarded as interesting, and these account for 1/5 of the total rauhaugite, the total volume of rauhaugite with 3.5 wt% P_2O_5 in sheets over 10 m calculated to a depth of 100 and 200 m respectively is 100 mill. and 200 mill. t.

7.4. INFRASTRUCTURE

The Sarfartôq Carbonatite Complex is situated 100 km from the airport of Søndre Strømfjord. The access to the sea (Søndre Strømfjord) is easy, through the flat, broad Sarfartoq Valley. Additionally it should be mentioned that the complex is situated in an area of local preservation.

7.5. SELECTED REFERENCES:

Larsen, L. M. 1980: Lamprophyric and kimberlitic dykes associated with the Sarfartôq carbonatite complex, southern West Greenland. Rapp. Grønlands geol. Unders. **100**, 65 - 69.

Larsen, L. M., Rex, D. C. & Secher, K. 1983: The age of carbonatites, kimberlites and lamprophyres from southern West Greenland: recurrent alkaline magmatism during 2500 million years. Lithos, **16**, 215 - 221.

Secher, K. 1976: Airborne radiometric survey between 60° and 69° N, southern and central West Greenland. Rapp. Grønlands geol. Unders. **80**, 65 - 67.

Secher, K. & Larsen, L. M. 1978: A new Phanerozoic carbonatite complex in southern West Greenland. Rapp. Grønlands geol. Unders. **90**, 46 - 50.

Secher, K. & Larsen, L. M. 1980: Geology and mineralogy of the Sarfartôq carbonatite complex, southern West Greenland. Lithos, **13**, 2, 199 - 212.

Secher, K. & Thorning, L. 1982: Detailed ground magnetic survey in the central part of the Sarfartôq Complex, southern West Greenland. Rapp. Grønlands geol. Unders. **110**, 32 - 38.

Secher, K. in press,a:Exploration of the Sarfartôq carbonatite Complex, southern West Greenland. Rapp. Grønlands geol. Unders. **128**.

Secher, K., In press,b:Phosphate resources in the Sarfartôq Carbonatite Complex, southern West Greenland. In: Phosphate Deposits of the World vol. 2), R. P. Sheldon and A. J. G. Notholt (eds.).

8. THE GARDINER COMPLEX

8.1. GENERAL GEOLOGY

The Tertiary Gardiner Complex consists of ultramafic cumulates probably associated with nephelinitic volcanism. The ultramafic series are cut by concentric and radiating dykes which can be grouped in 1) a melteigite-ijolite-urtite suite, 2) melilitolites and søvites and 3) magnetite-phlogopite-apatite-diopside-calcite/dolomite pegmatites.

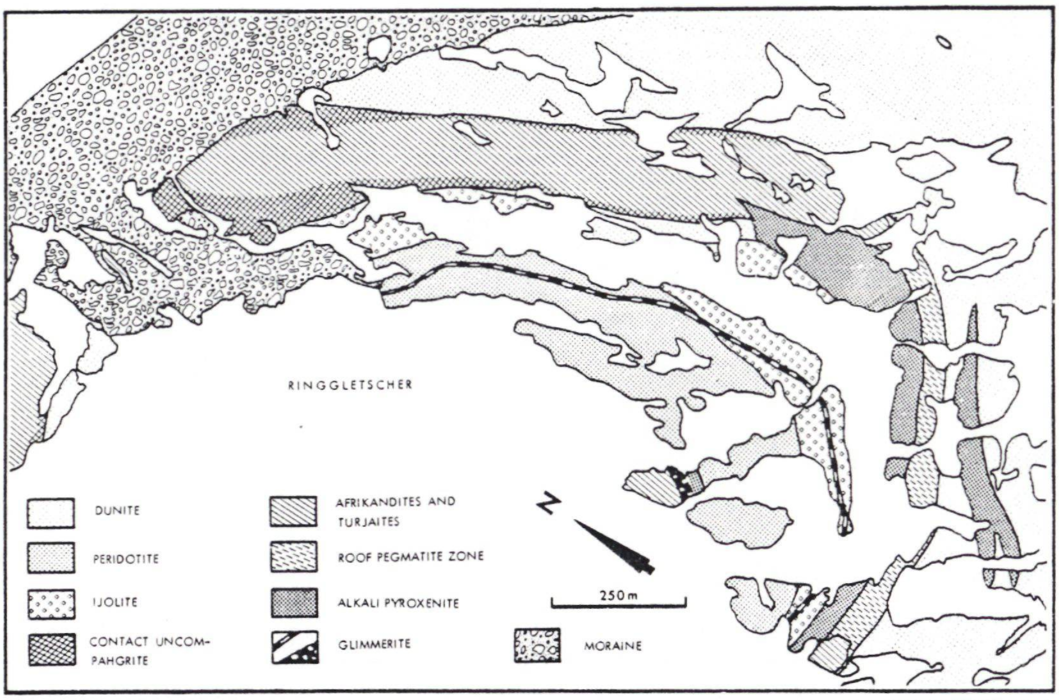

Fig. 69. Geological map of the central part of the Gardiner complex. Snow- and ice-covered areas are left blank. (From Nielsen, 1980, p.183).

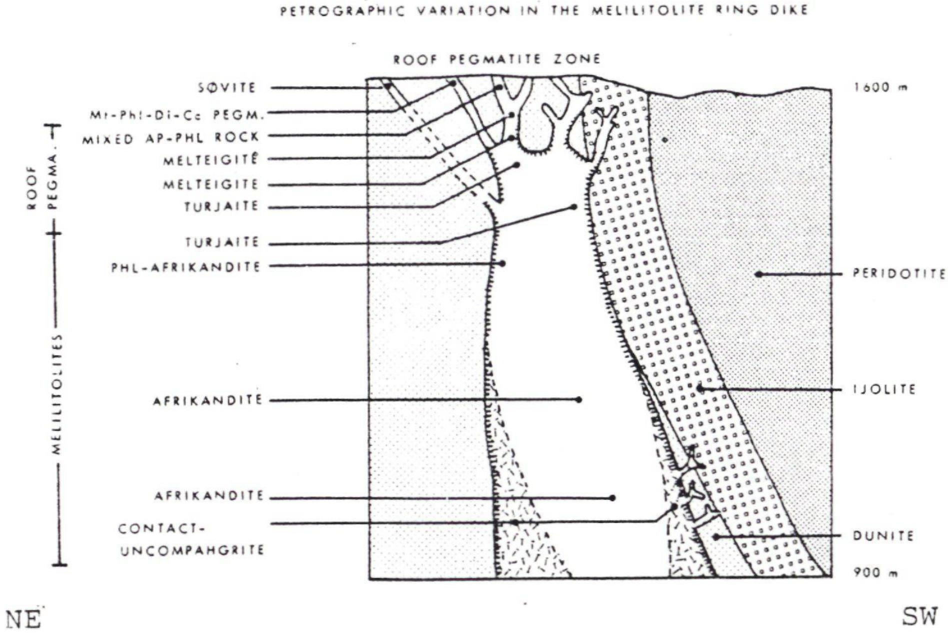

Fig. 70. Vertical section through the ring dyke. (From Nielsen, 1980, p.184).

The apatite-rich rocks are associated with the dykes, sheets and metasomatic rocks.

8.2. APATITE DISTRIBUTION

The apatite-rich rocks are:

1. An apatite-phlogopite ring dyke (glimmerite on fig. 69). This ring dyke is 8 m wide and has a diameter of about 2500 m and an approximate depth of 300 m. This gives 55 million tons of ore with an average grade of about 10% P_2O_5 (locally almost pure apatite rock).
2. A jacupirangite sheet (alkali pyroxenite on fig. 69). The dimensions of this are roughly 1200 x 200 x 200 m, which with an average density of 3 t/m^3 gives 144 million tons of ore with an average grade af 5% P_2O_5.
3. A metasomatic zone adjacent to the late magma chamber (contact between ijolite and afrikandites/turjaites on fig. 69). The volume of this zone is estimated to 125 million m^3 -> 375 million tons of ore with a grade ranging from 2 to 4% P_2O_5.
4. Magnetite-apatite-rich cumulates in the plutonic melilitolite ring dyke (afrikandite and turjaite on fig. 70). This ring dyke contains approximately 2.5 billion tons with a grade ranging from 1 to 5wt% P_2O_5.

The complex has not been investigated in detail and the figures given above are based on estimates (Troels Nielsen, personal communication, 1983).

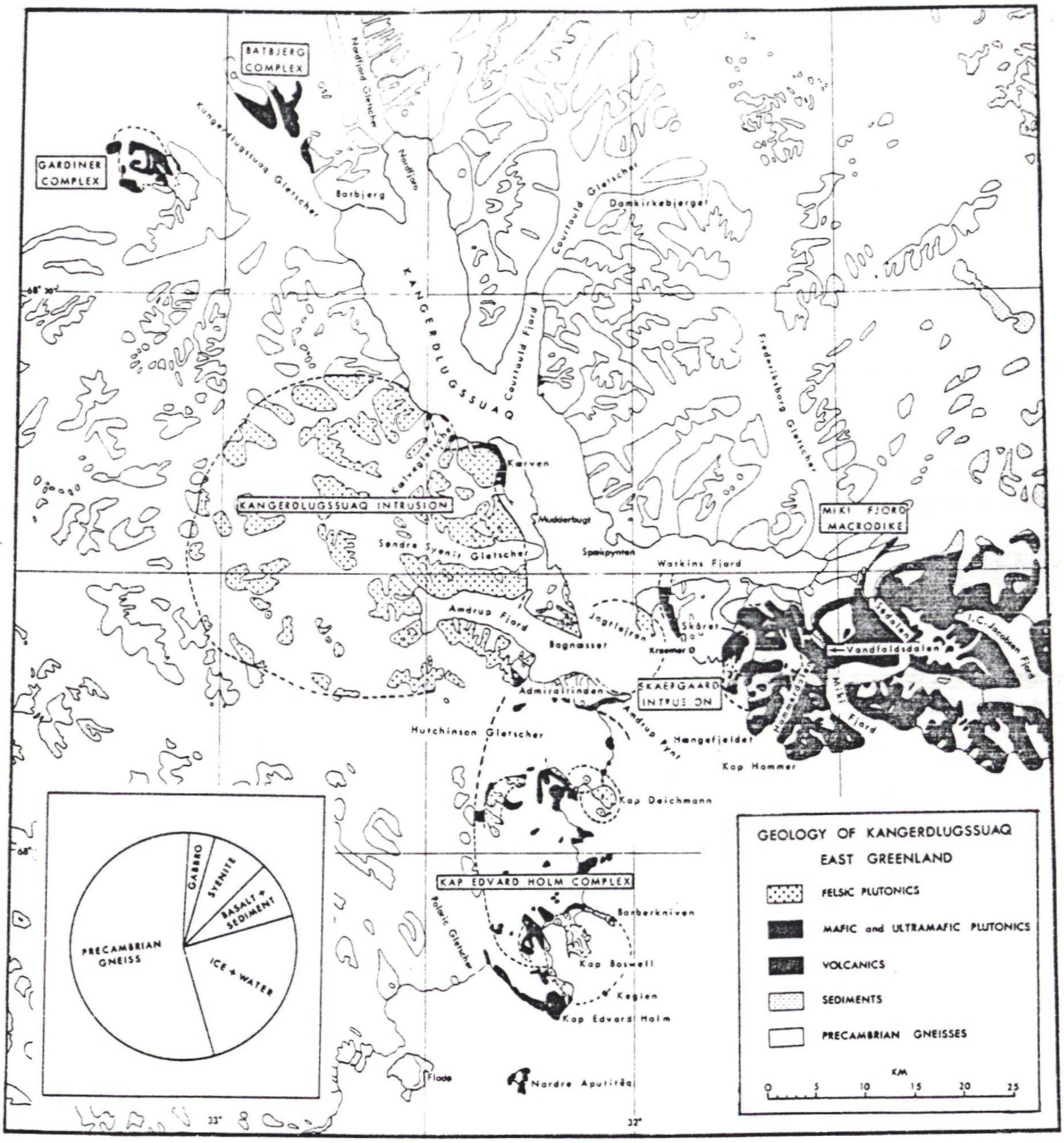

Fig. 71. Geology of the Kangerdlugssuaq area. Notice the remote position of the Gardiner complex.

8.3. CONCLUSION

The Gardiner complex is situated in a very remote part of Greenland, surrounded by glaciers (fig. 71) and hence only accessible from the air. Further the weather conditions are among the worst in the world. Because of these factors the occurrence must be regarded as having low priority as a source for phosphate.

8.4. SELECTED REFERENCES:

Brooks, C. K. & Nielsen, T. F. D. 1978: The Tertiary ultramafic alkaline ring complex at Gardiner Plateau, Kangerdlugssuaq, East Greenland: preliminary description. Proc. 1st International Symposium on Carbonatites, 1976. Pocos de Caldas, M. G., 227-230.

Brooks, C. K. & Nielsen, T. F. D. 1982: The Phanerozoic development of the Kangerdlugssuaq area, East Greenland. Meddr Grønland, Geoscience 9, 31 pp.

Frisch, W. & Keusen, H. 1977: Gardiner intrusion, an ultramafic complex at Kangerdlugssuaq, East Greenland. Bull. Grønlands geol. Unders. 122,62 pp.

Gleadow, A. J. W. & Brooks, C. K. 1979: Fission track dating, thermal histories and tectonics of igneous intrusions in East Greenland. Contrib. Mineral. Petrol. **71**, 45-60.

Nielsen, T. F. D. & Johnsen, O. 1978: Titaniferous clinohumite from Gardiner Plateau complex, East Greenland. Mineral. Mag. **42**, 99-101.

Nielsen, T. F. D. 1979: The occurrence and formation of Ti-aegirines in peralkaline syenites. An example from the Tertiary ultramafic alkaline Gardiner complex, East Greenland. Contrib. Mineral. Petrol. **69**, 235-244.

Nielsen, T. F. D. 1980: The petrology of a melilitolite, melteigite, ijolite, nepheline, syenite and carbonatite ring dike system in the Gardiner complex, East Greenland. Lithos **13**, 181-197.

Nielsen, T. F. D. 1981: The ultramafic cumulate series, Gardiner complex, East Greenland. Cumulates in a shallow level magma chamber of a nephelinitic volcano. Contrib. Mineral. Petrol. **76**, 60-72.

Nielsen, T. F. D. & Buchardt, B. 1985: Sr-C-O isotopes in nephelinitic rocks and Carbonatites, Gardiner Complex, East Greenland, Chem. Geol. **53**, 3/4 (in press).

9. SUMMARY AND CONCLUSION ON THE PHOSPHATE POTENTIAL

Qaqarssuk Carbonatite Complex

During the intrusion of the carbonatite, the phosphate has been redistributed. The søvite has generally low apatite content, whereas rock-types as silico-søvite, rauhaugite, ultramafic metasomatic rocks and late magnetite-apatite-pyrochlore-rich rocks form 10 to 15 m thick, steeply dipping sheets with 3.5 to 8.5 wt% P_2O_5 on average. Appr. 4 mill. t of rock with 4.4 wt% P_2O_5 (on average) is localised on the basis of outcrops (chip sampling) and drilling carried out during Nb exploration by Kryolitselskabet Øresund A/S. Drilling with the specific purpose of localising apatite-rich rocks is likely to indicate further resources.

Rocks with up to 15 wt% Nb_2O_5 have been found in the complex, and so far 3.5 mill.t of Nb ore with 0.5 wt% Nb_2O_5 or 1.2 mill. t with 0.8 wt% Nb_2O_5 down to 200 m has been localised so far. During the present investigation magnetite-apatite-pyrochlore-rich rocks were located in areas not yet drilled, and additional resources could be found by drilling on these showings found by soil geochemistry and radiometry.

Lanthanide-rich carbonatite veins up to 4 m thick with lanthanide concentrations ranging from 1.5 to 4 wt% (0.2 to 0.6 wt% Nd) are present (average over veins > 2m). These lanthanide-rich carbonatites can be localised with soil geochemistry as well as with radiometry (Th).

Further the magnetite appearing in the magnetite-apatite-pyrochlore rock has a V content of appr. 0.3 wt%.

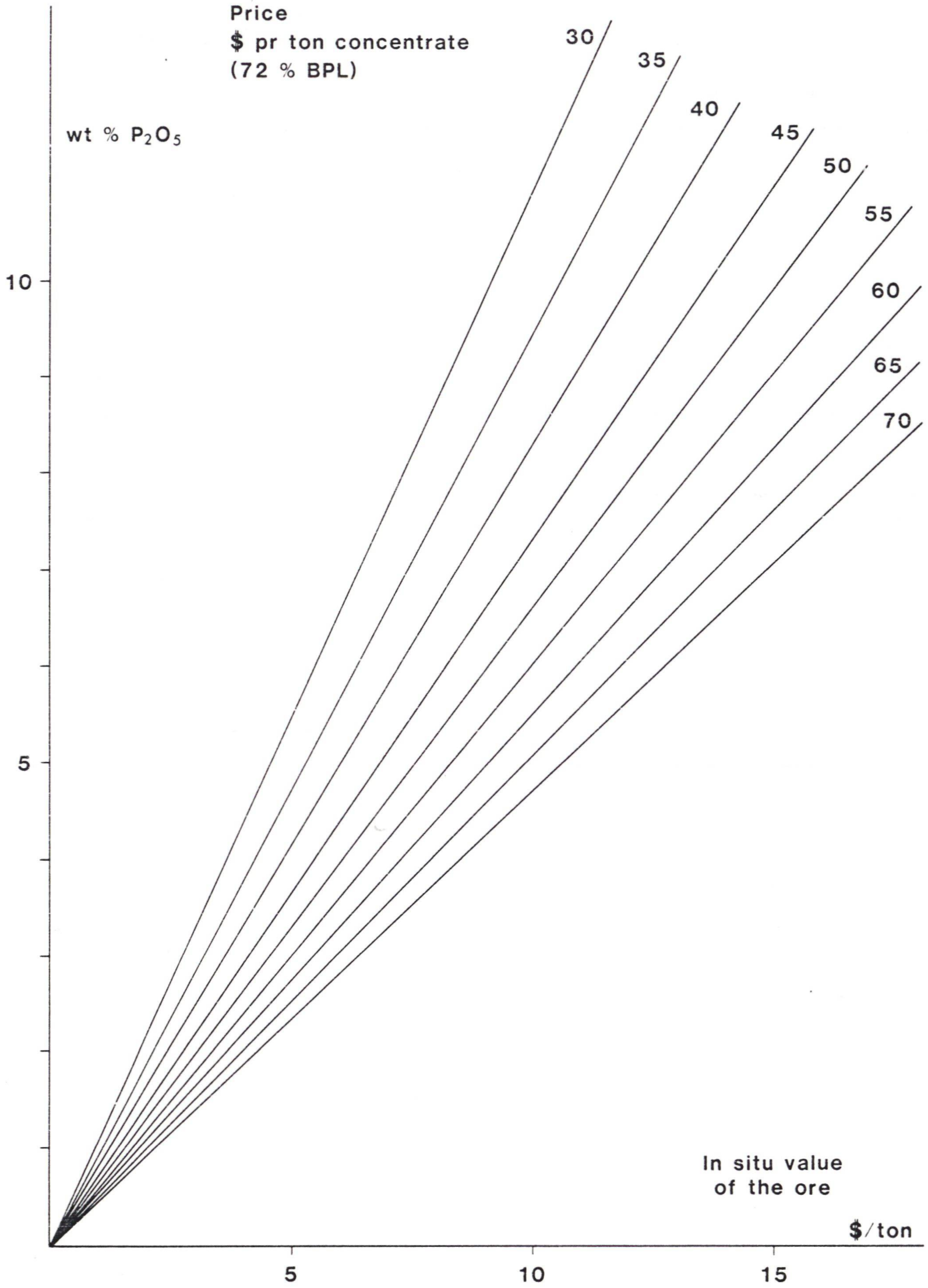
Price
$ pr ton concentrate
(72 % BPL)
wt % P_2O_5
30
35
40
45
50
55
60
65
70
10
5
In situ value
of the ore
$/ton
5
10
15

Fig. 72.

It must be concluded that the grade and tonnage of the apatite-enriched rocks, which probably are present in the complex, are too limited and the location to remote, to provide possibilities for large scale phosphate mining operations, as seen e.g. in Siilinjärvi. On the other hand do the magnetite-apatite-pyrochlore-rich rocks provide possibilities for a small scale mining operation.

Approximately 1 mill t of rock with 8.5 wt% P_2O_5 and 0.8 wt% Nb_2O_5 is indicated by the drilling. The ore is essentially composed of magnetite, apatite, phlogopite, alkali amphibole, calcite and pyrochlore. The rock could either be shipped directly or with a small degree of processing - separation by magnetic and gravitational methods. The in situ value of such an ore is for the phosphate appr. 13 mill.$ (fig. 72) and for the Nb 88 mill $ (columbite with a grade of 65% and Nb:Ta=10:1 is assumed worth 3.25$/lb (Tron, 1985)). Apart from the above-mentioned, the V-rich magnetite may be economic to exploit as well.

Qassiarssuk

Carbonatite lava flows with P_2O_5 contents of 3.5% (on average over 1 to 2 m) are common in the area, but the grade varies considerably in the volcanic and volcaniclastic sequence. These carbonatite lavas forms near surface horizontal sheets and they are localised in an area with existing infrastructure, and hence easily accesible. The geology of the area is, however, incompletely known, and further investigations are needed before the extent of the apatite carrying carbonatites can be evaluated.

Alkaline silicic rocks in the Gardar igneous province

Syenites with P_2O_5 contents between 1.5 and 3.5 wt% have been found in several alkaline igeneous complexes in South Greenland. These further contain 3 to 5 modal% magnetite with 0.3 to 1.9 wt% V. The geological evolution of these igneous complexes is relatively well known, but only limited knowledge exists about the extent of the apatite-enriched rocks. It should be noticed that the Gardar alkaline igneous province in many other respects is very similar to the Kola alkaline igneous province.

Sarfartôq Carbonatite complex

Appr. 100 to 200 mill. t of apatite-rich rauhaugite with 3.5 wt% P_2O_5 is localised here, based on observation of surface showings. No drilling has been carried out so far. Apart from the phosphate, small, high-grade pyrochlore deposits are found with average grade of 15 wt% Nb_2O_5.

Gardiner Igeneous Complex

Although large amounts of apatite-rich rocks are present, the location is too remote to be of economic interest at the moment.

Recommendation.

Further exploration for igneous apatite occurrences in Greenland should focus on:

1. Prefeasibility studies on the apatite and pyrochlore-rich rocks in the Qaqarssuk Carbonatite Complex, in a "small scale mining" context. This should be supported by further drilling on radiometric and soil geochemical anomalies.
2. Drilling on the apatite-rich rauhaugite at Sarfartôq combined with drilling on the small high grade pyrochlore rocks.
3. Investigation of the apatite-enriched rocks in the Gardar alkaline igneous complexes, and possible secondary deposits of apatite and vanadium -rich magnetite derived from weathering of the alkaline complexes.

10. ACKNOWLEDGEMENTS

Thanks are due to L. Keto, Kryolitselskabet Øresund A/S for permission to investigate drill-core and to use geophysical data obtained by the company, to J.C. Bailey for trace element analyses (XRF), to H. Bollingberg for trace element analyses (OAS), Danish Natural Science Research Council, Contract j. nr. 11-4964) to G. Asmund for Cd (ASV) analyses, to E. Leonardsen for X-ray identification of several minerals, to J. Rønsbo for guiding the microprobe analyses and J. Fløng for technical assistance during the probe work. INAA analyses were financed by Statens Naturvidenskabelige Forskningsråd. Further thanks are due to J. Halskov for drafting of the figures and maps, to Aase Hasselsteen who typed the manuscript, to M. Kjærgaard, K. B. Olsen and T. Boiesen for their enthusiastic geophysical field work, data handling and assistance in the field, to I. Rytved for laboratory work, data handling and moral support. Special thanks to K. Secher and L. M. Larsen for valuable discussions and comments on the manuscript. Publication of this report is authorised by the Director of the Geological Survey of Greenland.

11. REFERENCES:

Aleksandrov, I. V., Sin'kova, L. A. & Ivanov, V. I. 1969: Experimental study of the behaviour of rare-earth elements and yttrium as applied to the hydrothermal process. In Khitarov N. K. (edit.). Problems of geochemistry 285-294, Israel program for scientific translation.

Andersen, A. T. & Greenland, L. P. 1969: Phosphorus fractionation diagram as a quantitative indicator of crystallisation differentiation of basaltic liquids. Geochim. Cosmochim. Acta **33**, 493.

Anon, 1983: The Soviet Union's phosphate rock industry: Latest developments. Phosphorus and Potassium **126**, 29-32.

Anon, 1985: Phosphate rock: U.S. will lose cost advantage. Mining Journ. 1985, april **12**, 250.

Armbrustmacher, T. J. 1979: Replacement and primary magmatic carbonatites from the West Mountains Area, Fremont and Coster Counties, Colorado. Econ. Geol. **74**(4), 888 - 901.

Bagdasarov, Yv. A. 1971: Types of apatite metasomatite in carbonatite complexes. Doklady. Earth Sci. Sect. **199**, 2, 129-131.

Le Bas, M. J. & Handley, O. D. 1979: Variation in apatite composition in ijolitic and carbonatitic igneous rocks. Nature, **179**, 54-56. Mineralog. Mag.

Le Bas, M. J. 1981: Carbonatite magmas. Min. Mag. **44**, 133-140

Belashow, Yv. A. & Krigman, L. D. 1975: The effects of alkalinity and volatiles on rare-earth separation in magmatic systems. Geochem. Internat. **12**, 165-170.

Bergman, S. C. 1979: The significance of accessory apatite in the REE modelling of magma genesis. Trans. Am. Geophys. Union **60**:412.

Bergstøl, S. 1972: The jacupiraugite at Kodal, Vestfold, Norway. Mineralium Deposita, **7**, 233-246.

Brooks, C. K. & Nielsen, T. F. D. 1980: The Tertiary ultramafic alkali ring complex at Gardiner Plateau, Kangerdlugssuaq, East Greenland: preliminary description. Proc. 1st International Symposium on Carbonatites, 1976. Pocos de Caldas, M. G. 227-230.

Brooks, C. K. & Nielsen, T. F. D. 1982: The Phanerozoic development of the Kangerdlugssuaq area, East Greenland. Meddr Grønland, Geoscience **9**, 30 pp.

Brögger, W. C. 1921: Die Eruptivgesteine des Kristiania Gebietes IV. Das Fengebiet in Telemarken, Norwegen. Kong. Norske Vid. Selsk. Skr. I Mat. Nat. bl. **9**, 1-408.

Christensen, L. H. and Damsgaard, E. 1985: Neutron activation analysis at the Danish Reactor DR3. IAEA-SR **119**,10,15 pp.

Cockbain, A. G. 1968: The crystal chemistry of apatites. Mineral Mag. **36**, 654 - 660.

Companhia Brasileira de metalurgica e mineracao 1984: Carbonatite complexes of Brazil: Geology. Sao Paulo, CBMM, 44 p.

Cook, P. J. 1984: Spatial and temporal controls on the formation of phosphate deposits - A review. In: Phosphate minerals (edit.) O. Nriagu and P. B. Moore Springer, 242-274.

Cullers, R. L. & Medaris, G. J. 1977: Rare earth elements in carbonatite and cogenetic alkaline rocks: examples from Seabrook Lake and Callander Bay, Onterio. Contrib. Mineral. Petrol. **65**, 143-153.

Cullers, R. L. & Graf, J. L. 1984: Rare earth elements in igneous rocks of the continental crust: predominantly basic and ultrabasic rocks. In Henderson, P. (edit.) Rare earth element geochemistry. Developments in geocheistry 2. Elsevier, Amsterdam 1984, **237-274**, 510 pp.

Currie, K. L. & Ferguson, J. 1972: A study of fenitisation in mafic rocks with special reference to the calender Bay Complex. Can. Journ. Earth Sci. **9**, 1254-1261.

Currie, K. L. 1976: The alkaline rocks of Canada. Geol. Surv. Canada. Bull. **239**, 228 pp.

Drake M. J. & Weill, D. F., 1972: New rare earth element standards for electron microprobe analysis. Chem. Geol. **10**, 179-181.

Dumonceau, J., Bigot, S., Trevil, M., Fanchere, I. & Fromage, F. 1978: Determination de constantes de formation des tetracarbonato-Lanthanides (III) C. R. Acad. Sc. Paris Serie **C 287**, p. 325-327.

Eby, G. N. 1975: Abundance and distribution of the rare earth elements and yttrium in the rocks and minerals of the Oka carbonatite complex, Quebec. Geochim. Cosmochim. Acta. **39**, 597-620.

Emeleus, C. H. 1964: The Grønnedal-Ika alkaline complex, South Greenland, Meddr om Grønland, **172**, 3. 75 pp. Bull. Grønlands Geol. Unders.

Erdosh, G. 1979: The Onterio Carbonatite Province and its phosphate potential. Econ. Geol. **74**, 331-338.

Fleischer, M. & Altschuller, Z. S. 1969: The relationship of rare earth composition of minerals to geological environment. Geochim. Cosmochim. Acta, **33**, 727-732.

Fleischer, M. 1983: Distribution of the lanthanides and yttrium in apatites from iron ores and its bearing on the genesis of the Kiruna type. Econ. Geol. **78**, 5, 1007-1010.

Flynn, R. T. & Burnham, C. W. 1978: An experimental determination of rare earth partition coefficients between a chloride containing vapour phase and silicate melts. Geochim. Cosmochim. Acta4**2**2. 685-701.

Frietsch, R. 1974: The occurrence and composition of apatite with special reference to iron ores and rocks in Northern Sweden. SGU, Ser. C, 694 Årsbok **67**, 67,1, pp 49.

Frietsch, W. & Keusen, H. 1977: Gardiner Intrusion, an ultramafic complex at Kangerdlugssuaq, East Greenland. Bull. Grønlands geol. Unders. **122**, 62 pp.

Gittins, J., Macintyre, R. M. & York, D. 1967: The ages of carbonatite complexes in eastern Canada. Can. Journ. Earth Sci, **4**, 651-655.

Gleadow, A. J. W. & Brooks, C. K. 1979: Fission track dating, thermal histories and tectonics of igneous intrusions in East Greenland. Contrib. Mineral. Petrol. **71**, p. 45-60.

Gold, D. P. 1963: Average chemical composition of carbonatites. Econ. Geol. **58**, 988-991.

Gold, D. P. 1966: The average and typical cheical composition of carbonatites. Int. Min. Assoc., 1964 meeting, India, 83-91.

Gothenborg, J. & Pedersen, J. L. 1976: Exploration of the Qaqarssuk carbonatite complex, 1975, Part II, Kryolitselskabet Øresund A/S, unpubl. company report.

Gothenborg, J., Keto, L.& Pedersen, J. L. 1977: Exploration of the Qaqarssuk carbonatite complex 1976. Kryolitselskabet Øresund A/S. Unpubl. company report.

Gunnarsson, O. 1983: Heavy metals in fertilizers. Do they cause environmental and health problems? Fertilizers and agriculture **85**, 27-42.

Hamilton, D. L., Freestone, I. C., Dawson, I. B. & Donaldson, C. H. 1979: Origin of carbonatites by liquid immiscibility. Nature **279**, 52-54.

Hanekom, H. J., van Staden, C. M. v. H., Smit, P. J. & Pike, D. P. 1965: The geology of the Palabora Igneous Complex. South Africa Geol. Survey Mem. **54**, 185 p.

Hedges, M. M., Wall, V. J. & Bloom, M. S. 1985: Hydrothermal transport and deposition of uranium: Modelling and implications. *In* Concentration mechanisms of uranium in geological environments, (Nancy 1985), Extended abstract, 241-243.

Hogarth, D. D. 1977: Classification and nomenclature of the pyrochlore group. Amer. Mineral. **62**, 403-410.

Hutton, M. 1983. The environmental implications of cadmium in phosphate fertilizers. Phosphorous & Potassium **123**, 33-36.

Jones, P. B. 1983: Mesozoic rifting in the western Arctic ocean basin and its relationship to Pacific seafloor spreading. *In* A. F. Embry and H. R. Dalkwill (eds). Proc. Third Int. Symp. Arctic geology and geophys. Memr. Can. Soc. Petrol. Geol. **8**, 83-99.

Kapustin, Yn. L. 1977: Distribution of Sr, Ba and REE in apatite from carbonatite complexes. Geochem. Internat. **16**, 4, 71-79.

Kay, I. M., Young, R. A. & Posner, A. S. 1964: Crystal structure of hydroxyapatite. Nature **104**, 1050-1052.

Kjærgaard, M. & Olsen, K. B. 1985: Shallow-seismic, geoelectric and magnetitc investigation of the the Qaqarssuk carbonatite complex, West Greenland. Rapp. Grønlands geol. Unders. **125**, 140-144.

Kjærgaard, M. & Olsen, K. B. 1985: Geoelectric and seismic investigations at Qaqarssuk. Lab. for Geophysics, University of Aarhus. Unpubl. report (in Danish) 64 p.

Knudsen, C. 1984: Apatite mineralisation in carbonatite and ultramafic intrusions in Greenland. E.E.C. Contract MSM-119-DK. Interim report No. 2, pp 7.

Knudsen, C. 1985: Apatite mineralisation in carbonatite and ultramafic intrusions in Greenland. E.E.C. Contract MSM-119-DK. Interim report No. 3, pp 32.

Knudsen, C. 1985: Apatite mineralisation in carbonatite and ultramafic intrusions in Greenland. E.E.C. Contract MSM-119-DK. Interim report No. 4, pp 34.

Knudsen, C. 1985: Investigation of the Qaqarssuk carbonatite complex, southern West Greenland, Rapp. Grønlands geol. Unders. **125**, 35-40.

Knudsen, C. in press: Apatite accumulation in the Qaqarssuk Carbonatite Complex, southern West Greenland. *In* R. P. Sheldon and A. J. G. Notholt (eds), Phosphate deposits of the World (Vol. 2).

Knudsen C. & Secher, K., 1984: Apatite mineralisation in carbonatite and ultramafic intrusions in Greenland. E.E.C. Contract MSM-119-DK. Interim report No. 1, pp 23.

Kofoed, A. D. & Klausen, P. S. 1983: Influence on the cadmium content of soil (and crops. Investigations from long term field experiments in State Researche Station Askov 1874 - 198). Tidsk. Planteavl **87**, 23-32.

Koster van Groos, A. F. 1975: The effect of high CO_2 pressure on alkalic rocks and its bearing on the formation of alkalic ultrabasic rocks and the associated carbonatites. Am. J. Sci. **275**, 163-185.

Kosterin, A. V. 1959: The possible modes of transport of the rare earth by hydrothermal solutions. Geochemistry (USSR), English translation 381-387.

Kreidler, E. R. & Hummel, F. A. 1970: The crystal chemistry of apatite: structure fields of fluor- and chlorapatite. Amer. Mineral. **55**, 170-184.

Kunzendorf, H. & Secher, K. In press: Dispersion of niobium and phosphorus in soil overlying the carbonatite complex Qaqarssuk, southern West Greenland. J. geochem. Explor. In press.

Kunzendorf, H. & Sørensen, P. 1982: Reconnaissance geochemical sampling in the Qaqarssuk Carbonatite Complex, West Greenland, RISØ, Unpubl. internal report, 51 pp.

Kurki, I. and Juhava, R. 1971: Report on the exploration work in Søndre Isortoq Area, 1970. Kryolitselskabet Øresund A/S, unpubl. company report.

Kurki, I., Juhava R. & Gothenborg, J. 1973: Report on the exploration work in Søndre Isortoq area 1972, Kryolitselskabet Øresund A/S. Unpubl. company report.

Landa, E. A., Krasnova, N. I., Tarnovskaya, A. N., & Shergina, Yu. P., 1983: The distribution of Rare Earths and Yttrium in apatite from alkali-ultrabasic and carbonatite intrusions and the origin of apatite mineralisations. Geochem. International **20**, 1, 77-87.

Larsen, L. M. 1979: Distribution of REE and other trace elements between phenocrysts and peralkaline undersataturated magmas exemplified from the Gardar igneous province, South Greenland, Lithos **12**, 303-315.

Larsen, L. M. 1980: Lamprophyric and kimberlitic dykes associated with the Sarfartôq carbonatite complex, southern West Greenland. Rapp. Grønlands geol. Unders. **100**, 65-69.

Larsen, L. M. & Pedersen, A. K. 1982: A minor carbonatite occurence in southern West Greenland: the Tupertalik intrusion. Rapp. Grønlands geol. Unders. **110**, 38-43.

Larsen, L. M., Rex, D. C. & Secher, K. 1983: The age of carbonatites, kimberlites and lamprophyres from southern West Greenland: recurrent alkaline magmatism during 2500 mill. years. Lithos **16**, 215-221.

Liebau and Konitnig S. 1978: Phosphorus. *In* Wedepohl, K. H. (ed.) Handbook of geochemistry Vol. II-2, Springer, Berlin p. B1-019.

Lundberg, B. & Smellie, J. A. T. 1979: Painirova and Mertainen iron ores: Two deposits of the Kiruna iron ore type in northern Sweden. Econ. Geol. **74**, 5, 1131-1152.

Mariano, A. N. 1976: The application of cathodoluminescence for carbonatite exploration and characterization. Proc. First. Internat. Symposium on Carbonatites. Dept. Nat. da Producao Mineral, Brasilia.

Mc Birney, A. R. & Nakamura, K. 1974: Immiscibility in late-stage magmas of the Skaergaard intrusions. Carnegie Institution, Annual Report of the Director Geophysical Lab. 1973-1974, 348.

McConnel, D. 1973: Apatite. Its crystal chemistry, mineralogy, utilization and geologic and biologic occurrences. Springer, Vienna.

Mew, M. 1985: Phosphate rock. Mining Ann. Rev. 1985, 124-126.

Mitchell, R. H. & Brunfelt, A. G. 1975: Rare earth element geochemistry of the Fen alkaline complex, Norway. Contrib. Mineral. Petrol. **52**, 247-259.

Moore, P. B. 1973: Pegmatite phosphates 1973: Descriptive mineralogy and crystal chemistry. Miner. Rec. **4**, 103-130.

Møller, P. and Morteani, G. 1983: On the geochemical fractionation of rare earth elements during the formation of Ca-minerals and its application to problems of the genesis of ore deposits. *In* The significance of trace elements in solving petrogenetic problems and controverses (edit.) Augustithis, S. S., Theophrastus, Athens.

Nash, W. P. 1972: Apatite chemistry and phosphorous fugacity in a differentiated igneous intrusion. Am. Miner. **57**, 877-886.

Nash, W. P. 1984: Phosphate minerals in terrestrial igneous and metamorphic rocks. In Phosphate minerals (edit.) Nreiagu, J. O. & Moore, P. B., 215-241.

Nielsen, T. F. D. & Johnsen, O. 1978: Titaniferous clinohumite from Gardiner Plateau complex, East Greenland. Mineral. Mag. 42. 99-101.

Nielsen, T. F. D. 1979: The occurrence and formation of Ti-aegirines in peralkaline syenites. An example from the Tertiary ultramafic alkaline Gardiner complex, East Greenland. Contrib. Mineral. Petrol. **69**, 235-244.

Nielsen, T. F. D. 1980: The petrology of a melilitolite, melteigite, ijolite, nepheline, syenite and carbonatite ring dike system in the Gardiner complex, East Greenland. Lithos **13**, 181-197.

Nielsen, T. F. D. 1981: The ultramafic cumulate series, Gardiner complex, East Greenland. Cumulates in a shallow level magma chamber of a nephelinitic volcano. Contrib. Mineral. Petrol. **76**, 60-72.

Nielsen, T. F. D. & Buchardt, B. 1985: Sr-C-O isotopes in nephelinitic rocks and Carbonatites, Gardiner Complex, East Greenland, Chem. Geol. **53**, 3/4.

Norrish, K. & Chappel, B. W. 1977: X ray fluorescence spectrometry: *In* Zussman, I. (edit.). Physical methods in determinative mineralogy 2nd. ed. Academic Press, London 201-272.

Plant, J. A., O'Brien, C. Tarney, J. & Hurdley, J.: In prep. Geochemical criteria for the recognition of high heat producing granites.

Poty, B. P., Leroy, I. & Caret, M., 1974: Les inclusions fluides dans les minberais des gisements d'uranium intra granitiques du Limonsin et du Forez (Massif Central, France): In: Formation of uranium ore deposits 569-582, IAFA, Vienna.

Prins, P. 1973: Apatite from African carbonatites. Lithos. **6**, 133-144.

Puchet, H. & Emmermann, R. 1976: Bearing of rare earth patterns of apatites from igneous and metamorphic rocks. Earth Planet. Sci. Lett. **31**, 277-286.

Reedman, J. H. 1984: Resources of phosphate, niobium, iron, and other elements in residual soils over the Sukulu carbonatite complex, Southern Uganda. Econ. Geol. **79**, 716-724.

Ringwood, A. E. 1955: The principles governing trace element distribution during magmatic crystallisation. Part I: The influence of electronegativity. Part II: The role of complex formation. Geochim. Cosmochim. Acta **7**, 189-202 and 242-254.

Rosenberg, P. E. 1967: Subsolidus relations in the system $CaCO_3$ -$MgCO_3$ -$FeCO_3$ between 350° and 550°C. Am. Mineral 52, 787-796.

Samonikova, V. O. 1984: Some composition trends in the Yukspor apatite-nepheline ores and underiying rocks. Geochem. int. **21**, 1, 77-82.

Samoylov, V. S. & Smirnova, Ye. V. 1980: Rare-earth behaviour in carbonatite formation and the origin of carbonatites. Geochem. Int. **17** (6), 140-152.

Sauerbeck, D.: Zur Bedeutung des Cadmiums in Phosphatdüngemitteln. Landbauforschung Völkerude, **32**, 4, 192-197.

Secher, K. 1977: Airborne radiometric survey between 63° and 66° N, southern West Greenland. Rapp. Grønlands geol. Unders. **85**, 49-50.

Secher, K. 1980: Distribution of the radioactive mineralisations in central West Greenland. Rapp. Grønlands geol. Unders. **100**, 61-65.

Secher, K. 1983 (a): Noritic rocks and associated nickel-copper-sulphide occurrences in Sukkertoppen district, central West Greenland. Rapp. Grønlands geol. Unders. **115**, 30-34.

Secher, K. 1983 (b): Karbonatitforekomster i Vestgrønlnad - anvendelige mineralske resourcer? Forskning i Grønland, 2/83, 8-14.

Secher, K. in press(a): Exploration of the Sarfartôq Carbonatite Complex, southern West Greenland. Rapp. Grønlands geol. Unders. 128.

Secher, K. In press(b): Phosphate resources in the Sarfartôq Carbonatite Complex, southern West Greenland. *In* Phosphate Deposits of the World (vol 2), R. P. Sheldon & A. J. G. Notholt (eds).

Secher, K. & Larsen, L. M. 1978: A new Phanerozoic carbonatite complex in southern West Greenland. Rapp. Grønlands geol. Unders. **90**, 46-50.

Secher, K. & Larsen, L. M. 1980: Geology and mineralogy of the Sarfartoq Carbonatite Complex, Southern West Greenland. Lithos. **13**, 199-212.

Secher, K. and Thorning L. 1982: Detailed ground magnetic survey in the central part of the Sarfartôq Complex, southern West Greenland Rapp. Grønlands geol. Unders. **110**, 32 - 38.

Smith, I. V. 1981: Halogen and phosphorous storage in the Earth. Nature **289**, 5800, 752-765.

Sommerauer I. & Katz-Lehnert, K. 1985: A new partial substitution mechanism of CO_3^{2-}/CO_3OH^{3-} and SiO_4^{4-} for PO_4^{3-} group in hydroxyapatite from the Kaiserstuhl alkaline complex (SW-Germany). Contrib. Mineral Petrol. **91**, 360-368.

Sommerauer J. and Katz-Lehnert, K. 1985: Trapped phosphate melt inclusions in silicate-carbonate-hydroxyapatite from comb-layered alvikites from the Kaiserstuhl carbonatite complex (SW Germany). Contrib. Mineral Petrol. **91**, 354-359.

Steward, J. W. 1970: Precambrian alkaline-ultramafic/karbonatite volcanism at Qaqssiarssuk, South Greeland. Grønlands Geol. Unders., Bull. **84**.

Stormer, J. C. and Carmichael, I. S. E. 1971: Fluorine-hydroxyl exchange in apatite and bbiotite: A potential igneous geothermometer. Contrib. Miner. Petrol. **31**, 121-131.

Sørensen, I. 1975: X-ray fluorescence spectrometry at GGU. Rapp. Grønlands geol. Unders. **75**, 16-18.

Taborsky, 1962: Geochemie des apatite in Tiefengesteinen am Beispiel des Odenwaldes. Beitr. Miner. Petrogr. **8**, 354.

Tron, A. R. 1985: Niobium and Tantalum. Mining Ann. Rev. 1985, 96-97.

Upton B. G. J. 1960: The alkaline igneous complex of Kûngnât Fjeld. South Greenland. Bull. Grønlands Geol. Unders. **27**, 145 pp.

Upton, B. G. J., Stephenson, D. and Martin, A. R. The Tugtutôq older giant complex: Mineralogy and geochemistry of an alkali gabbro-augite syenite-foyaite association in the Gardar Province of South Greenland. In press.

Vartiainen, H. & Paarma, H. 1979: Geological Characteristics of the Sokli Carbonatite Complex, Finland. Econ. Geol. **74**, 1296-1306.

Vartiainen, H. 1980: The petrography, mineralogy and petrochemistry of the Sokli carbonatite massif, northern Finland. Bull. Geol. Surv. Finland **313**, 126 pp.

v. d. Veen, A. H. 1963: A study of pyrochlore. Nederlands Geol. Minbouwkd. Gen. Verh. Geol. Ser. **22**, 188 pp.

Vuotovesi, T. 1974: Qaqarssuk carbonatite complex. Unpubl. MSc thesis (in Finnish - translated to English by T. Tukiainen. GGU).

Wakefield, Z. T. 1980: Distribution of cadmium in phosphate fertilizer processing in "Cadmium seminar". The Fertilizer Institute, Washington Nov. 1980 p. 141.

Watson, E. B. 1979: Apatite saturation in basic intermediate magmas. Geophys. Res. Lett. **6**, 937-940.

Watson, E. B. 1980: Apatite and phosphorous in mantle source regions: An experimental study of apatite/melt equilibria at pressures to 25 kbar. Earth Planet Sci. Lett. **51**, 322-335.

Watson, E. B. & Green, T. H. 1981: Apatite/liquid partition coefficients for the rare earth elements and strontium. Earth Planet. Sci. Lett. **56**, 405-421.

Wendlandt, R. F. & Harrison, W. J. 1979: Rare earth partitioning between immiscible carbonate and silicate liquids and CO_2 vapor: results and implications for the formation of light rare-earth-enriched rocks. Contrib. Mineral. Petrol. **69**, 409-419.

Wolley, A. R. 1982: A discussion of carbonatite evolution and nomenclature, and the generation of sodic and potassic fenites. Mineral. Mag. **46**, 13-17.

Wyllie, P. J. 1966: Experimental studies of carbonatite problems. The origin and differentiation of carbonatite magmas. In O. F. Tuttle & J. Gitins (edit.) "Carbonatites" 311-352. Interscience Publishers. New York.

Wyllie, P. J., Cox, K. G. & Biggar, G. M. 1962: The tiabit of apatite in synthetic systems and igneous rocks.

Wyllie, P. J. and Tuttle, O. F. 1964: Experimental investigation of silicate systems containing two volatile components; part III: The effects of SO_3, P_2O_5, HCl and Li_2O, in addition to H_2O, on the melting temperatures of albite and granite. Am. J. Sci. **262**, 930.

Qaqarssuk Carbonatite Complex
Geological map of the core
1:2000

By Christian Knudsen,GGU,1985

The map is based on out crop mapping by CK, drill core and magnetic anomaly data obtained by Kryolitselskabet Øresund A/S.

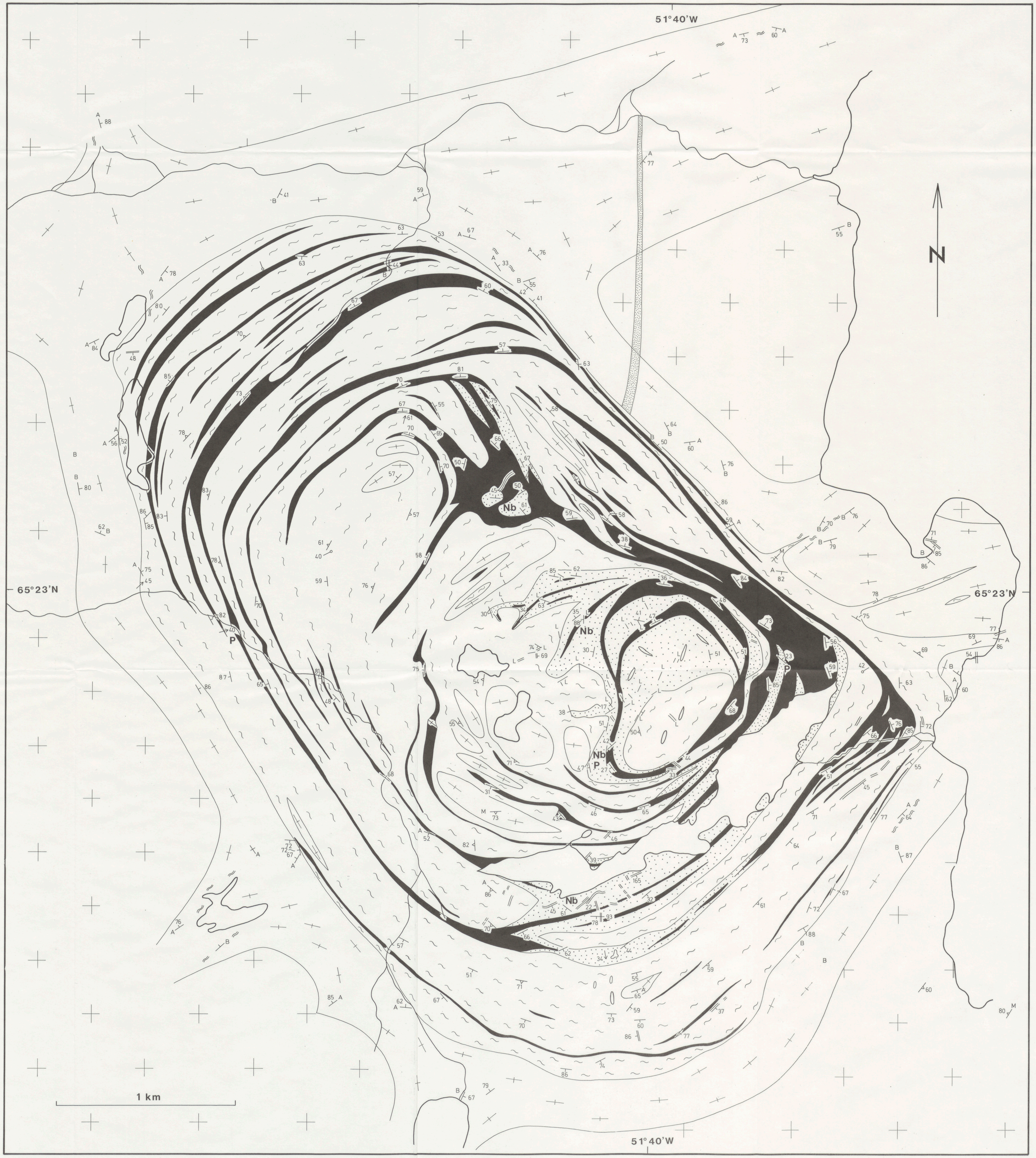

Qaqarssuk Carbonatite Complex

Geological map
1:10000
By Christian Knudsen
Geological Survey of Greenland 1985

⁙	Silicic ultramafite (glimmerite, hornblendite and pyroxenite < 50 % carbonatite)
◢	Carbonatite (>50 % carbonatite)
∼	Fenite (<50 % carbonatite)
⤫	Altered basement (quartz bearing)
+	Basement, little altered
▥	Dolerite dyke
30	Late søvite veins (dip of late søvite veins)
L 89	Lanthanide-rich carbonatite veins (dip of lanthanide-rich carbonatite veins)
59 A	Radioactive shear zone Strike and dip of radioactive ankerite vein
65 B	Strike and dip of beforsite and lamprophyre dykes
35	Strike and dip of layering in carbonatite and ultramafite
83	Strike and dip of foliation in fenite and altered basement
45	Fold axis
M	Mylonite
P	Phosphate-rich rocks
Nb	Phyrochlore-rich rocks